



Crowd Management at Train Stations in Case of Large-Scale Emergency Events

Anna Lisa Braun

IAS Series

Band / Volume 54

ISBN 978-3-95806-706-6

Forschungszentrum Jülich GmbH
Institute for Advanced Simulation (IAS)
Zivile Sicherheitsforschung (IAS-7)

Crowd Management at Train Stations in Case of Large-Scale Emergency Events

Anna Lisa Braun

Schriften des Forschungszentrums Jülich
IAS Series

Band / Volume 54

ISSN 1868-8489

ISBN 978-3-95806-706-6

Bibliografische Information der Deutschen Nationalbibliothek.
Die Deutsche Nationalbibliothek verzeichnet diese Publikation in der
Deutschen Nationalbibliografie; detaillierte Bibliografische Daten
sind im Internet über <http://dnb.d-nb.de> abrufbar.

Herausgeber und Vertrieb: Forschungszentrum Jülich GmbH
Zentralbibliothek, Verlag
52425 Jülich
Tel.: +49 2461 61-5368
Fax: +49 2461 61-6103
zb-publikation@fz-juelich.de
www.fz-juelich.de/zb

Umschlaggestaltung: Grafische Medien, Forschungszentrum Jülich GmbH

Druck: Grafische Medien, Forschungszentrum Jülich GmbH

Copyright: Forschungszentrum Jülich 2023

Schriften des Forschungszentrums Jülich
IAS Series, Band / Volume 54

D 468 (Diss. Wuppertal, Univ., 2022)

ISSN 1868-8489
ISBN 978-3-95806-706-6

Vollständig frei verfügbar über das Publikationsportal des Forschungszentrums Jülich (JuSER)
unter www.fz-juelich.de/zb/openaccess.



This is an Open Access publication distributed under the terms of the [Creative Commons Attribution License 4.0](https://creativecommons.org/licenses/by/4.0/), which permits unrestricted use, distribution, and reproduction in any medium, provided the original work is properly cited.

List of abbreviations

AG	Arbeitsgruppe (Working Group)
CroMa	Project founded by the German Federal Ministry of Education and Research (BMBF) – “Crowd Management in Verkehrsinfrastrukturen”
<i>fro-re</i>	front to rear
ICE	Intercity Express
JuPedSim	Jülich Pedestrian Simulator
JPScore	Simulation tool of JuPedSim
JPSreport	Evaluation tool of JuPedSim for the analysis of pedestrian trajectories
KapaKrit	Project founded by the German Federal Ministry of Education and Research (BMBF) – “Optimierung der Verkehrskapazität von Bahnhöfen im Krisen- und Katastrophenfall”
LOS	Level-of-Service
MSA	Merkur Spiel-Arena
PED	Platform Edge Doors
RE	Regional Express
<i>re-fro</i>	rear to front
SB	Stadt Bahn (City Train)
USA	United States of America
WA	Waiting Area
wt	Waiting Time

Abstract

In the past decades, various countries around the world have experienced disaster events that required large-scale evacuation. The causes of such events are both natural, such as the occurrence of extreme weather events or earthquakes, and human-made, such as incidents in nuclear power plants, terrorist attacks or war. Thus, although there is experience in the field of large-scale evacuations, planning and implementation are often inadequate, especially with regard to the use of public transport. This work is intended to close existing gaps and overall improve the planning.

However, since the road network in Germany, especially in the metropolitan area of North Rhine-Westphalia, offers little capacity, the attention of this thesis is focused on the means of railway transport, which offers a road-independent network and has therefore great potential in this field. In a direction-independent event, the railway network is mainly determined by the capacity of the train stations. Therefore, in this thesis, the pedestrian dynamics inside a train station is investigated in order to evaluate and increase its capacity in the case of increased passenger volumes. The results are thus not only applicable to the planning of large-scale evacuations, but can also be used, for example, for the transport planning of major events.

In particular, a methodology is presented which, in a first step, enables the identification of critical bottlenecks in the station system under consideration by means of simulation studies. Based on this, in a further step, simulation studies will be presented that examine the targeted use of various crowd management measures to reduce the bottlenecks and thus increase the overall capacity of the system while ensuring the safety of all persons. In a final step, the influence of varying different system components, such as the width of staircases or the length of access routes, is investigated. The results can be applied in the planning of new buildings or building conversions, but also in the planning of measures for large-scale events with a huge amount of passengers.

Kurzfassung

In den letzten vergangenen Jahrzehnten kam es in verschiedenen Ländern der Welt zu Schadensereignissen, welche eine großräumige Evakuierung mit sich zogen. Die Ursachen solcher Ereignisse sind sowohl natürlich, wie das Auftreten von extremen Wetterereignissen oder Erdbeben, als auch menschengemacht, wie Störfälle in Atomkraftwerken, terroristische Anschläge oder Krieg. Obwohl es also Erfahrungen in dem Bereich großräumiger Evakuierungen gibt, sind die Planung und Umsetzung, besonders in Bezug auf den Einsatz von öffentlichen Transportmittel, oft unzureichend. Diese Arbeit soll dazu beitragen, bestehende Lücken zu schließen und die Planung insgesamt zu verbessern.

Da das Straßennetz in Deutschland, besonders im Ballungsgebiet Nordrhein-Westfalen jedoch wenig Kapazität bietet, richtet sich die Aufmerksamkeit dieser Arbeit auf die Verkehrsmittel der Schiene, welche mit einem straßenunabhängigen Netzwerk großes Potential in diesem Bereich bieten. Bei einem richtungsunabhängigen Ereignis wird das Schienennetzwerk hauptsächlich von der Kapazität der Bahnhöfe bestimmt. Daher wird in dieser Arbeit die Fußgängerdynamik in Bahnhöfen untersucht, um ihre Kapazität bei stark erhöhten Fahrgastaufkommen zu bewerten und zu erhöhen. Die Ergebnisse finden somit nicht nur bei der Planung von großräumigen Evakuierung Anwendung, sondern können beispielsweise auch für die Verkehrsplanung von Großveranstaltungen eingesetzt werden.

Im Speziellen wird eine Methodik vorgestellt, welche es in einem ersten Schritt mittels Simulationsstudien ermöglicht, kritische Engstellen in dem zu betrachtenden System zu identifizieren. Darauf aufbauend werden weitere Simulationsstudien vorgestellt, welche den gezielten Einsatz verschiedener Crowd Management Maßnahmen untersuchen, um diese Engstellen zu reduzieren und somit die Gesamtkapazität des Systems zu erhöhen und gleichzeitig die Sicherheit aller Personen zu gewährleisten. In einem letzten Schritt wird der Einfluss der Variation verschiedener Systemkomponenten, wie die Breite von Treppen oder die Länge von Zugangswegen, untersucht. Die Ergebnisse können bei der Planung von Neu- oder Umbauten von Gebäuden, aber auch bei der Planung von Maßnahmen bei Großveranstaltungen angewendet werden.

Acknowledgements

This thesis was written during my time as a research assistant at the Institute for Advanced Simulation – Civil Safety Research (IAS-7) at the Research Centre Jülich. At this point, I would like to express my thanks for the great time and the support:

First, I would like to thank my doctoral supervisor Prof. Dr. Lukas Arnold, as well as Prof. Dr. Armin Seyfried, who not only advised me on technical issues, but also supported me in many other ways.

Very special thanks also go to Dr. Mohcine Chraibi and Tobias Schrödter, as well as the other team members of the department *Pedestrian Dynamics - Modelling*. They implemented the technical requirements for the simulation software JuPedSim, without which my work would not have been possible. Furthermore, they were always available to help me with questions and issues, and I could count on quick support at any time.

I also thank all my colleagues from the research centre and the colleagues from the departments *Computational Civil Engineering* and *Computersimulation für Brandschutz und Fußgängerverkehr* at the University of Wuppertal for their great support and the friendly working atmosphere.

Of course, my family and friends should not go unmentioned. Even though they were not able to support me professionally, they made a significant contribution to the success of this work, through their understanding in stressful times, putting up with bad moods or, especially in the final year, allowing me time by supporting me with childcare.

Last, I acknowledge the partial funding of this work by the German Federal Ministry of Education and Research (BMBF) within the KapaKrit project (13N14620). The needed computing time for the multivariate analysis was conducted on a computing cluster funded by the BMBF within the CoBra project (13N15497).

Table of Contents

1. Introduction	1
1.1. Motivation	1
1.1.1. Large-Scale Emergency Events using Railway	1
1.1.2. Abstraction and Crowd Management	2
1.2. State of the Art	3
1.2.1. Capacity of Train Stations in a Large-Scale Evacuation Context – Scientific Studies and other Concepts	3
1.2.2. Crowd Management at Train Stations	4
1.2.3. Station Processes – From Regular to Evacuation Operation	7
1.2.3.1. Waiting Behaviour at Train Stations	7
1.2.3.2. Boarding Times	8
1.2.4. Level-of-Service Concept	9
1.2.5. Jülich Pedestrian Simulator	11
1.2.5.1. New Features in JPScore	11
1.2.5.2. Geometry Structure, Router and Operational Model	14
1.2.5.3. Model Limitations of JPScore	15
1.2.5.4. JPSeditor, JPSreport and JPSvis	15
1.2.5.5. Software Version	15
1.3. Objectives and Approach	16
1.4. Thesis Outline	17
2. Methodology	19
2.1. Setup	19
2.1.1. Geometries	19
2.1.2. Train Types	25
2.2. Hand Calculation	27
2.3. Simulation Studies	28
2.3.1. Zero Cases	28
2.3.2. Operational and Tactical Crowd Management Measures	28
2.3.2.1. Train Arriving Intervals and Waiting Areas	29
2.3.2.2. Time Schedules	30
2.3.2.3. Filling Platforms	31
2.3.2.4. Multivariate Crowd Management Measures	32
2.3.3. Variable Geometries	33
2.4. Evaluation Theory	34
3. Evaluation and Result	37
3.1. Zero Cases	37
3.1.1. Multi-directional Zero Case	37
3.1.2. Uni-directional Zero Cases	40

3.2. Parameter Studies	42
3.2.1. Train Arriving Intervals and Waiting Areas	42
3.2.1.1. Multiple WAs and a Five-Minute Time Schedule	42
3.2.1.2. Multiple WAs and a Ten-Minute Time Schedule	44
3.2.1.3. Single WA and a Ten-Minute Time Schedule	45
3.2.2. Time Schedules	47
3.2.3. Filling Platforms	53
3.2.3.1. Inflow Rate	54
3.2.3.2. Filling Process	58
3.2.3.3. Door Status	59
3.2.3.4. Train Types	61
3.2.3.5. Overall Assessment	62
3.2.3.6. Double-sided Filling	63
3.2.4. Multivariate Crowd Management Measures	68
3.2.4.1. Densities	69
3.2.4.2. Total Evacuation Times	73
3.2.4.3. Filling Processes – Distribution of Passengers over the Platform	75
3.2.4.4. Interim Conclusion	78
3.3. Applicability to Variable Geometries	79
3.3.1. Hand Calculation	80
3.3.2. Densities	80
3.3.3. Maximum Evacuation Times and Peoples Distribution along the Event Access Area	86
3.3.4. Interim Conclusion	90
4. Conclusion	93
5. Outlook	95
A. Initial conditions of JPScore	101
B. Evaluation Final	105
C. Evaluation Easy	111

List of Figures

1.1. Crowd management concept at the station “Merkur Spiel-Arena/Messe Nord” in Düsseldorf (Germany)	5
1.2. Route guiding system with barriers, queuing system, waiting area and inflow regulation to the main station of Dortmund (Germany) in case of a football derby (before kick off)	6
1.3. Sketch of a fundamental diagram of the Level-of-Safety with traffic light colour coded classification	10
1.4. Example of the functionalities of waiting areas	12
1.5. Event-based door statuses in JPScore with internal and external control mechanisms and their influence on the walking strategy of the agents.	13
2.1. Train station setup 1	21
2.2. Train station setup details	21
2.3. Train station setup 2: Different platform lengths, a vestibule in front of the entrance hall and four entrance doors.	22
2.4. Train station setup 3: Separated platforms with a small tunnel section between the staircases to generate agents by source.	23
2.5. Train station setup 4: Whole station with equal platforms and six entrances.	23
2.6. Floor-fields with routing to the right staircase of platform 3 before and after the adaption of the <i>room</i> -structure.	24
2.7. Visualisation of the trajectories for the same time step in the simulation with a geometry before and after the adaption of the <i>room</i> -structure.	24
2.8. Setup 5: Variable geometry, avoiding a routing around 90-degree corners.	25
2.9. Examples of the different train types	26
2.10. Route choice to calculate the longest path for the hand calculation.	27
2.11. Waiting areas inside the station	29
2.12. Illustration of the filling processes front to rear (<i>fro-re</i>), <i>mixed</i> and rear to front (<i>re-fro</i>)	32
2.13. Analysis methods A and C of JPReport	34
2.14. Overview of measurement areas and lines for the evaluation of the trajectory data of the simulation	35
3.1. Location of measurement areas and lines in setup 1	38
3.2. Densities of the multi-directional zero case.	38
3.3. Flow of the multi-directional zero case.	39
3.4. Density of the zero case with an unidirectional inflow.	40
3.5. Flow of the zero case with an unidirectional inflow.	40
3.6. Densities of variation A with mean values and standard deviation.	42
3.7. Specific flow of variation A.	43

3.8. Densities of variation B with mean values and standard deviation. . . .	44
3.9. Specific flow of variation B.	45
3.10. Densities of variation C with mean values and standard deviation. . . .	46
3.11. Specific flow of variation C.	46
3.12. Location of measurement areas and measurement lines in setup 2. . . .	47
3.13. Evacuation times of the different station sections.	49
3.14. Trajectories for filling platform 1.	49
3.15. Densities with mean values and standard deviation for filling platform 1.	50
3.16. Trajectories for filling platform 3.	50
3.17. Densities with mean values and standard deviation for filling platform 3.	50
3.18. Trajectories for filling platform 5.	51
3.19. Densities with mean values and standard deviation for filling platform 5.	51
3.20. Measurement lines and areas for the different platforms of setup 3. . . .	53
3.21. Maximum evacuation times for different inflow rates.	54
3.22. Visualisation of the trajectories in the staircase area for different inflow rates and filling processes	55
3.23. Maximum densities for the ICE with different inflow rates.	56
3.24. Time-dependent densities for the ICE and the door status <i>open</i>	56
3.25. Time-dependent densities for the ICE and the door status <i>close</i>	57
3.26. Distribution of passengers over the platform at the example of the RE and an inflow rate of 2 s^{-1}	58
3.27. Visualisation of trajectories for the filling processes <i>re-fro</i> and <i>fro-re</i> . .	59
3.28. Boarding times in dependency of the door statuses.	60
3.29. Overview of the evacuation times, considering all crowd management measures.	62
3.30. Overview of the evacuation times, considering all crowd management measures for the double-sided case.	63
3.31. Boarding Times for the filling process <i>re-fro</i> in the double-sided case. .	64
3.32. Maximum densities for the ICE with different inflow rates for the double- sided case.	64
3.33. Time-dependent densities for the door statuses <i>open</i> and <i>close</i> as func- tion of the filling process for a double-sided ICE filling	65
3.34. Time-dependent densities for the door statuses <i>open</i> and <i>close</i> as func- tion of the filling process for a double-sided RE filling	66
3.35. Measurement areas and measurement lines for setup 4.	68
3.36. Measurement lines at transitions for the analysis of the different station sections in setup 4.	69
3.37. Maximum densities for different inflow rates at the example of platform 5.	69
3.38. Time-dependent densities as a function of the filling process for the example of platform 2 with an inflow rate of 4 s^{-1}	71
3.39. Densities in dependence of the door opening times for the filling process “100”	72
3.40. Densities in dependence of the door opening times for the filling process “-100”	72
3.41. Time-dependent delay in rising densities at the example of the filling process “100” on platform 5 with an inflow of 6 s^{-1}	73

3.42. Passing times of 75% of the passengers at the transitions between the station sections with different inflow rates.	74
3.43. Maximum passing times at the transitions between the station sections with different inflow rates.	74
3.44. Passenger distribution with an inflow of 2 s^{-1}	76
3.45. Passenger distribution with an inflow of 4 s^{-1}	76
3.46. Passenger distribution with an inflow of 6 s^{-1}	76
3.47. Measurement areas and lines for setup 5.	79
3.48. Setup 5, including obstacles.	79
3.49. Time-dependent densities for a corridor of 10 m, a staircase of 4 m, an inflow rate of 2 s^{-1} , and a door opening time of 10 min.	81
3.50. Time-dependent densities for a corridor of 50 m, a staircase of 4 m, and an inflow rate of 4 s^{-1}	84
3.51. Time-dependent densities for a one-sided filling with obstacle, a corridor of 10 m, a staircase of 4 m, and an inflow rate of 2 s^{-1}	85
3.52. Time-dependent densities for a double-sided filling with obstacle, a corridor of 10 m, a staircase of 4 m, and an inflow rate of 2 s^{-1}	85
3.53. Time-dependent densities of the filling process “100” (<i>re-fro</i>) for the double-sided filling with obstacle, a corridor of 90 m, a staircase of 8 m, and an inflow rate of 4 s^{-1}	86
3.54. Maximum evacuation times for different inflow rates, a corridor of 90 m and a staircase of 4 m.	87
3.55. Distribution over the <i>Event Access Area</i> in dependency of the filling process for the maximum number of people.	88
3.56. Distribution over the <i>Event Access Area</i> in dependency of the filling process for 50% of the people.	89
3.57. Distribution over the <i>Event Access Area</i> with obstacle in dependency of the filling process for the maximum number of people.	89
3.58. Distribution over the <i>Event Access Area</i> with obstacle in dependency of the filling process for 50% of the people.	90
B.1. Time-dependent densities as a function of the filling process for the example of platform 5 with an inflow rate of 4 s^{-1}	106
B.2. Time-dependent densities as a function of the filling process for the example of platform 3 with an inflow rate of 6 s^{-1}	107
B.3. Time-dependent densities as a function of the filling process for the example of platform 3 with an inflow rate of 8 s^{-1}	108
B.4. Time-dependent densities as a function of the filling process for the example of platform 3 with an inflow rate of 12 s^{-1}	109
C.1. Time-dependent densities for the filling processes “100” to “20” (<i>fro-re</i>) a corridor of 10 m, a staircase of 4 m, an inflow rate of 2 s^{-1} , and a door opening time of 2 min.	112
C.2. Time-dependent densities for the filling processes “100” to “20” (<i>fro-re</i>) a corridor of 10 m, a staircase of 4 m, an inflow rate of 2 s^{-1} , and a door opening time of 6 min.	112

C.3. Time-dependent densities for the filling processes “100” to “20” (<i>fro-re</i>) a corridor of 90 m, a staircase of 4 m and an inflow rate of 2 s^{-1}	113
C.4. Time-dependent densities for the filling processes “-100” to “-20” (<i>re-fro</i>) a corridor of 50 m, a staircase of 6 m and an inflow rate of 4 s^{-1}	113
C.5. Time-dependent densities for the filling processes “-100” to “-20” (<i>re-fro</i>) a corridor of 50 m, a staircase of 8 m and an inflow rate of 6 s^{-1}	114
C.6. Time-dependent densities for the filling processes “-100” to “-20” (<i>re-fro</i>) a corridor of 50 m, a staircase of 10 m and an inflow rate of 8 s^{-1}	114
C.7. Time-dependent densities for the double-sided filling, a corridor of 10 m, a staircase of 4 m, and an inflow rate of 2 s^{-1}	115
C.8. Time-dependent densities for the double-sided filling, a corridor of 50 m, a staircase of 6 m, and an inflow rate of 4 s^{-1}	116
C.9. Time-dependent densities for the double-sided filling, a corridor of 50 m, a staircase of 8 m, and an inflow rate of 6 s^{-1}	117
C.10. Time-dependent densities for the double-sided filling, a corridor of 50 m, a staircase of 10 m, and an inflow rate of 6 s^{-1}	118
C.11. Time-dependent densities with obstacle for a corridor of 90 m, a staircase of 8 m, and an inflow rate of 2 s^{-1}	119
C.12. Time-dependent densities with obstacle for a corridor of 90 m, a staircase of 8 m, and an inflow rate of 4 s^{-1}	119
C.13. Time-dependent densities with obstacle for a corridor of 90 m, a staircase of 8 m, and an inflow rate of 8 s^{-1}	120

List of Tables

1.1. Level-of-Safety classification	9
2.1. Train station setups overview	20
2.2. Train specifications in relation to the train doors	26
2.3. Variations of train arriving intervals and waiting times	30
2.4. Additional train type specifications.	31
2.5. Parameter variations of different crowd management measures.	31
2.6. Parameter variations of the multivariate crowd management measures, considering inflow rates, door statuses and filling processes.	33
3.1. Hand calculation vs. simulation: Walking times for a single passenger. .	48
3.2. Hand calculation vs. simulation: Evacuation times for train capacities. .	48
3.3. Example of a time schedule with departure times for one hour using both entrances	52
3.4. Boarding and evacuation times for different door statuses of the RE. . .	60
3.5. Comparison of the different train types with the results of an <i>open</i> door status, the filling process <i>re-fro</i> and an inflow rate of 2 s^{-1}	61
3.6. Hand calculation: Filling times for different staircase widths.	80
3.7. Hand calculation: Passing times at the entrance for different inflow rates. .	80

1. Introduction

1.1. Motivation

1.1.1. Large-Scale Emergency Events using Railway

Nature and human made hazards, like hurricanes, wildfires, terrorist attacks, incidents in chemical facilities and nuclear power plants or recent events such as the war in the Ukraine make it necessary to evacuate a huge number of people in a very short time. For such events, a large evacuation radius with several 100,000 people can be expected. Hence, the main focus of most of the studies regarding large-scale evacuations, which include reviews of past events and approaches for improvement and planning, is the management of the evacuation vehicles and its route planning [1]. Examples like the evacuation in case of hurricanes Katrina and Rita (USA), which were conducted with private vehicles and busses, show that large-scale evacuations with only road-dependant vehicle cause huge problems, like kilometre-long time-consuming traffic jams, a lack of fuel and broken cars, which further impaired the evacuation [2]. Besides this, in case of Katrina people without a private vehicle, who are dependant on public transportation were strongly neglected, which additionally hindered the evacuation. Though this is not an individual case and has to receive more attention to the evacuation planning [3]. The reasons for people having no private vehicles are numerous [4] and will become more important in the future as many people will give up their vehicles and use alternatives like car sharing or public transportation [5]. However, public transportation modes, which are used for large-scale evacuations, are mostly buses. There are also numerous studies on it, like route choice for multiple pickup and delivery points [1][6][7][8][9]. Nevertheless, these are also road-dependant vehicles.

In other countries, for example in Germany especially in the conurbation of North Rhine-Westphalia, the roads are already heavily congested during daily rush hours [10]. An evacuation with only road-dependant vehicles would hardly be possible. The working group (AG) Fukushima, which was founded in Germany after the nuclear disaster in Fukushima in 2011, for example, advises to use trains for a large-scale evacuation [11], as does the concept of Vesuvius [12][13], which will be further described in section 1.2.1. Nevertheless, there are hardly studies about the pedestrian dynamics inside a station in case of large-scale emergency events, which can be a limiting factor for the capacity of the whole railway system. Hence, this thesis aims to fill the existing gaps in this context. Therefore, the pedestrian dynamics within a train stations in case of a large-scale emergency event with increased passenger volumes will be investigated. In particular, critical bottlenecks of the system should be identified in order to increase the capacity of the station and to ensure the safety of the passengers, by introducing different crowd management measures.

1.1.2. Abstraction and Crowd Management

A train station can be seen as a path network. Unidirectional streams of passengers of different strengths flow through it. The network itself has natural bottlenecks, like cross-section narrowing or staircases, that have to be passed and at which congestion and crowding can occur depending on the strength of the passenger flow. Thereby, the occurrence of congestion is not a major problem at first. The decreasing flow of people only reduces the performance of the system. However, if the densities reach a very high level due to congestion, people can start pushing, which can quickly lead to dangerous situations. This problem also exists in the case of traffic access to large events or evacuations of buildings.

In April 1989, thousands of football fans poured into the already overcrowded Hillsborough Stadium in Sheffield, England. 96 people were crushed to death, 766 suffer injuries, some of them serious¹. In December 1999 at the “Air & Style” snowboard showdown with approximately 22,000 visitors at the Bergisel Stadium in Innsbruck a crush of people ensued, with a fatal outcome for six of the people involved, four patients in coma since then and 38 injured²³. The concentration of visitors has arisen at one exit of the stadium. Thereby, structural conditions, darkness and the slightly sloping and slippery path exacerbated the dangerous situation. Another particularly serious event was the Loveparade in Duisburg in July 2010 where 21 people died, and at least 652 people were injured. Big mistakes have already been done in the planning phase of the event. This is shown by the expert report of professor Gerlach of the institute “Straßenverkehrsplanung und Straßenverkehrstechnik” of the Bergische Universität Wuppertal, which was prepared as part of the court proceedings to clarify the events surrounding the Loveparade. The unsuitability of the venue for the expected number of spectators, the underdimensioning of the separation systems at the entrance and the transition area between the event area and the access were the main causes of the backlogs and the resulting crowding, which ended fatally for some spectators. Additionally, the situation was further aggravated by the insufficient coordination of measures in the overall context.

These are just a few examples of events where the path networks had safety-relevant bottlenecks that were not detected in advance or were incorrectly classified in terms of safety. Hence, a central question is how the processes in the path network can be optimised to ensure the safety of every single person. For the entrance situation at a stadium, for example, only the tickets of spectators were checked, in the past. Nowadays, it is usual that at least the bags are controlled and for the very latest times during the Covid-19 pandemic additionally the “green pass” needed to be controlled. This is time-consuming and makes it necessary to install additional queuing systems to avoid high densities, pushing and other dangerous situations at the entrances.

It cannot be ruled out that in the event of a large-scale evacuation, similar problems may arise when entering a train station or accessing the platforms. Even under normal circumstances, there are situations at train stations that lead to an overload of the infrastructure and to the evacuation of the station or individual platforms. A

¹<https://www.spiegel.de/geschichte/fussballtragoedie-von-hillsborough-a-948256.html>

²<https://tirol.orf.at/stories/3022526/>

³<https://www.springermedizin.de/toedliche-zwischenfaelle-durch-menschengedraenge-bei-grossverans/8005192>

current example for overcrowded platforms and trains in Germany, is the nationwide introduction of the *9-euro-ticket* in summer 2022 ⁴.

1.2. State of the Art

1.2.1. Capacity of Train Stations in a Large-Scale Evacuation Context – Scientific Studies and other Concepts

Large-scale evacuation means thousands of people need to be evacuated and want to use the train station infrastructure at the same time. As mentioned in chapter 1.1.1, the AG Fukushima recommends to use trains for the evacuation [11]. However, the author is not aware of any concepts or scientific studies on how a train station can be used in this context. The official planners of Neaple in Italy elaborated a concept for the high risk event of a volcano eruption of the Vesuvius [12][13]. The concept is comprehensive and detailed. The evacuation area is divided into four areas, which would be affected with varying severity. According to the area, the evacuation priority and the time schedule are set. The most affected area will be evacuated first. The areas are divided into smaller sections. Thereby, for every section it is precisely defined which transport modes should be used, which route should be taken and which safe area should be headed for. Among cars, busses and ships, also trains should be used for the evacuation. There is a detailed list of the expected people and required vehicles. Nevertheless, there is no evidence of crowd management planning at the stations. As outlined in section 1.1.2 crowd management at train stations is an important aspect to ensure the safety of all people and should therefore be taken into account.

Another example of using trains for an evacuation is given by VanLandegen and Chen [14]. They modelled an evacuation of the Pentagon by using the metro station. This is a small-scale example, but as there are only two lines which can be used to evacuate the 23,000 employees, it can be transferred to a large-scale evacuation with more people but also more usable platforms and lines. In the study, pedestrian simulation and traffic simulation are combined. It is assumed, that people do not need more than ten minutes to leave the Pentagon. The time from the Pentagons exit to the metro entrance is modelled by pedestrian simulation. Afterwards, the output of the pedestrian simulation is used as input for the traffic simulation. It is analysed how long it takes until the people arrive at their destination station, which is defined as the nearest to their homes. But again, the pedestrian dynamic and the derived crowd management inside the departure station is not modelled.

In both studies, it remains open whether there is congestion when entering the station and boarding the trains. In order to increase the safety of the people, a closer look at the pedestrian dynamics would be necessary. Apart from the evacuation context, there are other concepts on how to deal with excessive high passenger volumes at train stations or at least at several platforms. This includes daily rush hours, on the one hand and special events like sport games or concerts, where many people use public transportation and especially at the end of the event all people flock to the traffic

⁴<https://www.derwesten.de/panorama/vermishtes/9-euro-ticket-deutsche-bahn-chaos-fahrgaestevolle-zuege-ueberfuellung-pfingsten-id235532603.html>

modes at the same time, on the other hand. These concepts are shown in the following section.

1.2.2. Crowd Management at Train Stations

Huge main stations in Germany, like Hamburg or Frankfurt, handle up to 500,000 passengers per day (d^{-1}) [15]. Cologne handles about 300,000 d^{-1} and Dortmund around 100,000 d^{-1} . Smaller main stations handle even less, like Bochum with 100,000 d^{-1} . In case of a large-scale evacuation thousands of people are dependant on public transportation and many of them will go to the station to be evacuated by train. Nevertheless, there are a lot of examples of stations that are already struggling with high passenger volumes, without a concrete case of evacuation. In Germany, it was most recently the impact of the *9-euro-ticket*. The ticket was a measure to relieve the financial burden on the population due to the effects of the war in Ukraine. Nevertheless, it causes many struggles with overcrowded stations and trains⁵. Besides this, there are also many stations which struggle with high densities during the daily rush hours. If more people constantly enter the station than can be transported by incoming trains, this inevitably leads to a gathering of people in the station and on the platforms. To avoid dangerous situations, this leads to the necessity of crowd management measures, like regulating the inflow to the station. Therefore, it is important to know the bottlenecks of a station in advance. Pu et. al. [16] give an overview of bottlenecks in stations, which can be divided into two kinds, ordinary bottlenecks, which occur due to insufficient capacity of the available structure and controllable bottlenecks like security and ticket gates. The latter are facilities where regulation can be carried out. The results show, that the most efficient regulation is carried out by using all available facilities, in this case security and ticket gates. Jiang et. al. [17] show how to regulate the inflow based on real time data. Railings in front of the station, ticket vending machines and ticket gates, as well as closing individual partial accesses are mentioned as possible regulation options. Hoogendoorn et. al. [18] compare stations with and without access gates and refer to the influence of their location.

These examples of daily business inflow regulation are predominantly conducted with permanently installed facilities and come close to the expectations of what happens in the event of a large-scale evacuation at a train station. Many people want to use the trains at the same time, which leads to waiting situations and overcrowding and should be countered with crowd management measures, like the inflow regulation with predominantly permanently installed facilities, as shown in the examples. However, there are non-daily business situations, which make it necessary to handle huge crowds in a short time, like concerts or sport events, and therefore need to consider further crowd management measures. At event venues, like stadiums, there are also permanently installed facilities for ticket controlling, which serve also as inflow regulation. In addition, temporally facilities, are used to create queuing systems, which prevent high densities and pushing at the entrance. Such portable devices can be used individually and are adaptable to the respective situation. Hence, such systems can also be transferred to extraordinary inflow situations at train stations. The station at the event location

⁵<https://www.tagesspiegel.de/berlin/bahn-chaos-wegen-9-euro-ticket-ueberfuellte-zuege-ungeplante-stopps-starker-andrang-wegen-rueckreisen-erwartet/28401170.html>

“Mercur Spiel-Arena (MSA)” in Düsseldorf (Germany) is one example of it. Here, the exhibition grounds and the MSA share a train station with two platforms. Accordingly, this is regularly used by a huge number of people. In many cases, this leads to overcrowding on the platform. Hence, several solid installed facilities and individually applicable measures have been applied. In the first step, half-height platform edge doors (PED) have been permanently installed. These are barriers with fixed openings for the train doors, which are kept close until a train arrives and thus preventing the risk of people falling into the tracks. However, the installation of the PED also leads to heavy crowding in front of the doors, which can cause people to be injured. To avoid this, a crowd management concept was developed by Bernd Belka, the security manager of the company “Special Security Services Deutschland” (SPECSEC) [19]. This concept provides for the use of additional temporary crowd management facilities to control the flow of people at the station in case of an event in the MSA. In addition, security personnel will be deployed to distribute people on the platform. Figure 1.1 shows a sketch of the concept with the location of temporary facilities and security personal. Nevertheless, the success of such concepts always presupposes that the staff employed are appropriately trained. The implementation of this concept could be observed during field observation made during the project CroMa⁶.

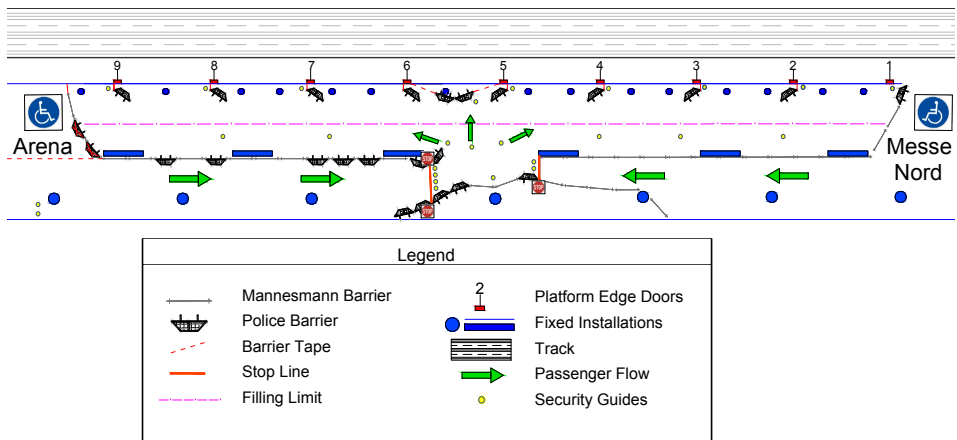


Figure 1.1.: Sketch by Olga Sablik, with own translation and little supplements, of the crowd management concept at the station “MSA/Messe Nord” in Düsseldorf, Germany, developed by Bernd Belka (SPECSEC) using the example of the set-up from the field observation made during the CroMa project on 24.09.2019.

Another example for crowd management at train stations in case of extraordinary events, where crowd control is conducted by temporarily facilities like barriers and entrance systems, is the main station of Dortmund (City in Germany). In case of football games, especially in case of a derby, there are inflow restrictions to the station

⁶Project funded by the German Federal Ministry of Education and Research (BMBF) – “Crowd Management in Verkehrsinfrastrukturen”

and also barriers and other facilities to steer the crowd through the station to the platforms but also to separate the fans of the rival clubs. These measures could also be necessary during an evacuation, e.g. to evacuate women and children (or families) first, or to organise special queues for those in need of help. In Dortmund, the federal police elaborate individual concepts for each event. Picture 1.2 was made during the event of a football derby in 2019, before the kick-off. It shows a route guidance system for the football fans of the external club, with barriers, queuing system, waiting area and inflow gates in front of the entrance of the subway station of the main station of Dortmund. The fans who come by train from the external city need to change at the main station from the train to the metro, which drives to the stadium. So, they are guided from the platform inside the train station to the waiting area in front of the subway station. From there, every few minutes, corresponding to the interval of the arriving metro trains, 300 fans, which is the capacity of one metro train, were allowed to enter the station, as long as all fans have caught a metro to the stadium. After the event, when the fans arrived back at the main station, in order to avoid a clash of the fan groups, the external fans were directed from the subway via the rear entrance



Figure 1.2.: Photos by Mohcine Chraibi with own supplements. Route guiding system with barriers, queuing system, waiting area and inflow regulation to the main station of Dortmund (Germany) in case of a football derby (before kick-off). The fans are standing in the waiting area and every few minutes 300 people were allowed to enter the station, corresponding to the capacity of one train.

directly to the nearest platform. For this purpose, the corresponding train is diverted to this platform and the route to the platform is partly equipped with privacy fences. Nevertheless, external equipment is not hold up at every train station and has to be procured from supra-regional storage. As this is time-consuming, the focus to regulate the inflow to the station should lie on its available facilities in case of a high-risk large-scale evacuation.

1.2.3. Station Processes – From Regular to Evacuation Operation

In case of a large-scale evacuation the daily railway operations have to be transferred to an evacuation operation. To what extent this is done depends on the incident and the resulting evacuation radius. As this work was part of the project KapaKrit⁷, this question was discussed with different railway operators, who provide the railway infrastructure in Germany, and the federal police, who are responsible for securing the train stations and have experience with other events with a huge number of passengers, as shown in the previous section. At the assumption, that a large-scale emergency event is considered, these parties recommend suspending the daily railway operations on a large scale in a regulated manner in order to implement appropriate evacuation operations afterwards. The federal police also needs some time to prepare evacuation measures according to the situation and to provide sufficient personnel. Hence, once the station is empty, no operational and tactical measures for crowd management inside the station will be influenced by alighting passengers.

Consequently, the processes inside a station like ticket controlling, boarding and alighting or waiting differ significantly from the daily business or an emergency evacuation of a train or the whole station, like in [20]. Nevertheless, it is important to look at the daily business for different reasons. On the one hand, as shown in the previous section, it is important to know which kind of facilities can be used in a station to regulate the inflow if the one-way traffic dominates. On the other hand, as will be outlined in the next section peoples' behaviour on daily business is from interest, for example, how do they contribute over the platform while waiting for a train, and how can special facilities like PED influence this behaviour.

1.2.3.1. Waiting Behaviour at Train Stations

Most of the studies for railway processes of platforms concern the boarding and alighting process, because it has a huge influence on the dwell time of a train at the daily operation. Another important aspect is the waiting behaviour of passengers on the platforms. How people distribute over the platform and where they preferably wait influences the boarding and alighting process significantly [21]. This is also an important aspect for the evacuation context, because it may lead to crowd management measures on the platforms to decrease the boarding and therefore the evacuation times.

Küpper analysed the waiting behaviour of people by using trajectory data from two stations in Switzerland [22]. She identifies the area around platform accesses to be one of the most commonly waiting places. Also, areas around ticket machines, showcases

⁷Project founded by the German Federal Ministry of Education and Research (BMBF) – “Optimierung der Verkehrskapazität von Bahnhöfen im Krisen- und Katastrophenfall”

and walls are used to wait for the train [22] [23]. Less common are areas with a long distance to the platform accesses. Thereby, the choice of the waiting area is strongly dependant on the time remaining until a train arrives. The closer it gets to arrival, the more people tend to wait near the accesses and do not distribute over the platform. Besides this, the affiliation of a group and the number of people belonging to it also plays a role in waiting behaviour. While single persons and small groups up to three people walk longer distances to their waiting places, larger groups tend to wait directly at the accesses [24].

In general, most of the people do not use the whole platform length, which is a problem that also has to be expected in the event of an evacuation. Even field observations at the train station “MSA/Messe Nord”, where the guiding concept, shown in figure 1.1 and described in section 1.2.2, was used due to the high number of passengers after an event in the MSA, showed this behaviour. This results in almost empty wagons, while others are very crowded. An exception to this behaviour is the arrival of an Intercity Express (ICE), which is a common long-distance railway traffic mode in Germany. Here, people usually have reserved seats and distribute according to the expected train car order, to enter the right wagon. This was also observed during own field observations at the main station of Dortmund (Germany) during the church day 2019.

Another aspect which influences the waiting behaviour and therefore the boarding process is the exact knowledge about the door position. This phenomenon can be observed, especially with the use of PED. They are usually used in metro stations for climate reasons, but also for safety reasons to avoid dangerous situations, like people falling into the tracks [25]. Thereby, the design of the PED is various. When using it for climate reasons in metro stations, they are carried out as walls, which separate the platform from the tracks. Using PED only for safety reasons, like shown in section 1.2.2 for the station “MSA/Messe Deutz” in Düsseldorf (Germany), they are carried out as half-height barriers. But all form a barrier to the tracks, with doors at the places where the doors of the train will be. In metro lines with trains having all the same design, this is well implementable, and the passengers wait next to the doors to enter the arriving train. Therefore, the waiting areas are often marked on the floor to ensure that the waiting passengers do not block the way for those disembarking. For platforms with various train designs, the usage of PED leads to difficulties because they may not match the train doors [26]. Nevertheless, the safety and the equal distribution of the passengers will be increased.

1.2.3.2. Boarding Times

An important factor when considering passenger flows within a station is also the boarding times of the trains. These represent the initial parameter of the train station system and are therefore not to be neglected. When researching boarding times, the comprehensive studies by Weidmann [27] should be mentioned in particular, which are often cited in this context. Among other things, the influence of different boarding heights depending on the type of train and the platform height, but also of luggage is examined. In regular railway operations, however, the boarding process is often influenced by the alighting process, as in most cases they overlap. Additionally, the trains are not empty, which additionally influences the flow for the boarding process. For these reasons, an individual consideration of the filling of an empty train with these

values is only possible to a limited extent.

In the context of a bachelor thesis supervised by the author [28] and in the context of the research project KapaKrit, further field observations were therefore made, which were carried out at times when there was as high a proportion of boarding passengers as possible, so that the influence of alighting passengers is kept as low as possible. However, an attempt was made to choose boarding times that are as accurate as possible. These are listed in more detail in chapter 2.1.2.

1.2.4. Level-of-Service Concept

In the case of an evacuation, the safety of the passengers is just as important as during an event or in the regular operation of a railway system. In order to ensure passengers safety, the volume of passengers in the train station must be qualitatively assessed. For this purpose, an appropriate classification of the passenger flow is necessary.

In 1963 Oeding investigated the relationship between traffic density and walking speed in pedestrian flows by means of field studies and, for large numbers of people, also by means of experiments. He developed a level-based classification for pedestrian traffic facilities, which reflects how walking behaviour changes at certain densities. Based on these classification levels, Fruin developed the Level-of-Service (LOS) concept [29], which was later adapted by Weidmann [30] and others. The number of levels varies greatly. While Fruin describes six levels, Weidmann has nine. Holl et al. compare the known LOS concepts, which shows that not only the number but also the threshold values of the classification levels differ greatly, cf. table 3 [31]. Nevertheless, most of the studies, listed in this table, declare densities of 1.5 m^{-2} and 2.5 m^{-2} to be a limit for emergence of heavy crowding. These values can be used to evaluate the densities inside the station from the simulation studies done in this thesis.

Additionally, Holl et al. transferred the LOS concept to a Level-of-Safety concept, for the assessment of pedestrian traffic at major events [31]. This is limited to three levels, which are colour-coded according to a traffic light system and classified as described in table 1.1. These classifications are furthermore described in an exemplary fundamental diagram, see figure 1.3. There is a slight kink at the transition between the green and the yellow area, but the speed continues to increase, while in the red area there is a steady decrease in speed.

Colour	Criteria
Green	Mutual interference between pedestrians may occur, but the free choice of walking speed is not significantly affected.
Yellow	Pedestrians are often forced to change their speed. Local disruptions can already have an impact on the traffic flow as a whole.
Red	The traffic volume exceeds the capacity of the facility. Significant obstructions and traffic jams may occur. Safety-critical situations must be expected.

Table 1.1.: Level-of-Safety classification, cf. [31].

Within a station, there are no possibilities for evasion when very high densities occur. A quick assessment of the passenger volume and the quick initiation of measures to

restrict the inflow are highly relevant to passenger safety. The proposed classification of only three levels for the assessment of the passenger volume is therefore considered reasonable and chosen for the assessment of the passenger volume within the station in case of a large-scale evacuation.

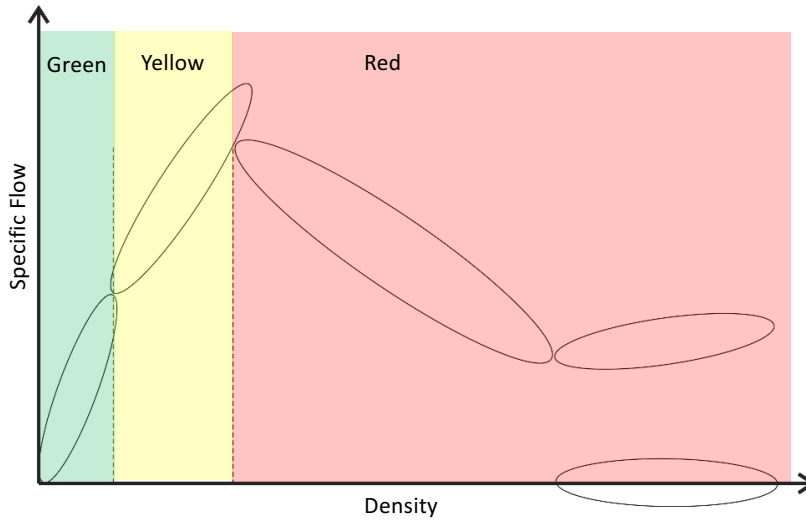


Figure 1.3.: Sketch of a fundamental diagram of the Level-of-Safety with traffic light colour coded classification, cf. [31].

1.2.5. Jülich Pedestrian Simulator

For the simulation studies, the Jülich Pedestrian Simulator (JuPedSim) is used. JuPedSim is a software tool for simulation and analysis of pedestrian dynamics, which is mainly maintained at the Research Center Jülich (FZJ). It is divided into four parts, *JPScore*, the simulation tool, *JPSeditor*, for creating geometries and configuration files, *JPSreport*, the evaluation tool for analysis of pedestrian trajectories, and *JPSvis* a visualisation tool for visual inspection of trajectories. The main reason to use this software was its open-source character, allowing further development and expansion of the software for the research purpose of crowd management at train stations in case of large-scale emergency events. Numerous requirements for the simulation tool JPScore were defined and implemented with the help of the developer team at Institute for Advanced Simulation - Civil Safety Research (IAS-7). In the following subsection, the main relevant new developments of JPScore, are presented in detail. The further subsections present the geometry structure and the models used for the simulation with JPScore as well as their limitations. Additionally, an overview about the software version and the usage of the other parts of JuPedSim is given.

1.2.5.1. New Features in JPScore

The most important new or further developed functions are, the possibility to define waiting people, which are called agents in JPScore, to assign different functions and properties to doors, to model train arriving and departures and to create new incoming passengers during the simulation in a very detailed way. These and other functions and models used in this work are presented in the following.

Waiting Areas and Door Functionalities

The most important functionality simulating the passenger flow in a train station is the modelling of waiting passengers. Therefore, two features were implemented, the waiting areas (WAs) [32], and the door status. WAs are closed polygons defined inside the building, which are used as an interim goal and offer two operating options: waiting and distribution. Figure 1.4 shows an example of the usage of WAs. In the configuration settings of the simulation with JPScore, agents must be assigned a defined goal, which can be an exit door or a WA as an interim goal. The agents' (blue dots) defined goal is the waiting area WA-1. This WA has a defined waiting time (wt) of 60s and targets WA-2 as the next goal with a probability of 100%. WA-2 has a wt of 30s and targets the next goals WA-3a to WA-3d with probability of 20% or 30%. At last, WA-3a to WA-3d target an exit, which is the nearest train door. In other words, to summarise the defined schedule, the agents walk from their starting points to WA-1, wait for 60s, walk to WA-2 and wait for another 30s before they are distributed to WA-3a, 3b, 3c, or 3d with probabilities of 20% or 30% and reach at last their final train door.

Another property of the WAs which has to be considered, is its capacity, i.e. the maximum number of agents fitting in one WA. If a WA has been defined with a maximum number of agents and the number of waiting agents is reached, the agents in the previous WA will remain waiting, even if the waiting time is over.

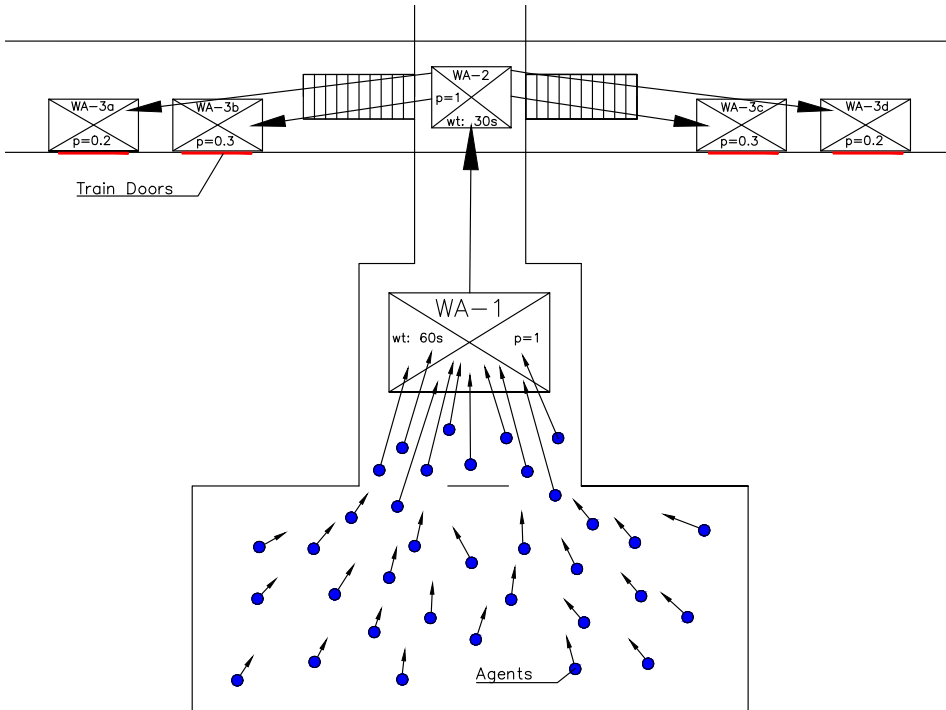


Figure 1.4.: Example of the functionalities of waiting areas (WAs). The first interim goal of the agents is WA-1, after the defined waiting time (wt) they are led to WA-2 and from there to WA-3a to WA-3d in front of the train doors by defined percentages (p).

The second feature to model waiting passengers was implemented by adoption of different door statuses. Doors have various properties. They can be assigned a flow rate and a maximum number of agents to pass through. Moreover, doors can also have three statuses, *open*, *closed* or *temporally closed*. Each status has a different effect on the walking strategy of agents. An open door can be passed as usual. A closed door will not open again and leads to re-routing of agents, whereas a temporally closed door can be open again and leads to waiting. Waiting therefore means, the agents walk to the door which is temporally closed and wait in front of it until it opens again, for example if a train has already been arrived, but the doors are still closed.

Figure 1.5 shows the doors' statuses and their control options. On the one hand, the doors' statuses can change during the simulation by different events, which are timed operations and have to be defined in the configuration file of the simulation. This can be used to open or close a door at defined times, for example, to regulate the inflow to the station building in dependency of the train arriving interval. On the other hand, changing the door statuses is triggered internally to consider the flow rate of a door and the maximum number of agents, which are fixed values, which have to be defined in the configuration file of the simulation. If a maximum number of agents is set for

a door, it will close automatically if this number is reached. This was implemented to model train doors, representing limited capacity. If a door flow has been defined, this flow is checked continuously, following a defined time interval. Does the actual flow exceed the defined door flow, the door status is set to temporally closed and will be set to open again once the flow matches the defined one.

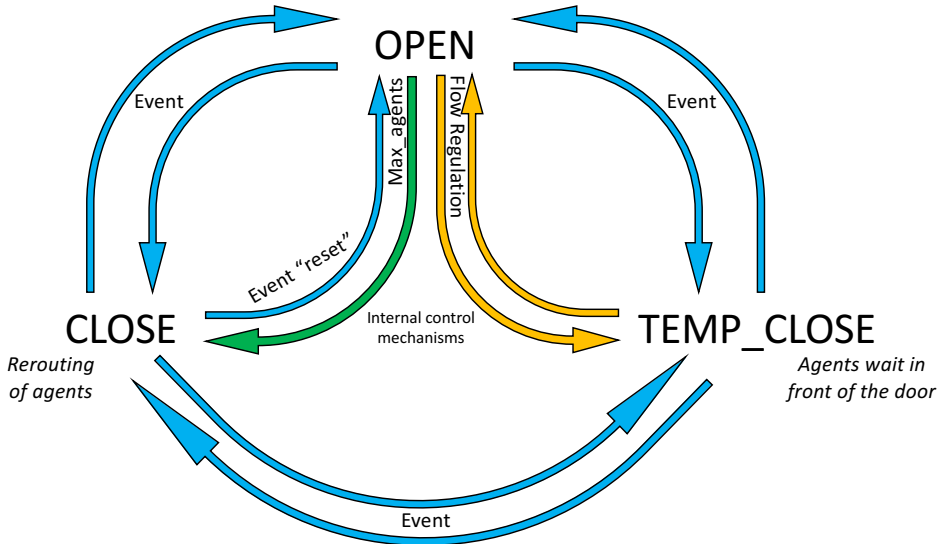


Figure 1.5.: Event-based door statuses in JPScore with internal and external control mechanisms and their influence on the walking strategy of the agents.

Another feature for setting door statuses, which is important to model train departures and arrivals at the same platform, is the possibility to reset the status of a door. If a train door was closed because the maximum number of agents or the departure time has been reached, the door can be reset, which represents the next train arrival. Then, the number of agents is set to zero and the door opens again.

As a train usually has several doors, another implementation for the train modelling was made, the time schedules. These are an extension of the single door events and correspond to events for multiple doors. Doors which belong to the same train and hence share some train-specific properties, e.g. the door flow rate, can be grouped. Afterwards, the door status for each group can be changed by a defined time schedule.

Sources

To simulate an evacuation in the given context, it is necessary to introduce new agents into the running simulation. This is realised via the *sources*. Originally, a source could be used to insert a defined number of agents with a defined time frequency. However, since, for example, arriving buses were also to be depicted, a refined design of the source-interface was necessary. By means of the following scenario, the new sources-design is depicted: 12 busses, each with a capacity of 50 passengers, are to

arrive at intervals of 5 minutes. The depiction of these arrivals was previously possible. In addition, the alighting process should be depicted: every two seconds, 5 passengers alight from the bus. For this purpose, the functionalities of percentage and rate were introduced. The respective input parameters are defined as follows. A bus with 50 agents ($N.create=50$) arrives every five minutes ($frequency=300$) until 12 busses have arrived ($agents.max=600$). And for each bus every 2 seconds ($rate=2$) 5 agents ($percentage=0.1$) alight from the bus. For more information, see the manual [33].

Trains

As mentioned above, trains are modelled as doors at the platform edges. Therefore, their position and properties like the flow rate are fixed values and the arriving and departure are considered by opening and closing these doors and resetting it for the next arrival. An adaption of their position or a change of the train type during the simulation is not possible. The studies in this work rely on this approach, to model the trains.

Nevertheless, one of the newest developments of JPScore is the train function, that enables the definition of different train types and a time schedule for their arriving and departure. Thereby, the train doors are not defined as part of the geometry, but separately in “train schedule” files. So, the doors only occur temporally during the dwell time of the specific train, which additionally enables the possibility to set the position of the trains, as also in reality trains do not stop at the same position every time. As the implementation of this function was only realised after most of this work had been completed, it was not used here.

1.2.5.2. Geometry Structure, Router and Operational Model

Geometry Structure

In the configuration file of the geometry, which is used for the simulation with JPScore, a special structure is needed. A one-level geometry consists at least of one *room* with one *subroom*. For multi-level geometries, each level has to be defined by at least one separated *room* with one *subroom*, whereas the connection between two levels, which is represented by a stair or an escalator, may only consist of a single *room* with a single *subroom*. This structure is especially important when looking at the router and the route-choice models.

Router and Operational Model

In all studies, the *Collision-free Speed Model* of Tordeux et al. [34] is used. The model prevents by definition overlapping of agents and can represent various self-organisation phenomena such as lane formation in bidirectional flows. Furthermore, the floor-field-router [35] is used, which calculates the shortest path between the doors within the same *subroom*. Here the geometry structure becomes important, as it affects the floor-field and therefore the routing of the agents. Chapter 2.1.1 will outline how the routing can be changed by sensibly defined *rooms*. All adjustments, such as the introduction of the WAs, were carried out for the floor-field router.

1.2.5.3. Model Limitations of JPScore

JuPedSim and especially JPScore have, as all software products, some model limitations. The most important ones, for this work, are as follows. As mentioned above, the floor-field router is used. The router, enables correct routing around corners in low density situations. The shortest path that leads around a corner is taken. However, with increasing density, congestion occurs in front of the corner, which is caused by the fact that all agents are routed around the corner following the shortest path. This happens regardless of how wide the geometry is behind the corner, compared to the width before the corner. For this reason, the geometry was partially adapted for the studies, which is described in detail in chapter 2.1.1.

Another difficulty arises when considering bidirectional flows. The phenomena that occur in such a case, like lane formation, are represented by the *Collision-free Speed Model* of Tordeux et al. [34], which is used for the simulation studies. However, the recently published work of Xu [36] shows, based on comparisons with experiments, that reality cannot be completely represented by this model. Therefore, Xu developed a model that represents reality fairly well. When the studies of this thesis were conducted, however, Xu's model was still in progress and had not yet been integrated into JPScore. The integrated *Collision-free Speed Model* can nevertheless be used, taking these findings into account. The results will be critically examined accordingly.

1.2.5.4. JPSeditor, JPSreport and JPSvis

Besides JPScore, the other parts of JuPedSim were also used for this work. The first geometries were created with JPSeditor. During the project KapaKrit, JPSeditor was further developed in order to be able to create configuration files. However, due to the complexity of variations for the simulation configurations, this function was not used in this work. The visualisation tool JPSvis was used to visually evaluate the results of the simulations. It is possible to create video clips or images of individual frames, in order to visually inspect the simulation results. This function was used especially in the first studies to assess critical bottlenecks. For the latter studies with several thousand simulation variants, a visual individual evaluation was no longer possible. For this reason, JPSreport was additionally used to evaluate the simulation data. This offers, among other, the possibility to calculate, pedestrian flows along defined evaluation lines or densities and speeds in defined evaluation areas, from the simulation data. A detailed description of the evaluation methods of JPSreport, which were used in this work, can be found in chapter 2.4.

1.2.5.5. Software Version

JuPedSim is a developing software, and many necessary adaptations have been made in JPScore to realize this work. Hence, several versions were used for the studies. The predominant part of the simulation studies for this thesis, which are described in chapter 2.3.2, were conducted with the same JPScore version of February 2020:

JuPedSim - JPScore version 0.8.4

Commit id v0.8.4-920-g705add1d [37].

The previous studies, described in chapter 2.3.1, have been conducted with previous

versions but have also been reproduced with the version of February 2020. An example of a configuration file of JPScore, showing the important modelling parameters, can be found in appendix A.

The evaluation methods of JPSreport, which were used for this work, did not change during the work time of this thesis. The version, which was predominately used, is:

JuPedSim - JPSreport version 0.8.4

Commit id v0.8.4-1026-g38c1884e.

1.3. Objectives and Approach

The existing concepts, known to the author, for the use of train stations in the case of large-scale emergency evacuations do not consider pedestrian dynamics within the stations. However, this plays a major role in the overall context, as it can be the limiting factor for the capacity of the whole railway system, especially in a direction-independent context. Therefore, the aim of this thesis is to investigate the pedestrian dynamics within train stations and to increase its capacity under the evacuation aspect by using special crowd management measures. For this purpose, a method is presented, which uses simulation studies to identify critical bottlenecks in a train station. Based on this, various crowd management measures are investigated with regard to their effectiveness in reducing the number of bottlenecks and thus increasing the capacity of a train station while at the same time preserving the safety of all passengers. The requirement of these measures is that they can be implemented with very little time, personnel and material effort. For this reason, mainly measures are considered which can be implemented with the existing facilities in a station, such as inflow regulation by opening or closing entrance doors or existing ticket control systems.

Since it is not possible, for organisational and cost reasons, to conduct an evacuation exercise for the corresponding scenario or field experiments on a similar scale at an existing train station, simulation studies are carried out. In this way, the interaction of all crowd management measures can be examined in detail. In addition, findings from field observations during events with particularly high passenger volumes at train stations are also used.

The knowledge gained from the simulation studies on crowd management measures at stations in the case of large-scale emergency events with increased passenger volumes can also be used for other application scenarios that occur spontaneously or do not allow the installation of material- and personnel-intensive measures for other reasons, such as overcrowding due to the *9-euro-ticket*. Furthermore, the detailed investigation of the interaction of different measures can also be used for the organisation of major events. Since comparable situations arise here before and after events, especially at the interfaces between the event site and the transport infrastructure due to the unidirectional flow of people, cf. project CroMa.

1.4. Thesis Outline

The thesis is further structured as follows. Chapter 2 *Methodology* is divided into three subchapters. First, the setups and the specific train types used for the investigations are described. In the next subchapter, the hand calculation is presented, which is used to check the plausibility of the simulation results. In the last subchapter, the simulation studies are presented. This includes the reference cases, which do not include any crowd management measures, the parameter studies, which examine the different crowd management measures and a transfer case to show the applicability to other non-station specific geometries. Chapter 3 *Evaluation* shows the results of the simulation studies presented in chapter 2. Chapter 4 gives a conclusion to the investigations, and chapter 5 gives an outlook on further investigation possibilities and needs.

2. Methodology

In this work, various studies were carried out to increase the capacity of train stations for the sudden occurrence of large crowds. For this purpose, both hand calculation methods and pedestrian simulations with JPScore were carried out. For both cases, entire station geometries and simplified models are considered. These are presented in the following first section 2.1, as well as an overview about the properties of three different train types. In the section 2.2 the hand calculation method is presented. And in section 2.3 the simulation studies with the corresponding parameter variations for the different crowd management measures are described. The last section 2.4 gives an additional overview of the analysis methods used to analyse the simulation data.

2.1. Setup

In the following subsection, different geometries, which are used for the hand calculation and the simulation studies, are presented. An overview is given as well as a detailed description. In particular, the differences and similarities between the geometries are highlighted. In a second subsection, three different train types and their relevant differences are shown, which is especially important for the simulation studies.

2.1.1. Geometries

This work was largely part of the research project KapaKrit. The subject of this project was the main train station in Dortmund. This is a station where trains go through, which is a common design for train stations in Germany. The general geometry is therefore based on this station design. The platform accesses are located under the tracks. A tunnel leads there from the entrance hall. Accordingly, the main entrance is at the entrance hall and a rear entrance is located at the other end of the tunnel. As mentioned above, both the entire station geometry and only individual sections are used for the investigations. Additionally, an abstraction of a train station geometry is used to analyse the influence of changing different geometry facilities. For modelling reasons, all setups are simplified and reduced to the basic components. This means on the one hand, that all walls and obstacles are straight. On the other hand, it means that variable facilities like rubbish bins or benches are not considered for most of the geometries.

Table 2.1 gives a brief overview of all setups used for the studies in this thesis. The differences are shown, as well as the setup numbers, which are used in the following. Setup 1 and 2 differ mainly in the usage of vestibuels and the platform lengths. Setup 3 only consists of different separated platforms and their accesses. Setup 4 is a full station, and is adapted to ensure a better corner routing. The last setup 5 represents any kind

of geometry and has variable components. A detailed description for each setup follows below.

Nr.	Preview	Usage	Geometry Specifications
1		First investigations - finding critical bottlenecks	Full station with one or two entrances
2		Further investigations - considering different train types	Full station with vestibules and different platform lengths
3		Investigation of different filling processes of the platforms	Separated consideration of platforms with different lengths
4		Final investigations - multivariate crowd management measures	Full station with optimised corner routing
5		Abstraction / idealisation	Idealised geometry with variations of stair widths and tunnel lengths

Table 2.1.: Train station setups overview

Setup 1 – Critical Bottlenecks

Setup 1 depicts an overall train station, figure 2.1. It can be separated in three sections, the entry hall, the tunnel and the platforms. The tunnel has two staircases for each of the five platforms. All platforms have the same length of 240 m. Figure 2.2 gives a more detailed view on important components. The entry hall is a rectangular with a dimension of 20 m × 20 m. The tunnel has a width of 10 m and a length of 110 m. The staircase width is 4 m and the length 10 m. The distance between the middle of the platforms is 20 m. As described in section 1.2.3 the station is empty, and the agents will directly be navigated to the platforms. Hence, ticket offices, shops and similarities, where people usually wait, are not modelled.

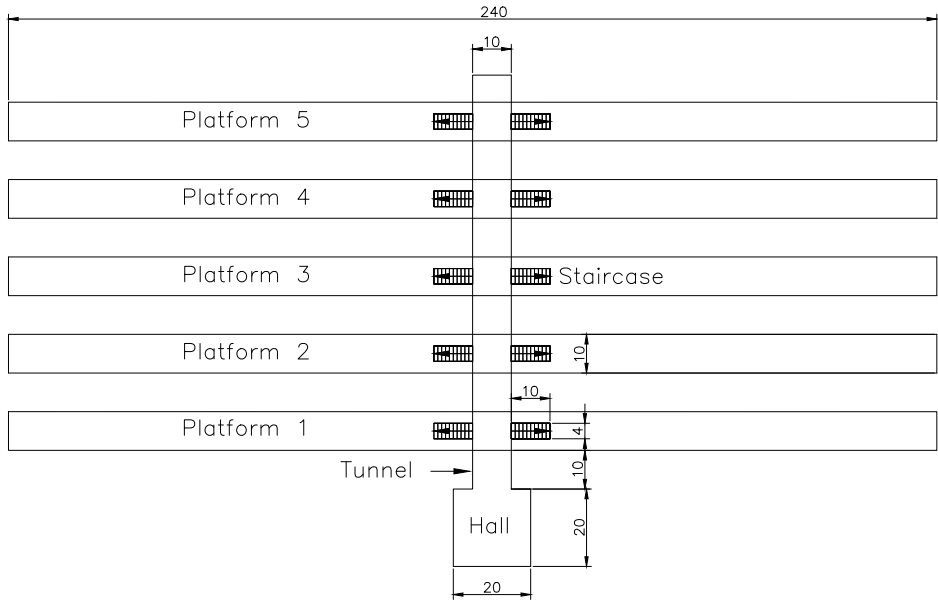


Figure 2.1.: Train station setup 1

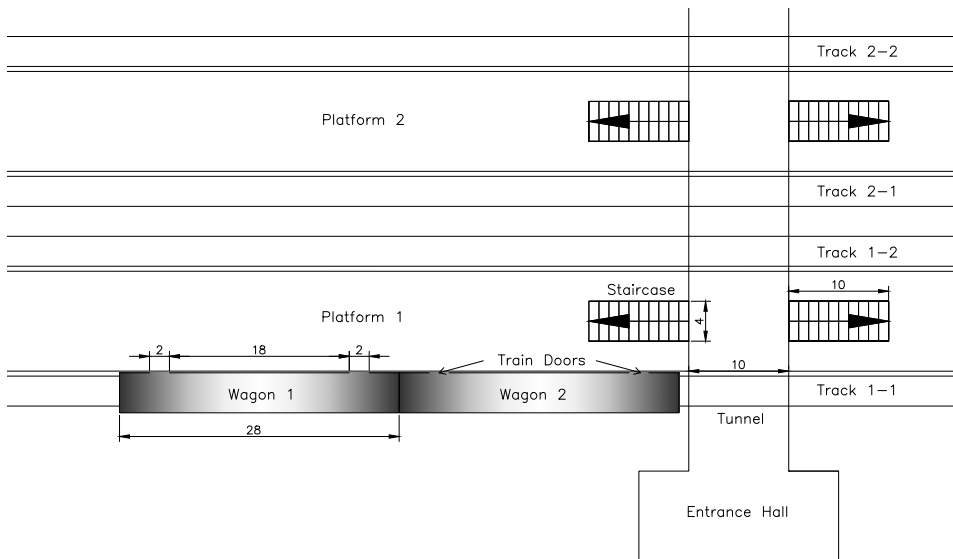


Figure 2.2.: Train station setup details

Setup 2 – Different Train Types

Setup 2 is an adaption of setup 1. The general dimensions do not differ. Nevertheless, this setup is used to analyse the influence of different train types. Long-distance trains

like the Intercity Express (ICE) are longer than the Regional Express (RE) or the City Train (SB). Accordingly, usually long-distance platforms are longer than platforms used exclusively by regional trains. Hence, the platforms in this setup have different lengths, see figure 2.3. For the simulations, an additional vestibule in front of the entrance is needed, to simulate the inflow through the entrance doors. This vestibule has a dimension of $50\text{m} \times 50\text{m}$. Four entrance doors, which are coloured in red in figure 2.3, connect the vestibule and the entrance hall. The two outer doors have a dimension of 2m and the inner have a width of 3m .

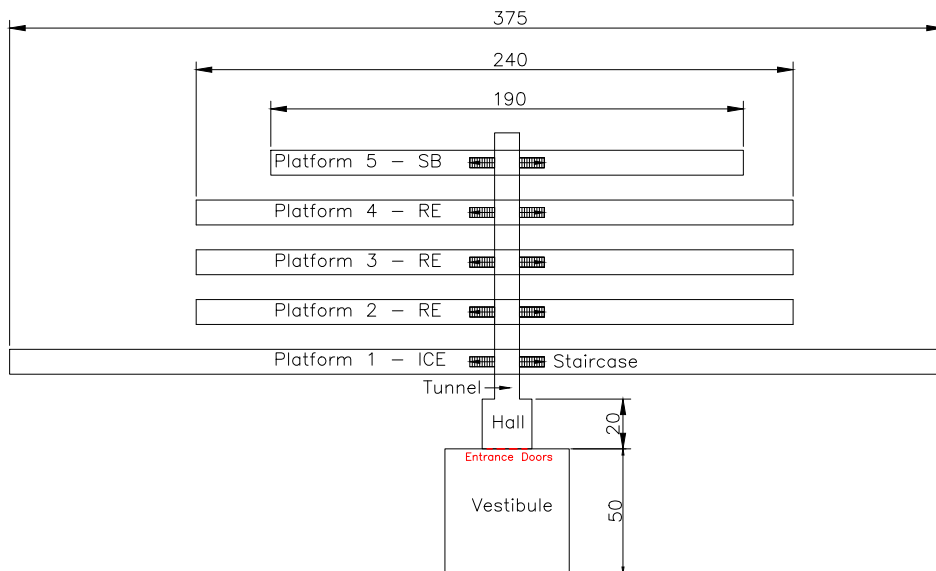


Figure 2.3.: Train station setup 2: Different platform lengths, a vestibule in front of the entrance hall and four entrance doors.

Setup 3 – Filling Processes

In chapter 1.2.5.3 the model limitations of the corner-routing, using the floor-field router, in JPScore were described. These were found in the first studies using setups 1 and 2, which will be outlined in section 2.3 and chapter 3. To investigate individual processes on the platform, without any influence of this limitation, the platforms for the different train types are considered separately. Thus, setup 3 is a reduction of setup 2. The dimensions are the same, but, in setup 3 the tunnel is cut at the above platform edges, see figure 2.4. The agents are therefore generated by source in the small tunnel section between the staircases.

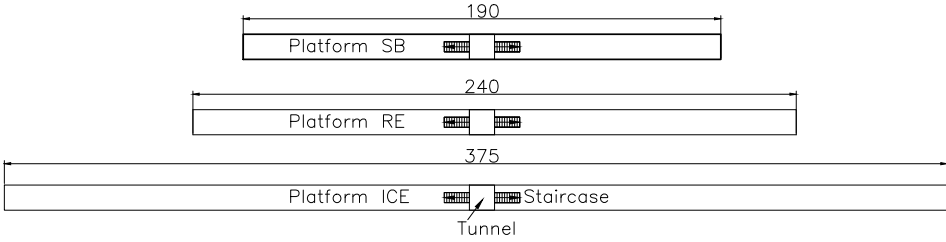


Figure 2.4.: Train station setup 3: Separated platforms with a small tunnel section between the staircases to generate agents by source.

Setup 4 – Optimised Corner Routing

Setup 4 describes an entire station again. Compared to setup 2, further standardisations have been made. All platforms have a length of 400 m, which corresponds to the length of an ICE platform, see figure 4. Additionally, the number of entrances has been increased to a total of six doors, which all have a width of 2 m. This was done to regulate the inflow by opening or closing individual doors. Besides this, the *room*-structure of the geometry model for the simulation with JPScore, which was described in section 1.2.5.2, was adapted to improve the corner routing for the floor-field router for high densities. The tunnel is separated into multiple *rooms*, one for each platform. Furthermore, in front of the staircases of the platform which should be filled, an additional *room* is added, which has two diagonally arranged transitions. Figure 2.6 shows the *room*-structure and the corresponding floor-fields with routing to the right staircase of platform 3 before (left) and after the adaption (right). In the original geometry, the agents are led from the tunnel entrance directly to the staircase. For the adapted geometry, it can be seen, that the overall routing is more precisely. Here, the agents are led to the transitions between the different tunnel sections first. At the

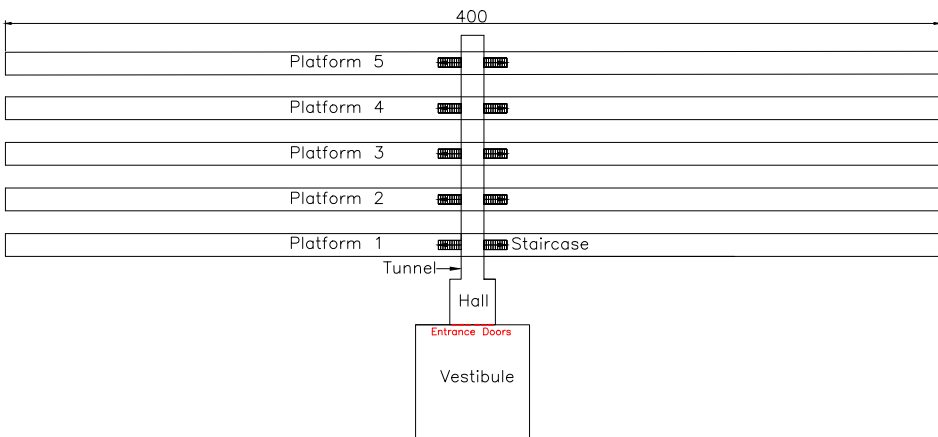


Figure 2.5.: Train station setup 4: Whole station with equal platforms and six entrances.

additional *room* in front of the staircases, due to the two diagonally arranged transitions, the floor-field ensures that a further arc is drawn around the corner. Figure 2.7 shows the visualisation of the corresponding trajectories for the same time step in the simulation before (left) and after the adaption (right) of the *room*-structure. Here, the improvement becomes clear once again. The available space in the corners is used more effectively, and the flow on the stairs is thus reduced to a lesser extent.

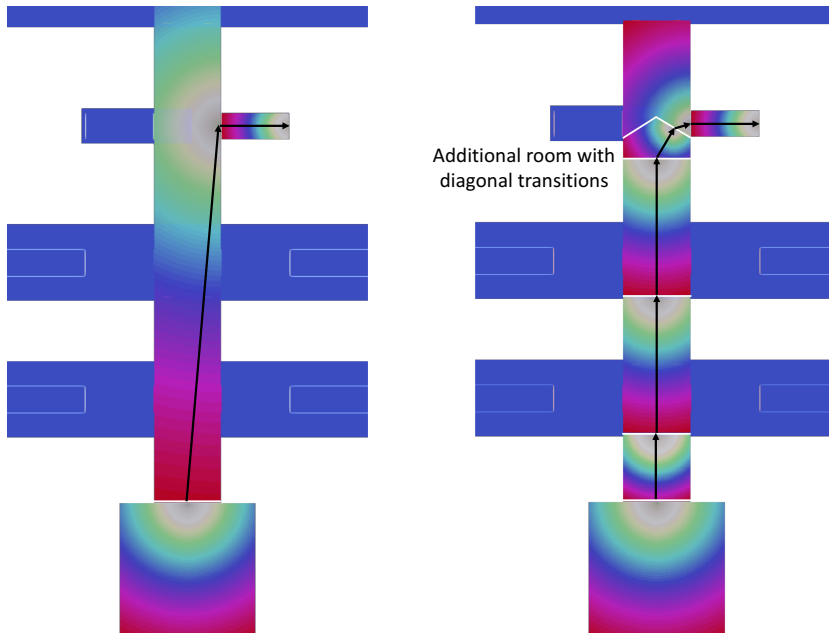


Figure 2.6.: Floor-fields with routing to the right staircase of platform 3 before (left) and after the adaption (right) of the *room*-structure. The colouring of the floor-fields represents the distance to the next transitions. Their values are set individual for each room to illustrate the differences between both cases.

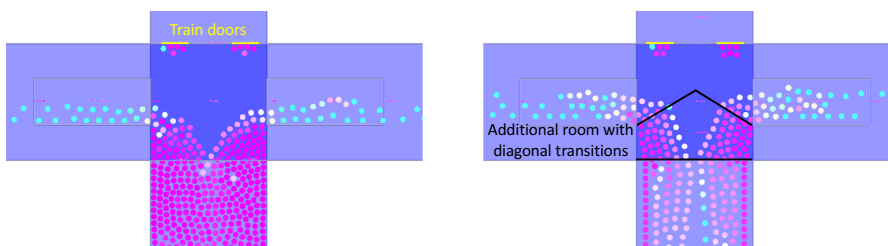


Figure 2.7.: Visualisation of the trajectories for the same time step in the simulation with a geometry before (left) and after the adaption (right) of the *room*-structure.

Setup 5 – Variable Geometry

The last setup to introduce is setup 5. It complies to two functionalities. On the one hand, it is a high simplification of a train station to avoid any kind of bottleneck, where passengers have to walk around a 90-degree corner. On the other hand, it can also be seen as an abstraction of a geometry, which can be used for any kind of crowd managed event. With regard to the train station geometry all elements, the vestibule, the entry hall, the tunnel, the stairs, and the platform were considered but renamed, see figure 2.8. Nevertheless, to improve the routing, the walls of the *Entrance Area* converge at an angle and the stairs and the *Event Access Area* are located at the end of the corridor in the walking direction of the agents. Additionally, following setup 4, six entrances, each with a width of 2 m are implemented to regulate the inflow to the building. To consider different walking distances from the entrances to the *Event Access Area*, the corridor length varies between 10 m and 90 m in 20 m steps. And, in order to represent different designs, the staircase width is varied between 4 m and 10 m in 2 m steps.

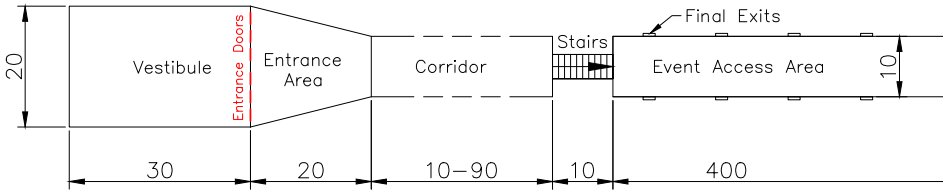


Figure 2.8.: Setup 5: Variable geometry, avoiding a routing around 90-degree corners.

2.1.2. Train Types

In Germany there are three train types, which are most commonly used in railway traffic, the ICE, the RE and the SB. They differ significantly from each other concerning door location and width, access height, number of seats and train car length. For the simulations, the trains are modelled as final exit doors at the platform edges. Nevertheless, to consider different entry times, resulting from differences of the access height and the inner train design, the doors can be defined with a specific outflow.

Figure 2.9 shows an example of train wagons for each of the three train types. The RE (top) corresponds to the DBpza 751 series. For the ICE (middle) the ICE-4 of the series 412 is chosen and the SB (bottom) is represented by the DB-series 423. Detailed information about wagon length, number and width of the train doors and the corresponding door flow can be found in table 2.2. In the case of the SB, it should be noted that the DB-series 423 consists of one train unit with four sections. The indicated length in table 2.2 corresponds to one section, which has three train doors, see figure 2.9. The dimensions of the trains come from [38], [39] and [40], and the door flow rates are chosen according to come from [27] and [28]. An ICE has only two small doors with a width of less than one metre at the edges of each wagon and stairs, which must be overcome. Accordingly, the door flow is quite low. The RE trains have also two doors with or without staircases. These doors are two or three times wider than

the ICE doors, so the door flow is also higher than in the ICE. As mentioned, the SB has three doors for each section and therefore the highest total opening width for a single passenger wagon, see table 2.2. The door flow is also the highest, because the doors are usually on ground level, which enables a faster boarding process than the usage of staircases.



Figure 2.9.: Examples of the different train types. Comparison between middle wagons of a RE (top) and a ICE (middle)⁹ and a whole SB (bottom)¹⁰.

Train type	ICE	RE	SB
Wagon length [m]	28.8	26.8	15.5
Doors per wagon	2	2	3
Door width [m]	0.9	1.9	1.3
Door flow [s ⁻¹]	0.45	0.95	1.1
Opening width [%]	6.25	14.18	25.16

Table 2.2.: Train specifications in relation to the train doors.

These specifications are used for studies with setups 2 and 3. For the final examinations using setups 4 and 5 a fictitious train was chosen with a door width of 120 cm. Furthermore, no outflow was defined, as the time difference, depending on the parameter composition, is negligible, and the time can be added via hand calculation in case of doubt.

⁸<https://www.maerklin.de/de/produkte/details/article/43568>

⁹<https://www.maerklin.de/de/produkte/details/article/43725>

¹⁰<https://www.roco.cc/de/product/39934-0-0-1000-0-1-0-403-0-002004-1/products.html>

2.2. Hand Calculation

The hand calculation is done to check the plausibility of the simulation data [41]. Therefore, the evacuation times are calculated in two ways. First, equation 2.1 [41] is used to calculate the time t_{evac1} , a single person needs to leave the geometry. Here, L_{max} is the maximum distance a passenger has to walk from the entrance to an exit, which is defined to be the train door, which is the furthest away, see figure 2.10. The value of v_{free} denotes the free walking speed of the passenger.

$$t_{evac1} = \frac{L_{max}}{v_{free}} [s] \quad (2.1)$$

For the second calculation, t_{evac} results from the flow J_s , with the transition width b and the number of passengers N , equation 2.2 [41].

$$t_{evac} = \frac{N}{J_s \cdot b} [s] \quad (2.2)$$

If multiple transitions or different flows have to be considered, for example by considering flat corridors and staircases, the calculation is done for the corresponding combinations and the highest values are chosen. This can be shown by the example of figure 2.10. The final exit is assumed to have a width of 2 m and the staircases of 4 m. The free walking speed is 1.2 m s^{-1} and 0.7 m s^{-1} at the staircases. For 1,000 agents t_{evac} at the final exit results in approximately 417 s and at the staircases t_{evac} results in 357 s. So 417 s would be chosen. But if considering a train with multiple doors as final exits their width have to be added up, which results in a lower value for t_{evac} , so the staircases would be the critical bottleneck for this calculation.

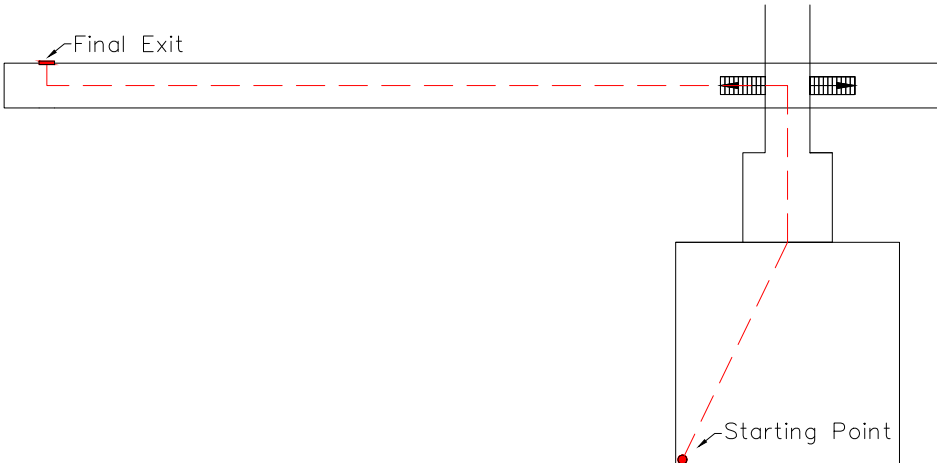


Figure 2.10.: Route choice to calculate the longest path for the hand calculation.

2.3. Simulation Studies

One of the highest goals of the large-scale evacuation planning is to ensure the safety of the evacuees by evacuating as many people as possible in the shortest time as possible. To ensure this, a wide range of factors must be taken into account. An important factor is the identification of critical bottlenecks. The bottleneck, with the highest threat for people using a train station at events with a huge amount of passengers, is to fall into the track when a platform gets overcrowded. Hence, it is assumed, that the evacuation train has already arrived, when the first passengers enter the platform. This assumption is comparable to the usage of PED and influences the waiting behaviour of the passengers as described in chapter 1.2.3.1.

Furthermore, every train station has individual bottlenecks, where a dangerous situation in case of crowding can arise. The simulation studies, presented here, are a practical tool to identify those bottlenecks and design appropriate operational and tactical crowd management measures.

2.3.1. Zero Cases

Zero cases are defined to be evacuation cases in which no operational or tactical crowd management measures are implemented. This means all entrances are used, and the passengers can unhindered pour into the station. In order to represent the unhindered passenger inflow in the simulation, sources, which continuously generate passengers, are defined in the front part of the entrance hall or in the vestibules. The only exception, which also applies here, is the assumption described in chapter 1.2.3, that the regular railway service has been discontinued. The station is accordingly empty and no disembarking passengers are to be expected.

In order to represent different entrance situations at train stations, a distinction is made between uni-directional zero cases and multi-directional zero cases in the following. In the multi-directional zero case, geometries are considered which have two or more not adjacent, opposite entrances. This can, independently of the assumption above, result in bi- or multi-directional passenger movements. Accordingly, an uni-directional zero case considers geometries, which have only one entrance, either because the geometry dictates this, or because all other doors were closed as a first measure. The aim of both variants is to find critical bottlenecks inside the station in order to derive appropriate crowd management measures.

2.3.2. Operational and Tactical Crowd Management Measures

This section gives an overview about the parameter studies, which were conducted to analyse different crowd management measures and various station designs. The aim of these studies is to decrease the evacuation time and ensure the safety of the passengers. They are structured as follows. First, different crowd management measures are introduced, structured in the order of their time operational capability. It starts with a study about measures to limit the inflow to the station regarding the train arriving interval. Further on, the platforms are considered separately to find an effective filling method. Another study considers the whole station and shows the interaction between

different measures for the inflow and the filling processes. Finally, the influence of different station designs, including all crowd management measures are shown.

2.3.2.1. Train Arriving Intervals and Waiting Areas

The first crowd management measure, which was considered, was to regulate the inflow to the different station sections depending on the train arrivals. This was also part of the authors' publication [42]. Nevertheless, some additional aspects are analysed, here. It is assumed, that one train at each of the five platforms will arrive at the same time. One train should carry about 640 passengers. So, 3,200 passengers enter the train station within a time interval mapping the interval of the train arrivals. The passengers are created by source in the first two meters of the entrance hall. The inflow is therefore set to twelve passengers per second, which corresponds to $1 \text{ s}^{-1} \text{ m}^{-1}$ at six doors with a width of 2 m. To regulate the inflow to the different section inside the station, waiting areas were set inside the entrance hall and inside the tunnel in front of the staircases. To model the waiting in front of the train doors, additional waiting areas are set in front of the doors. All waiting areas are shown in figure 2.11.

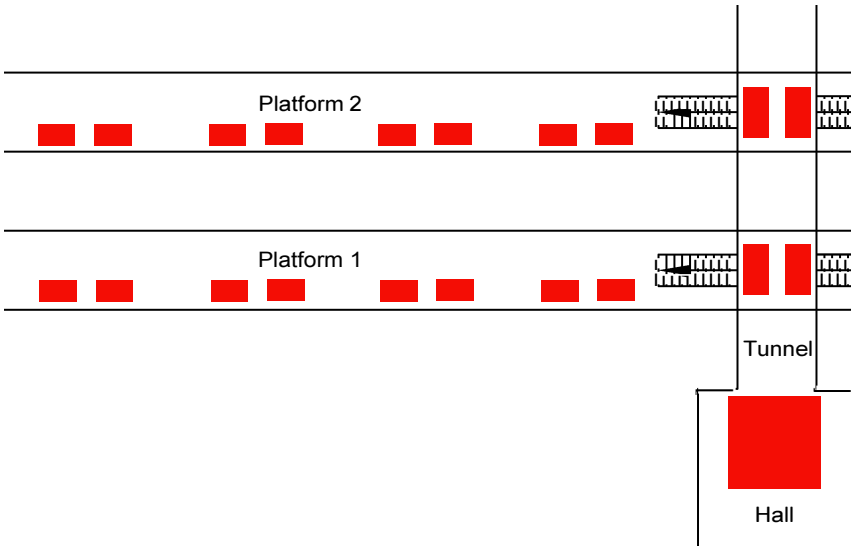


Figure 2.11.: Waiting areas inside the station

The waiting areas inside the tunnel are derived from crowd management measures, which were conducted by the federal police during a football game at the main station of Dortmund, see section 1.2.3. Three different variations of train arriving intervals and waiting times were investigated. These are shown in table 2.3. The waiting time in the hall is one minute for each variation of A to C. This ensures that stragglers can reach the platform before the next wave of passengers enters the station. In variation A and B the waiting time in the tunnel is another two minutes. This is an estimated time for the trains to depart and arrive again. The interval of arrivals is 5 minutes for variation A and 10 minutes for B and C. In variation C there is no waiting time in the

tunnel.

As mentioned in chapter 1.2.5.5, the studies in [42] were performed with an older JPSScore version. To ensure the comparability with further studies, which use JPSScore version 0.8.4-920, these studies were reproduced with this version, too. Therefore, some adaptations were made. As with JPSScore version 0.8.4-920 agents wait in front of temporally closed doors, the waiting areas are no longer used to set waiting times. This functionality is considered by setting closing and opening times of the transitions between the entrance hall and the tunnel, at the staircases and at the train doors. Nevertheless, the waiting areas inside the tunnel are used to distribute the passengers equally to the train doors.

Variation	wt_{hall} [s]	wt_{tunnel} [s]	Interval [min]
A	60	120	5
B	60	120	10
C	60	0	10

Table 2.3.: Variations of train arriving intervals and waiting times (wt).

2.3.2.2. Time Schedules

After assuming in section 2.3.2.1 the trains at each of the platforms will arrive and depart at the same time, here the platforms are considered separately. By separating the simulations in this way, the results can give an overview of the time, which is required to reach the different sections inside the station, depending on the distance of the platforms to the entrance. Setup 2 is used, which has vestibules and different platform lengths for three different train types. In the first studies, the passengers were created inside the entrance hall. So, the inflow process to the station was not considered. Now, the passengers start in the vestibule and enter the station by one of the four entrances. The number of passengers is therefore equivalent to the train capacity, which is listed in table 2.4. For the calculation of the capacity of an ICE, the middle car of the 13-car ICE-4 is taken as a basis, which has 88 seats [39]. This value is rounded up to 90 passengers per train car, which results in a capacity of 1170 passengers. Considering the total capacity of the train, which is only 918 seats due to lower-capacity cars [43], the assumption of 90 passengers per train car corresponds to an occupancy of about 120%. As discussions with the German railway operator indicate that a 200% seat occupancy rate is permissible, this is considered acceptable. The RE is accepted with 9 train cars. The DBpza 751 series has a capacity of 139 passengers per wagon [38]. This number is also slightly increased to 150 passengers per wagon, which results in an overall capacity of 1350 passengers. In case of the SB, it is assumed that three train units are strung together. A single unit has a capacity of 544 passengers, which already includes all standing and seating places [40]. With 12 doors, rounding down results in a value of 45 passengers per door. As most passengers might carry luggage or similar, this value is reduced to 40 passengers per door, which results in an overall capacity of 1440 passengers for three units. In addition to these capacity values, the overall train length, measured between the first and the last door, is also given in the table 2.4. Information about the door width and the outflow were given before, in table 2.2.

Train Type	Train Length [m]	Train Capacity	Door Capacity
ICE	372.9	1170	45
RE	236.2	1350	75
SB	195.2	1440	40

Table 2.4.: Additional train type specifications.

2.3.2.3. Filling Platforms

While the first crowd management measures are limited to timing the inflow, further measures are being investigated, which, on the one hand, further regulate the inflow and, on the other hand, take a closer look at the filling and outflow processes of the platforms. For each of the three variations of setup 3, which refer to the different train types, several variations in the inflow, the filling process, and the door status are considered, see table 2.5. All combinations of these variations result in a total of 81 different simulations.

Train Type	ICE	RE	SB
Inflow per Staircase [s^{-1}]	1	2	4
Filling Process	re-fro	fro-re	mixed
Door Status	open	close	open after 180 seconds

Table 2.5.: Parameter variations of different crowd management measures.

For the analysis, the platform can be separated into two areas, the left and the right one, divided by the staircases. A source between the staircases will produce the passengers by a defined flow. This is the inflow rate and set for each staircase to $1 s^{-1}$, $2 s^{-1}$, or $4 s^{-1}$. The filling process is the way the passengers are distributed over the platform, with or without special crowd management measures. Three different filling processes are taken into account, from the front to the rear train doors (*fro-re*), equal distribution (*mixed*) and from the rear to the front train doors (*re-fro*).

Figure 2.12 shows these processes and outlines the differences. On the upper platform, the *fro-re* process is illustrated. The first passengers (1) use the nearest train door (a) and the last passengers (3) the most distant one (c). As described in chapter 1.2.3.1, this scenario corresponds to the most realistic distribution without any regulations, compared to the daily passenger movements and waiting behaviour. Passengers tend to wait near the platform accesses and therefore choose the nearest doors and only walk to a rear door, in case the nearest doors are jammed. The process *re-fro*, on the lower platform, is the opposite of the *fro-re* process. The first passengers (1) will use the rear train doors (c), so the last passengers (3) entering the platform have the shortest way by using the nearest train doors (a). This corresponds to a maximum controlled distribution and has to be accompanied by security personal or the police. In the middle, the *mixed* process is shown. The equal distribution of this process means that for each source-dependant time step, one passenger per door enters the system. Accordingly, passengers (x, y, z) must reach the furthest door (c) the middle door (b) and the front door (a) in all time steps. For the filling times, this means that in an

undisturbed distribution in which the free walking speed is reached at all times, the *mixed* process takes a similar time as the *fro-re* process. The latter would only be a few time units longer due to the longer entry times, for accordingly not one but several passengers, corresponding to the door capacity. The *re-fro* process, on the other hand, would be faster by the walking time of the distance between the first and the last door, as long as this is greater than the boarding time of all passengers at one door.

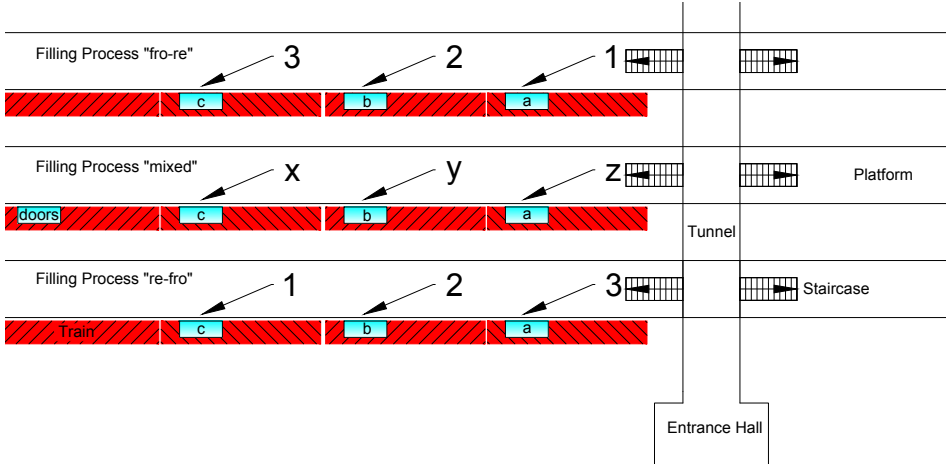


Figure 2.12.: Illustration of the filling processes *fro-re* (top), *mixed* (middle) and *re-fro* (bottom).

The door status is the status for the train doors, which is defined as the time the doors are kept closed, referring to the time when the first passenger enters the train station. A distinction is made between *open*, *close* and *open after 180 seconds*. When the status is *close*, the doors will open after 600 seconds. This corresponds to an average time, which is needed until the last passenger has entered the platform and reached its destination door. Here, the filling process is completely independent of the entry process to the train, stragglers excluded. For the status *open after 180 seconds*, the doors are closed for 180 seconds. It is expected that the filling process and the entry process will affect each other.

2.3.2.4. Multivariate Crowd Management Measures

In this section, the main studies of this thesis are presented. These are an extension of the studies from the last section, where the platforms were considered separately. Here, the entire station is taken into account by using setup 4. Furthermore, the crowd management measures used are extended. So, a multivariate analysis becomes possible. The aim is to compare the sensitive interactions of the different measures.

Table 2.6 gives an overview of the parameters, inflow, filling process and door status, which are used. As all measures should be usable without any kind of external items, the inflow rate corresponds to the number of entrance doors which can be opened. The door status is the time until the train doors will open after the first passenger has entered the platform. The filling process is an interaction of the processes *re-fro* or *fro-re*

and the process *mixed* from the previous studies. This is done to model the degree of implementation of the processes. If for example the process *re-fro* is aspired, some passengers might not follow the order and distribute wherever they want. These passengers are represented by the different proportion of the *mixed* process. The percentage values therefore show how many passengers follow the ordered process. Negative values represent gradations of *re-fro* and positive values of *fro-re*. The *mixed* values give the percentage of how many passengers do not follow the order and distribute equally.

Inflow rate [s^{-1}]:	2	4	6	8	10	12						
Door status [min]:	1	2	3	4	5	6	7	8	9	10		
Filling process:	-100	-80	-60	-40	-20	0	20	40	60	80	100	
ordered [%]:	-1.0	-0.8	-0.6	-0.4	-0.2	0	0.2	0.4	0.6	0.8	1.0	
mixed [%]:	0	0.2	0.4	0.6	0.8	1.0	0.8	0.6	0.4	0.2	0	

Table 2.6.: Parameter variations of the multivariate crowd management measures, considering inflow rates, door statuses and filling processes.

2.3.3. Variable Geometries

The last studies, which are presented, serve to demonstrate the applicability of the crowd management measures, which were shown in section 2.3.2.4, to variable geometries. As described in section 2.1 setup 5 is used for this purpose, which represents an idealisation of a train station on the one hand and the applicability to other geometries on the other hand. Hence, next to the crowd management measures, which were outlined in table 2.6, this studies also consider changes in the geometry, like different staircase width and the placing of obstacles.

For the comparison with and without obstacles, not all presented combinations of measures are used. In order to be able to make a statement about the positive or negative influence, random comparisons are sufficient. In order to nevertheless obtain a result that is as meaningful as possible, the cases were carefully selected. The two low inflow rates of $2s^{-1}$ and $4s^{-1}$ are chosen because the greatest changes are to be expected there. In addition, a higher inflow rate of $8s^{-1}$ is also considered. For the filling process the cases “ ± 100 ”, “ ± 60 ” and “0” are chosen. In this way, the two extreme processes *fro-re* and *re-fro*, but also a combination of the processes are mapped. It is the same with the door opening times, here the cases 2 min, 6 min and 10 min are considered. All together, when considering double-sided filling, these are still 540 variations, since additionally the width of the stairs is varied between 4 m and 8 m and the length of the tunnels between 10 m, 50 m and 90 m.

2.4. Evaluation Theory

The trajectory data from the simulations are evaluated in different ways. Especially for the first studies, the trajectories are visually evaluated by using JPSvis. In this way, by the local detection of congestion, initial conclusions can be drawn about critical bottlenecks in the system, from which further investigations can be derived. These critical areas can then be examined more closely in a further step, which is the analysis of the trajectory data with methods A and C of JPSreport. The differences of the methods are shown in figure 2.13.

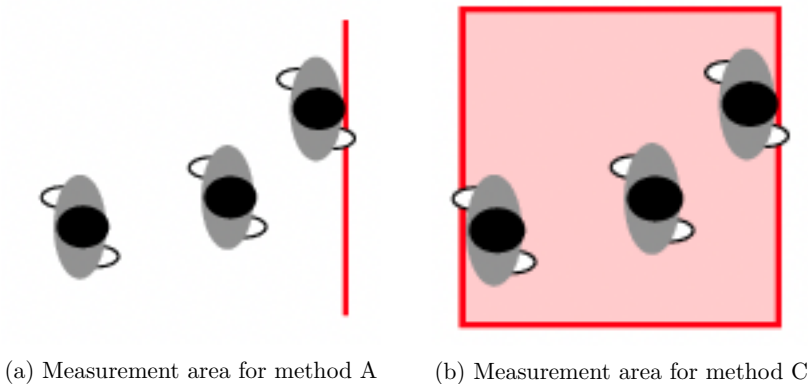


Figure 2.13.: Analysis methods A and C of JPSreport [33].

In method A, the data is evaluated at defined measurement areas. This enables the analysis of the $N(\Delta t)$ data, which contains information for each time step about the cumulative number of people who passed a measurement area. From this data also, the flow of people at the measurement area can be calculated. The measurement areas are for example defined at the entrances, at the crossings of the individual areas of the station and at the train doors. In this way, statements can be made about how long it takes individuals, a certain proportion, or all people to pass a certain area. These are important values, especially for the creation of time schedules. A more detailed overview about the location of the measurement area are given below.

In method C, on the other hand, the trajectory data is evaluated in defined measurement areas. In this way, it is possible to calculate the time-dependent density, which is defined as the number of persons (N) per measurement area (A), equation 2.3.

$$\rho(A) = \frac{N}{A} \quad [m^{-2}] \quad (2.3)$$

The placement of these measurement areas for this purpose is done taking into account the critical bottlenecks defined in the visual evaluation, which are, for example, at the tunnel entrance and in front of and behind the staircases. A detailed overview about the location of the measurement area is also given below. The resulting densities allow statements about safety. The criteria for assessing safety and comfort are provided by the Level-of-Service [29] and the Level-of-Safety [31]. For the context of emergency

events with extraordinary high passenger volumes, the limit values for the occurring congestion is set to the maximum of 1.5 m^{-2} to 2 m^{-2} .

Overview of measurement areas and areas

As the setups presented in section 2.1.1 differ from each other, also the location of the measurement areas and lines differ. Nevertheless, figure 2.14 shows the approximate position of both. A detailed overview will be given in the according sections of chapter 3 *Evaluation and Result*. For each setup there are measurement lines (red) immediately behind the entrance, at the transitions between the different station sections and in front of the train doors to measure the outflow. Additionally, for the studies considering the filling processes of the platforms, further measurement lines (green), which are located across the platforms are used to measure the distribution of the passengers along the platform.

The measurement areas to analyse the density, which are coloured in blue, are in front of the transition between the entrance hall and the tunnel, at the platforms behind of every staircase and in the tunnel in front of each platform. These positions are chosen to measure the density at the critical bottlenecks on the one hand, and on the other hand to investigate the influence of the platform location in relation to the entrance.

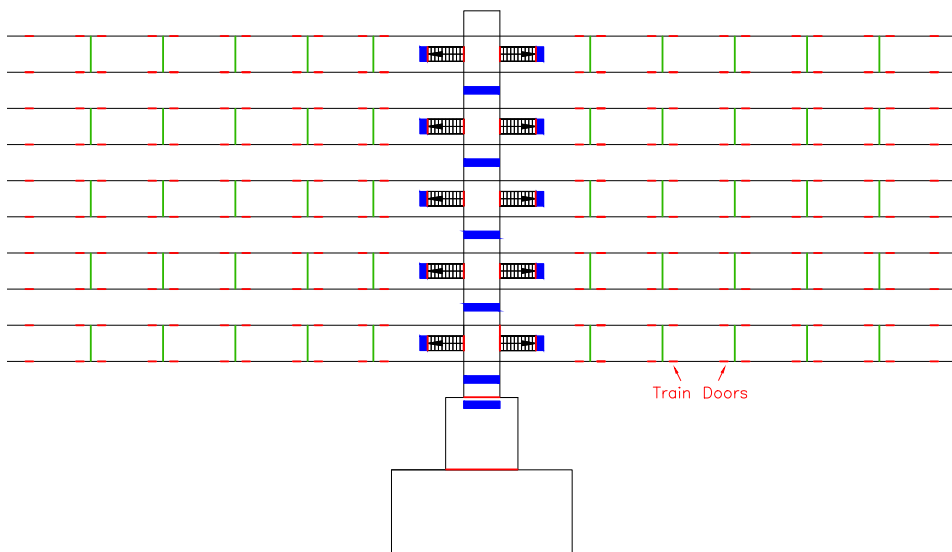


Figure 2.14.: Overview of measurement areas (blue), and general- (red) and additional measurement lines (green) for the evaluation of the trajectory data of the simulation.

3. Evaluation and Result

The aim of this work includes a methodology that uses simulation studies to investigate the increase in capacity of train stations with particularly high passenger volumes. For this purpose, in the first step, studies were carried out that do not take into account any crowd management measures. These are the zero cases and can be divided into uni- and multi-directional cases, which are determined by the use of side-by-side or opposite located entrances. The result of these studies is the identification of critical bottlenecks inside the station and are presented in the first section 3.1. This is followed by a parameter study in section 3.2 which examines the use of various crowd management measures. First, individual measures are implemented. Subsequently, a multivariate analysis of different measures is carried out to investigate their interaction. The last section 3.3 examines the applicability of the crowd management measures studied to variable geometries and the influence of obstacles.

The hand calculation, which was introduced in chapter 2.2, is used especially in the parameter studies. On the one hand, it is used to check the plausibility of the results. On the other hand, it serves to explain certain phenomena, such as the influence of the walking paths. Since the setups of the individual studies differ from each other and the calculation therefore does not provide generally valid results, the results of the manual calculation are presented in the corresponding sections of the simulation studies.

3.1. Zero Cases

The first simulation studies, which were carried out, were the zero cases. For these purpose, setup 1 was used, and no crowd management measures were considered, which means passengers can walk into the station without any regulations and chose any platform and train. Thereby, a distinction is made between multi- and uni-directional zero cases. The first one considers geometries with at least two opposite directed entrances, whereas the second one uses only one entrance. The results will show critical bottlenecks inside the station and will help to develop appropriate measures to handle huge crowds in emergency events. Therefore, different measurement areas and measurement lines are used to evaluate the densities and passenger flows. These are shown in figure 3.1. The IDs are used in the following to refer to the corresponding areas or lines.

3.1.1. Multi-directional Zero Case

The very first simulation study, which was carried out, was the multi-directional zero case. Therefore, beside the main entrance of setup 1, a second entrance at the end of the tunnel is considered. So, passengers flow into the station from two opposite directions. Both passenger groups want to reach one of the five platforms, which leads

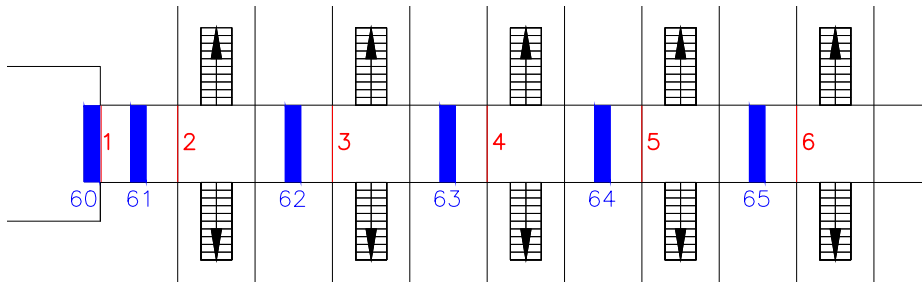


Figure 3.1.: Location of measurement areas (blue) and measurement lines (red) in setup 1, rotated view.

to a bidirectional flow inside the tunnel.

Figure 3.2 shows the density in the measurement areas with ID 60 at the entrance and IDs 61 to 65 inside the tunnel. Figure 3.3 shows the corresponding specific flow in this area at the measurement lines with IDs 1 to 6. As at the beginning of the simulation, the geometry is completely empty, the filling process is also displayed. In the first two minutes, the passengers steam into the station without major disruptions. During this time, the density and the specific flow rise. When the density inside the entrance hall reaches more than 1.5 m^{-2} (figure 3.2) the specific flow at the measurement line with ID 1 reaches a peak, which is an indicator that the critical density has almost been reached, and free walking is no longer possible, see figure 3.3. Only little later, the specific flow falls down. At this point, the density has reached almost 2 m^{-2} , see figure 3.2. The walking speed slows down and congestion occurs. In the exemplary fundamental diagram (figure 1.3) of the Level-of-Safety [31] this is described as a turning point. After this point, the densities in the simulation rise even higher, which would cause uncomfortable and even dangerous situations for all passengers.

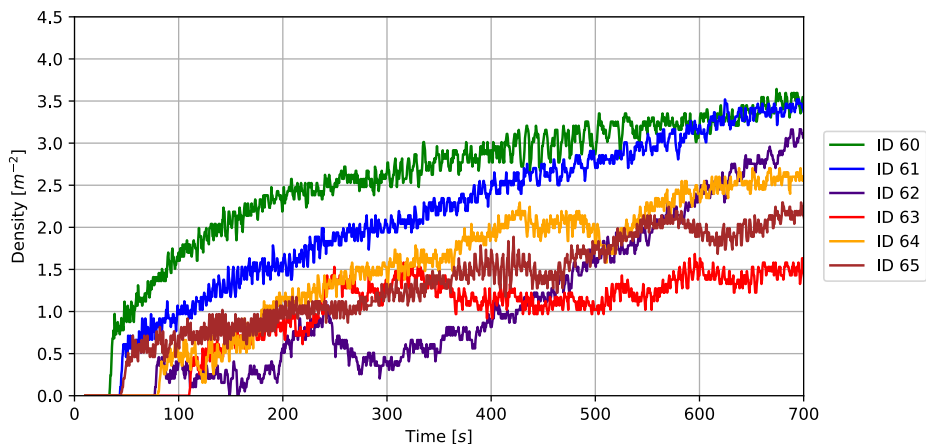


Figure 3.2.: Densities of the multi-directional zero case.

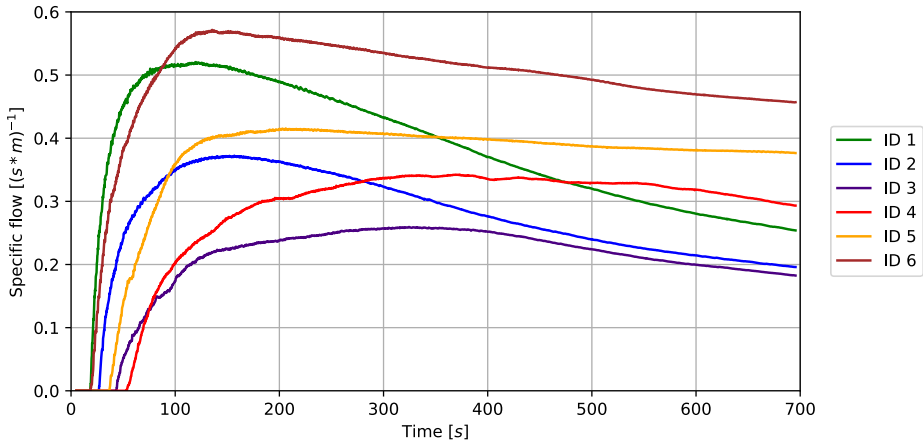


Figure 3.3.: Flow of the multi-directional zero case.

Another interesting aspect is the differences between the single measurement lines. The flow at the measurement line with ID 6 is a bit higher than at ID 1. This stems from the fact that passengers, using the back entrance, do not hit a bottleneck before entering the staircases. Passengers, who use the front entrance, have to pass the cross-sectional constriction between the entrance hall and the tunnel. This constitutes a bottleneck and reduces the flow. Additionally, it can be observed that the flow at the measurement lines further inside the tunnel are smaller than at the first measurement lines. The reason for this is that passengers are hindered by those, who enter the first platforms and also by oncoming passengers from the other entrance, who want to reach a rear platform. So, fewer passengers can reach the next measurement line in the same time.

Looking at the densities in figure 3.2, another aspect can be seen. The densities of the measurement areas in the entrance hall and the first tunnel section have a rather smooth curve, whereas the densities of the other areas show some larger fluctuations. As described above, the oncoming passengers and those, who enter the staircases to the first platforms, hinder the subsequent passengers to pass through. Hence, there is no constant inflow to the measurement areas and the densities have no constant level. If taking a very close look into the flow curves of ID 3, ID 4, and ID 5 in figure 3.3 these fluctuations can also be seen there.

As it is not clear if the high densities are caused by the unimpeded inflow to the station or if it is an effect of the bidirectional flow inside the tunnel section, both influences will be investigated in the following sections. First, the results of the unidirectional zero case show the influence of avoiding a bidirectional flow inside the station. Afterwards, in the parameter studies also different inflow regulations will be investigated.

3.1.2. Uni-directional Zero Cases

Multiple opposite entrances cause bidirectional flows from oncoming passengers inside the tunnel section. To avoid this, a first crowd management measure was to close one of the entrances, which also corresponds to a station having only one entrance. Figure 3.4 shows the density and figure 3.5 the specific flow for this case. There are similarities but also significant differences to the bidirectional case. The initial conditions are the same. The station is empty and the passengers steam into the station without any regulations. Hence, the densities and the flow also rise during the first two minutes. And also here, the flow reaches a peak when the density in the entrance hall reaches around 1.5 m^{-2} . With a density of almost 2 m^{-2} the flow falls off again.

What, in turn is particularly striking, is that the densities in the first two measurement areas with IDs 60 and 61 reach a very high level whereas the densities in the rear

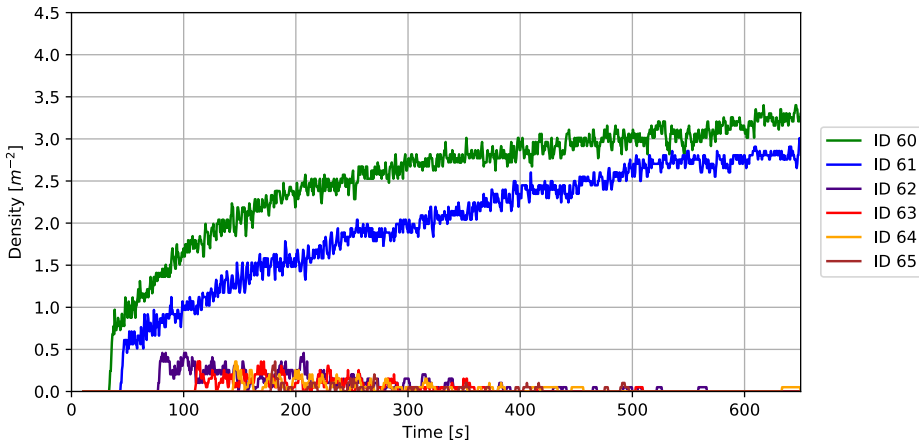


Figure 3.4.: Density of the zero case with an unidirectional inflow.

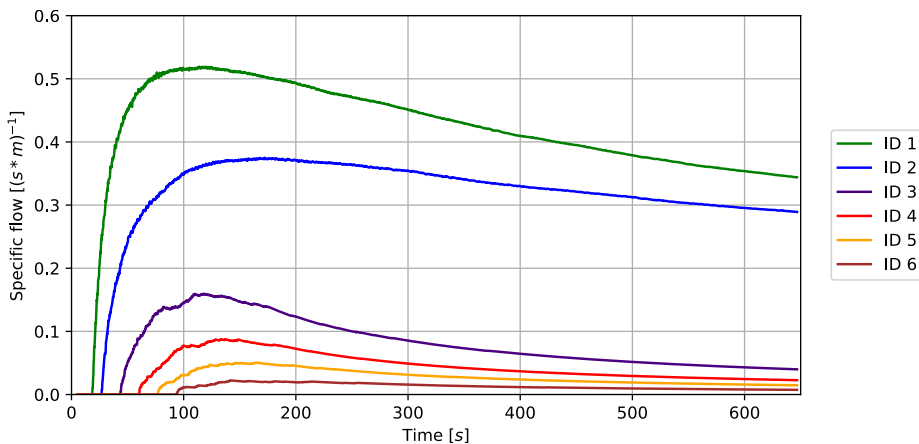


Figure 3.5.: Flow of the zero case with an unidirectional inflow.

measurement areas do not exceed 0.5 m^{-2} and drop almost to zero. The same can be observed for the flows at the rear measurement lines. Looking to the bidirectional case, the subsequent passengers are hindered by those, who enter the first platform accesses and also by oncoming passengers. However, in the uni-directional case, there are no passengers coming from the other entrance. Therefore, this effect is limited to the front areas. As the results show, the passengers, who enter the first platforms, hinder other passengers to reach the rear platforms. As this effect was also observed for the bidirectional case, and did not dissolve with closing one entrance, the next measure is to restrict the inflow to the station. This and further measures will be investigated in the next section.

3.2. Parameter Studies

The results of the zero cases showed that there is a great demand on regulation to handle huge crowds. The following sections therefore deal with different crowd management measures. First, a train arriving interval and waiting areas are set. Based on this, a time schedule is worked out and the filling processes of the platforms is taken into account. At the end, a multivariate analysis of different measures is conducted, and the findings are transferred to a variable geometry.

3.2.1. Train Arriving Intervals and Waiting Areas

The results of the uni-directional zero case, used only one entrance and showed that there is still dangerous crowding inside the station. For this reason, in the next studies, the inflow was restricted and waiting areas were arranged inside the station. Both are defined by the train arriving interval. The detailed variations A to C were shown in table 2.3 and figure 2.11 showed the locations of the waiting areas. As setup 1 is used, the measurement areas and measurement lines shown in figure 3.1 are still valid, so their designation will be used when describing the results in the following sections.

3.2.1.1. Multiple Waiting Areas and a Five-Minute Time Schedule

In this section, the results of variation A, a five-minute train arriving interval and waiting areas inside the hall and the tunnel are shown. As described in chapter 2.3.2.1 one train at each of the five platforms will arrive every five minutes. So, every five minutes a corresponding number of passengers flows into the station. Then the passengers wait for one minute inside the entrance hall and for another two minutes inside the tunnel in front of the staircases.

Figure 3.6 shows the mean values and the standard deviation of the densities for the measurement areas inside the entrance hall (ID 60) and inside the tunnel (IDs 61 to 65), cf. figure 3.1. The first thing which stands out is that the density continues to

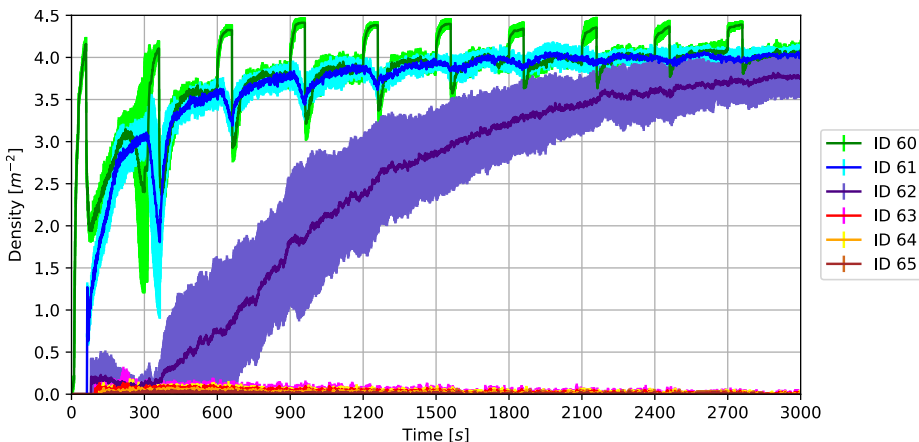


Figure 3.6.: Densities of variation A with mean values and standard deviation.

increase with each train arriving interval until it reaches a maximum. If looking into detail, the processes like opening and closing the WAs can be seen. The simulation starts with closed WAs. Hence, the densities inside the measurement area with ID 60 rises. When it falls off rapidly after 60 s the barrier of the WA in the entrance hall was opened. Nevertheless, the WAs in front of the staircases are still closed. When looking at the densities of ID 61, the curves rise steeply and then flatten out. The bend between these courses, show that the WAs in front of the staircases have been opened. Every 300 s new passengers flow into the station. At this point, the WA in the entrance hall is closed, to give the passenger inside the tunnel some time to reach the platforms. Hence, the density inside the measurement area with ID 61 drops and rises for ID 60. When the WA inside the entrance hall opens again, the WAs in front of the platforms close again to let passengers reach the train. At this point all passengers should have reached the platform, which, however, is not the case. So, the densities increase with the next interval.

Another thing that attracts attention are the low densities in the rear measurement areas. At the end of the first interval, when the WA inside the entrance hall is closed again, only rising densities in the tunnel section of the first platforms can be observed. Passengers, who want to reach one of the rear platforms, are hindered by those who want to reach the first platform, but need to wait in front of the staircases. Hence, only a few passengers can go through. But when the density in front of the first staircases drops, because the WA in the entrance hall was closed after 300 s, more passengers can reach the next platform. But here it is the same. Passengers, who want to reach a further platform, are blocked again by waiting passengers. These two blockages result in a very few passengers who reach one of the rear platforms.

Figure 3.7 shows the corresponding flow. At measurement line with ID 1, which is located directly behind the tunnel entrance, the intervals with new arriving passengers can also be seen. It can further be seen that the overall flow continues to decrease with each interval of newly arriving passengers. This is equivalent to the density increasing. The reason for these observations is that large congestion builds up in the area of the

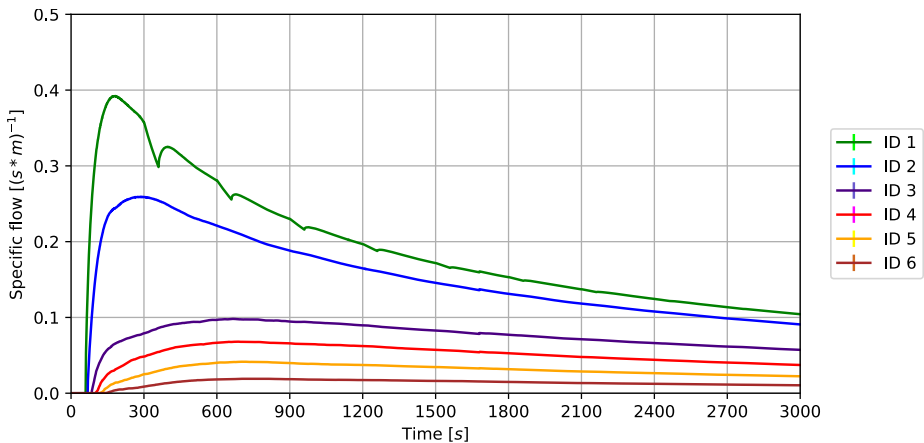


Figure 3.7.: Specific flow of variation A.

first platform staircases all the way back to the entrance hall. These do not dissipate before the next passengers enter the station. Accordingly, the backlogs are getting bigger and bigger, which can lead to fatal situations. There are two possible reasons for this, firstly, the interval is too short and secondly, the waiting times in the individual areas are too long. Both opportunities will be examined in the following, starting with a larger interval.

3.2.1.2. Multiple Waiting Areas and a Ten-Minute Time Schedule

In this section, the results of variation B (cf. table 2.3) are shown, which considers an adapted time interval from five to ten minutes. The waiting times inside the single waiting areas are the same as for variation A, one minute in the entrance hall and two minutes in front of the staircases. This in turn means passengers have more time in between to reach the next sections before the barriers close again and the waiting times begin. Both processes can be seen in the peaks and valleys and the steep and flat rising densities in the first two measurement areas (ID 60 and 61) in figure 3.8. Nevertheless, it can also be observed that the densities in the front areas rise to a very high level during the first interval and do not decrease again, whereas the densities in the rear tunnel areas are almost zero. The densities in front of the second platform staircases rises even faster as before.

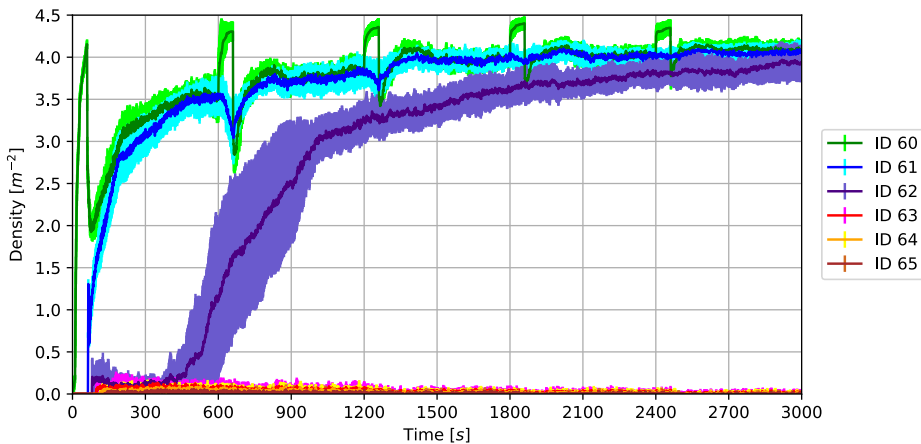


Figure 3.8.: Densities of variation B with mean values and standard deviation.

The flow curves in figure 3.9 show the same effect. Here the flow rises to a peak and falls off afterwards, for the measurement lines in the front area, whereas the flows of the rear areas stick on a very low level all the time. The reason for this is again that a huge congestion builds up in front of the first platforms, which causes a tailback into the entrance hall and hinders passengers to reach the rear platforms. At the end, the results are not much better than for the five-minute interval. This suggests that the interval is still too short or the waiting times for the next incoming passengers have to be adapted so that the actual passengers can reach their final goals. As the interval was already adapted, in the next step, the waiting times are adapted by setting those

inside the tunnel to zero. So, the passengers only wait in the entrance hall, which should avoid congestion in front of the staircases. The results of these are shown in the next section.

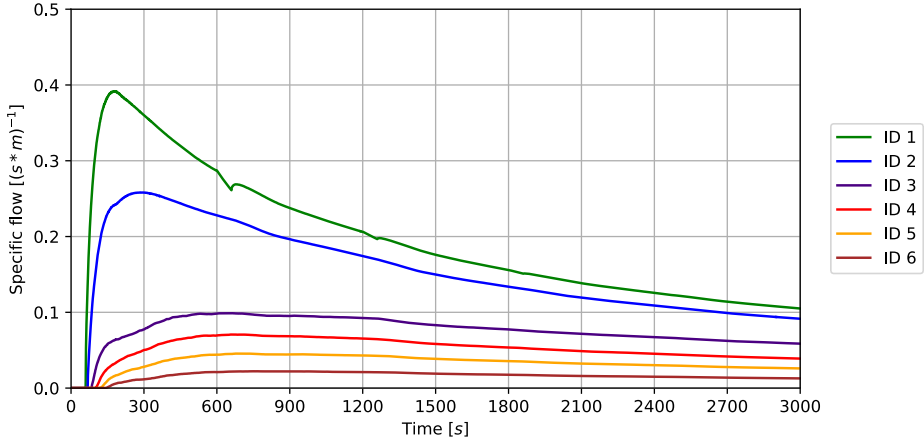


Figure 3.9.: Specific flow of variation B.

3.2.1.3. Single Waiting Area and a Ten-Minute Time Schedule

In this section, the results of the adapted waiting times of variation C are shown, cf. table 2.3. The interval of ten minutes is still valid, as well as the waiting time inside the entrance hall of one minute. The waiting areas inside the tunnel have been removed, as waiting passengers in variation B caused huge congestion with a tailback into the entrance hall, which blocked other passengers to reach the rear platform.

Figure 3.10 shows the densities of the six measurement areas. The peak in the measurement area with ID 60 at the beginning of each interval is caused by the closed WA. When it opens, the densities fall off and rise in the other areas. It is immediately noticeable that the course of all densities differ very much from the results of the previous studies. The densities in the entrance hall and in the tunnel in front of the first platform (ID 61) are still the highest, but do, except an initial peak, not reach a high-risk level. For the other measuring areas applies, the further away they are from the entrance, the lower are the densities. The reason for this is that fewer passengers have to pass through the individual areas. Another thing that attracts attention, is that all densities reach zero, before the next interval begins. Additionally, the flow curves in figure 3.11 drop down before ten minutes are over. Both are indicators that all passengers have reached their destination platform before new passengers enter the station. So, the next interval starts with an empty station again. Nevertheless, the waiting time inside the hall is necessary to ensure the departure and arriving of the trains before new passengers reach the platforms.

From this first view, this study shows good results. However, the densities in the entrance hall and in the tunnel sections of the first platforms have still a constant high level. As there is no way to swerve inside the station, especially inside the tunnel, this

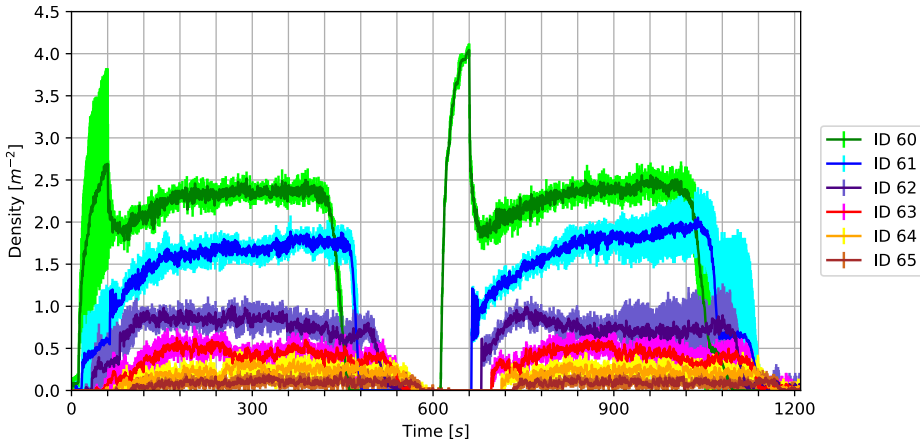


Figure 3.10.: Densities of variation C with mean values and standard deviation.

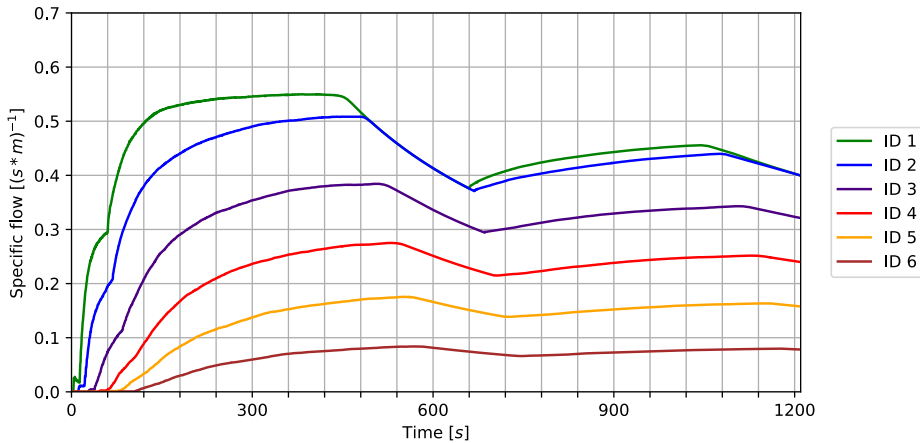


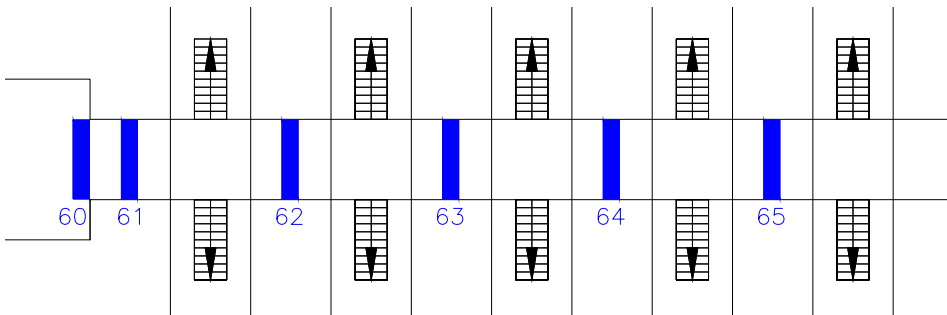
Figure 3.11.: Specific flow of variation C.

can lead to dangerous and fatal situations, e.g. if passengers start pushing. Densities should therefore not exceed 1.5 m^{-2} for a constant level or 2 m^{-2} for short peaks. Hence, further crowd management measure are taken into account to decrease the densities. These are shown in the following sections.

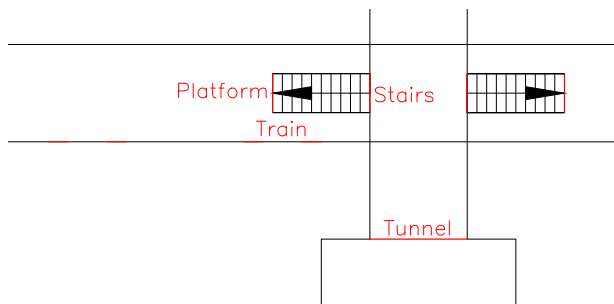
3.2.2. Time Schedules

In the previous studies, all platforms are filled at the same time, which caused several problems. Hence, this study deals with the individual consideration of filling the different platforms. Therefore, setup 2 is used, which has different platform lengths for different train types. The passengers start in the vestibule in front of the station and enter the station through one of the four entrance doors. There are no limitations or crowd management measures except the number of passengers entering the station at once, which correspond to the considered train capacity. The results give an overview about the times, passengers need to reach the different sections of the station. Therefore, several questions can be answered, e.g., how long does it take to refill the platforms or to fill the trains, but also when does the last passenger enter the tunnel or a staircase. To check the plausibility of the simulation data, the results are compared to the results of hand calculation with one and multiple passengers.

To evaluate the trajectory data of the simulations with regard to the resulting densities, different measurement area were defined. Additionally, the times, which are needed by the passengers to pass the transitions between the different station sections, are evaluated. Figure 3.12 shows the measurement areas and the transitions which are evaluated. Their IDs and designations will be used in the following.



(a) Measurement areas of setup 2, rotated view.



(b) Measurement lines at transitions between the different station sections.

Figure 3.12.: Location of measurement areas and measurement lines in setup 2.

Before looking at the overall results of the trajectory data of the simulations, the plausibility is checked. For the hand calculation of one passenger, equation 2.1, which

uses the pathway of the passenger, is used. The corresponding results and the data from the simulation are shown in table 3.1. The final exit is defined as the furthest train door. As can be seen, there are only negligible differences of a less than 15 s, which result from the route choice in the simulation. Here the shortest path is chosen, whereas in the hand calculation the middle of all transitions is used to calculate the path length, see figure 2.10.

transitions	hand calculation [s]	simulation [s]
hall/tunnel	18	17
staircase platform 1	35	31
staircase platform 3	67	63
staircase platform 5	101	96
final exit of platform 1	199	188
final exit of platform 3	179	168
final exit of platform 5	199	186

Table 3.1.: Hand calculation vs. simulation: Walking times for a single passenger.

For the hand calculation of multiple passengers, equation 2.2 is used. It uses the number of evacuees and the door with the smallest width in combination with the walking speed to calculate the evacuation time. The train doors have the smallest width, but as there are multiple, the staircases are chosen to be the critical bottleneck. So, the staircase width of 4 m and the free walking speed on stairs of 0.7 m s^{-1} as well as the train capacities serve as input parameter for the calculation. Table 3.2 shows the results for the different train types from hand calculation and the simulation data. The results show only little differences between 3 s and 37 s. To explain this range of differences, figure 3.13 can be used. It shows the minimum and maximum time values of the different station sections, which correspond to the times, which are needed until the first and the last passenger have passed the corresponding measurement lines. On the x-axis there is the platform number, and on the y-axis, there is the passing time in seconds. Over all, there are four points of interest: the transition between the entrance hall and the tunnel, the transitions between the tunnel and the staircases, the transitions between the staircases and the platforms and the transitions to the train doors, which all have been shown in figure 3.12b.

Train type	ICE	RE	SB
Capacity N	1170	1350	1440
Time _{stair} hand calculation [s]	418	482	514
Time _{stair} simulation data [s]	427	479	551

Table 3.2.: Hand calculation vs. simulation: Evacuation times for train capacities.

For each transition, the minimum, and maximum passing time is shown. When looking at the minimum and maximum times of the staircases, it can be found, that the minimum values rise with the distance between the entrance and the platform. These differences were also found in the calculation of one passenger. As the distances are not conducted in the equation for multiple passengers of the hand calculation, this explains

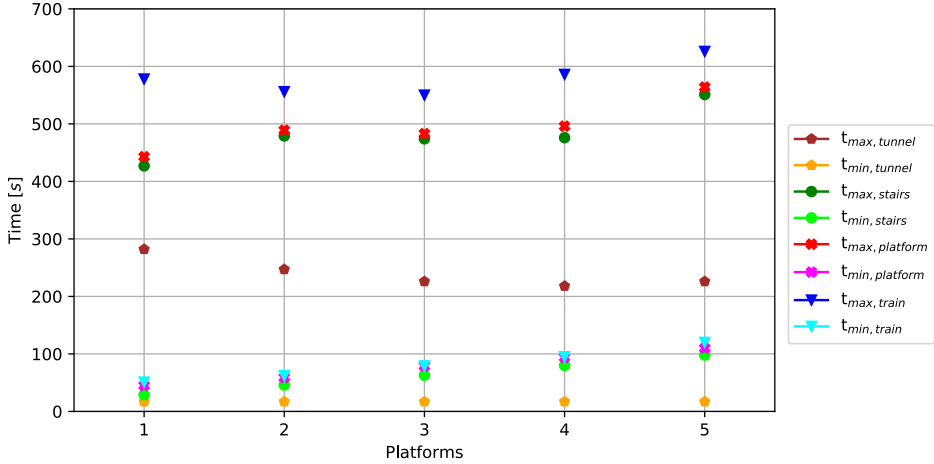


Figure 3.13.: Evacuation times of the different station sections.

the range in the differences. The differences of 37 s at the staircases can be found for the rear platform of the SB. The gap between the minimum values of the first and the last platform is more than 60 s, which can also be seen in table 3.1. As this is more than 37 s, it leads to the conclusion that the simulation data can be seen as plausible.

In the following, the simulation data will be examined in more detail to find individual bottlenecks and to work out a time schedule for the train departures. When looking deeper into the passing times in figure 3.13, some particularities can be observed. As mentioned, the minimum values increase with the distance of the platforms. In the maximum values, on the contrary, the time of the first platform is higher than the times for platforms 2 and 3. The reason for this can be seen in the trajectory visualisation and the densities in figures 3.14 to 3.19.

For the case of filling platform 1, the trajectories in figure 3.14 show, that congestion occurs in front of the staircases, which cause a tailback and more congestion inside the entrance hall. This can also be observed, when looking at the densities in figure 3.15. These reach a high level of 3 m^{-2} in the entrance hall (ID 60) and 2.7 m^{-2} in the measurement area in the tunnel with ID 61. Looking at the trajectories of platform 3 it can be found that the congestion that occurs in front of the staircases has a much smaller influence on the flow in the entrance hall, see figure 3.16. Figure 3.17 shows the

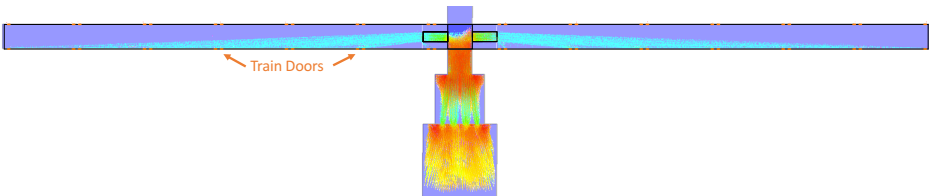


Figure 3.14.: Trajectories for filling platform 1.

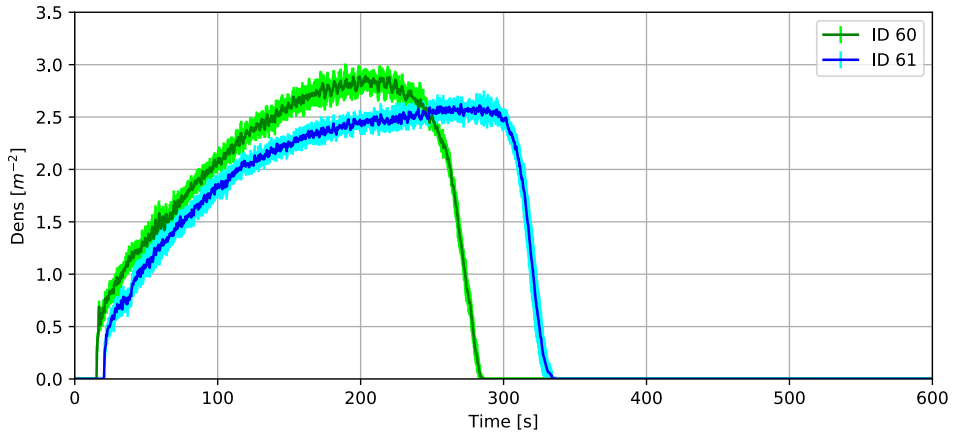


Figure 3.15.: Densities with mean values and standard deviation for filling platform 1.

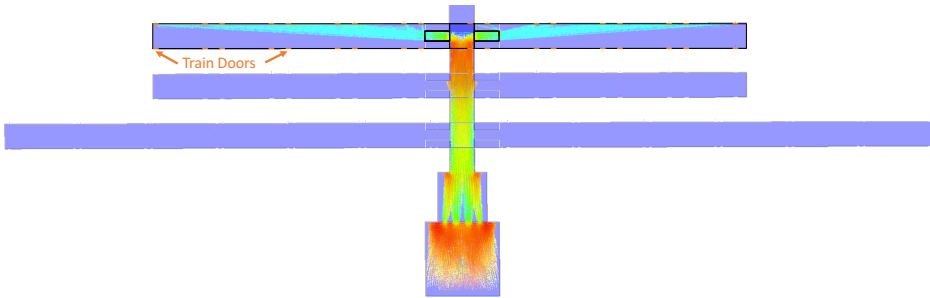


Figure 3.16.: Trajectories for filling platform 3.

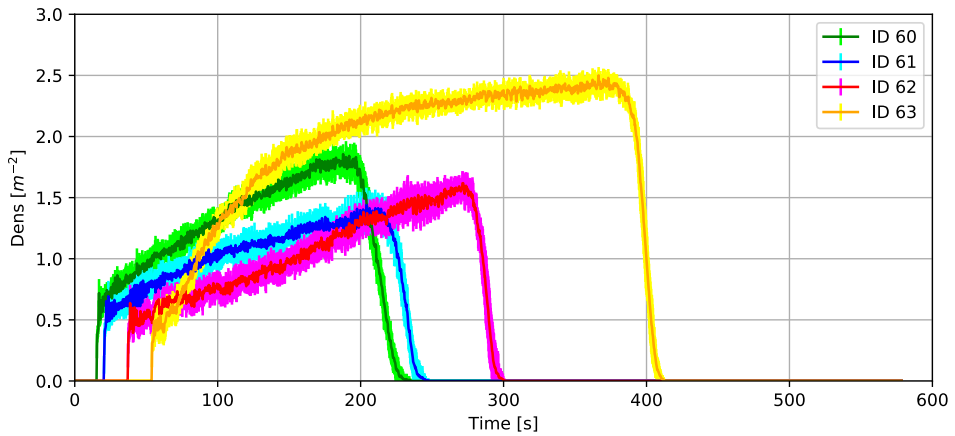


Figure 3.17.: Densities with mean values and standard deviation for filling platform 3.

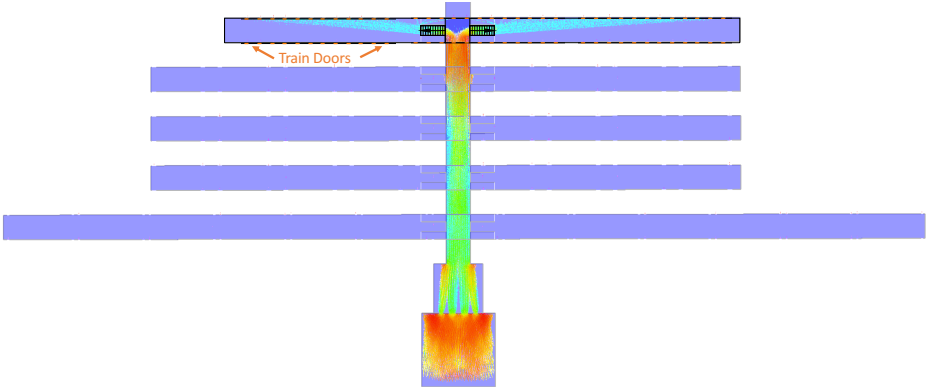


Figure 3.18.: Trajectories for filling platform 5.

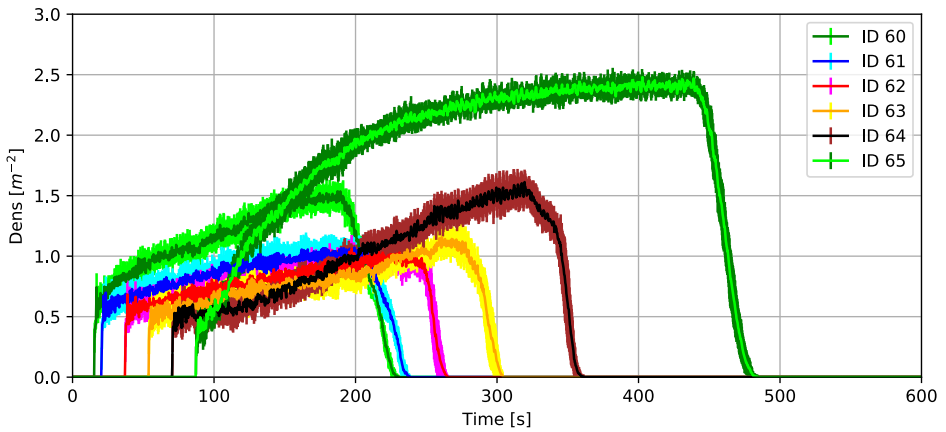


Figure 3.19.: Densities with mean values and standard deviation for filling platform 5.

corresponding densities. While the densities in the tunnel section of platform 3 (ID 63) reaches 2.5 m^{-2} , the density values in the entrance hall reach only 1.9 m^{-2} . In return, however, the densities in the tunnel section in front platform 2 (ID 62) increase, because of the tailback. For the rear platforms, the distance to the entrance hall is sufficient to avoid further tailbacks to the entrance area, see figure 3.18. Here, only the tunnel section in front of platform 4 (ID 64) is effected by the tailback. The little increase of density inside the entrance hall, which can be seen in figure 3.19, is caused by the cross-sectional constriction at the tunnel entrance.

So, the tailback into the entrance hall, which makes passengers need more time to reach the platforms, is the reason for the decreasing evacuation times with increasing distances between the entrance and the platform in figure 3.13. For the very rear platforms 4 and 5 this is not valid at all. As the influence of the tailback on the evacuation times decreases for the rear platforms, the influence of the walking times for longer distances to the rear platforms increases. Hence, the evacuation time increases from platforms 3 to 5, see figure 3.13.

Time Schedule

In the results of the previous studies in chapter 3.2.1, it was shown that it is not an optimal solution to fill all platforms at the same time, because huge congestion occurs, which can lead to dangerous crowding. So, the trains should depart with a specified time gap. Therefore, figure 3.13 provides the necessary results. The minimum times show, that the first passengers enter the stairs in less than two minutes. The difference between the first and the last passenger entering the stairs lies between 6.5 min and 8 min. As a different platform can be used for the next interval, it is not necessary to wait until the last passengers have finally entered the platform until the next passengers are let into the station. For the time schedule in this example, hence, a time interval of 7 min is defined to be possible. Additionally, the usage of both entrances is possible. To avoid a bidirectional flow, passengers, whose destination is a train at platforms 1 or 2 take only the main entrance, passengers whose destination platform is 4 or 5 take only the back entrance and the middle platform 3 can be reached from both entrances at different times. An example for a time schedule can be found in table 3.3. The dwell time was set to 3 min after the last passenger has entered the platform. Figure 3.13 shows that this is enough to fill the trains. With these settings and for this special geometry, a capacity of 21,000 agents/h can be reached.

platform	platform 1	platform 2	platform 3	platform 4	platform 5
departure	24	17	10 _{main}	10	17
times [min]	38	31	24 _{back}	31	38
	59	52	45 _{main}	45	52

Table 3.3.: Example of a time schedule with departure times for one hour using the main entrance for platforms 1 and 2, the back entrance for platforms 4 and 5, and both entrances for platform 3.

However, the densities inside the entrance hall and the tunnel reached high levels, up to 3.0 m^{-2} . As mentioned before and in reference to the Level-of-Service, densities should not exceed 1.5 m^{-2} for constant levels and 2 m^{-2} for shorter peaks, to avoid any kind of dangerous situations. As the high density values are caused by the uncontrolled inflow and the bottleneck of the staircases, on the one hand, there is a need for inflow regulations and other crowd management measures inside the station, to decrease the densities at any point. On the other hand, the bottleneck of the staircases includes a routing around a 90-degree corner, which was identified to be a model limitation of JPSScore. The influence of this limitation compared to the influence of the bottleneck itself is not considered to be significant. Nevertheless, since no solution to this model limitation had been found at the time these studies were carried out, the following studies, which are presented in the next section (3.2.3) and consider inflow regulations and other crowd management measures inside the station, were carried out with separated platforms in order to prevent a routing around 90-degree corners. In further studies, which are presented in chapter 3.2.4, the solution of a modified floor-field, which was shown in chapter 2.1.1, is pursued, which improves the corner routing and minimises its influence.

3.2.3. Filling Platforms

In the last presented studies, the filling process of the individual platforms were evaluated, and a time schedule could be elaborated. However, crowding with high densities were still found in some sections inside the station. This makes it necessary to optimise the processes to increase the capacity by simultaneously maintaining the safety of the passengers. Therefore, on the one hand, a multivariate analysis is conducted to show the interaction between the different crowd management measures, which were pointed out in section 2.3.2.3 and include different inflow rates, door statuses and filling processes. On the other hand, the usage of different train types is further investigated. As variations of these crowd management measures and their combinations are numerous, the analysis was done in several steps, which are presented in separated subsections. At the beginning, a combination with a single variable is determined, which corresponds to one of the crowd management measures. The results of changing this variable are analysed accordingly. The best result is then set as the input combination for the analysis of the next measure, with another variable as the degree of freedom. So, the best option for each variation can be found and at the end the best combination of these variations. The matters of interests are therefore the evacuation times, occurring congestion and critical densities, which are evaluated in defined measurement areas and at different measurement lines. Their location and designation can be found in figure 3.20.

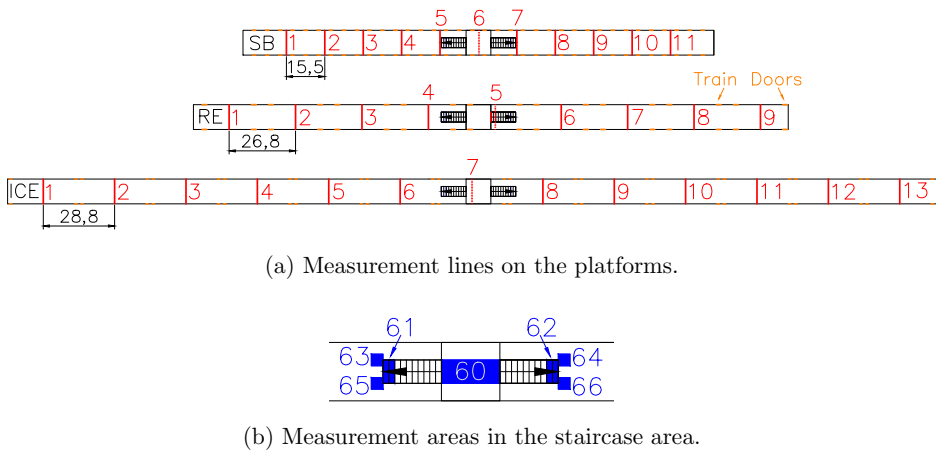


Figure 3.20.: Measurement lines and areas for the different platforms of setup 3.

In the first evaluation step, which is presented in subsection 3.2.3.1, the different inflow rates 1 s^{-1} , 2 s^{-1} and 4 s^{-1} are analysed. These inflow rates are set for each staircase, so the inflow rates for the whole platform have to be doubled. As the statuses of the train doors can have an influence on occurring congestion, the analysis is conducted with the open door status. The maximum evacuation times are analysed and the area of the staircases is observed, which is identified as a critical bottleneck. Therefore, the evacuation time is defined as the maximum time all passengers need to enter the platform and the train.

In subsection 3.2.3.2 examination of the filling processes *re-fro*, *fro-re* and *mixed* are shown. For this purpose, the distribution of the passengers on the platform is estimated, by analysing the data from the length measurement lines on the platform, see red lines in figure 3.20a. For the ICE and RE, which have two doors per wagon, these lines were set to the middle of each wagon. For the SB, which has three doors per wagon, the measurement lines were set between the wagons. The results will show the best filling process to guarantee an optimal boarding process to the trains.

In the third subsection (3.2.3.3) the influence of the different door statuses at the beginning of the filling process is shown. Therefore, the boarding times are compared. These are defined as the time differences between the first and the last passenger, who enters a train door. Additionally, in the last subsection (3.2.3.4) the three train types are compared. The aim is to find the best train to evacuate the most passengers in the shortest time. In case of an evacuation, all train types would be used, but it is necessary to know these dimensions to find an optimal time schedule and to calculate the capacity of the train station.

3.2.3.1. Inflow Rate

In the following, the influence of the different inflow rates is estimated. As mentioned above, two things have to be considered to find the optimal inflow rate. The first is the maximum evacuation time, which is an important value to make a statement about the number of passengers that can be evacuated in a defined time. Therefore, only the door status *open* is considered, because the others have an influence on the filling processes and therefore on the evacuation times. Secondly, a certain Level-of-Service should be maintained by avoiding high densities and resulting congestion.

Figure 3.21 shows the maximum evacuation times for the different inflow rates and filling processes for each train type. It can be observed, that the inflow rate of 1 s^{-1} has always significant higher evacuation times than 2 s^{-1} and 4 s^{-1} . In contrast to this, the difference in the evacuation times between 2 s^{-1} and 4 s^{-1} is marginal. This is an

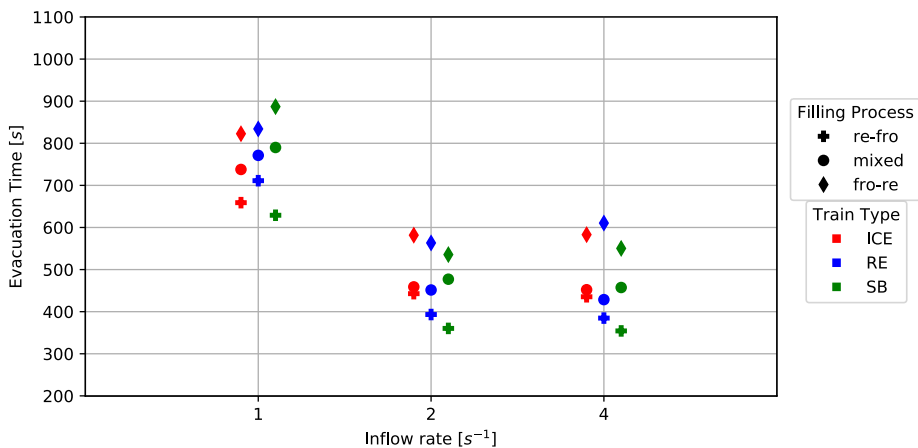


Figure 3.21.: Maximum evacuation times for different inflow rates.

indicator that the capacity of the staircases has been reached between these two inflow rates. An analysis of the flow rate at the beginning and the end of the staircases, showed that the highest reachable flow does not exceed 2.5 s^{-1} for each staircase. Hence, for the analysis of the next variations, the best inflow rate is set to be between 2 s^{-1} and 4 s^{-1} per staircase.

Another thing that can be observed in figure 3.21 is, that the evacuation time also varies between the different filling processes. The *re-fro* process shows overall the best results with the lowest evacuation times, whereas the *fro-re* process shows the highest times. Looking also at the visualisation of the trajectories in the staircases' area in figure 3.22, which shows three examples for the RE, it can be found that congestion mainly occurs for the filling process *fro-re* and at the end of the left staircase. The reason for this is the location of the train doors. The first train door, the passengers have to reach, is beside the staircase, which makes it necessary for the passengers to change their walking direction. During this process, they slow down, which causes congestion. At the opposite staircase, the train doors are located in walking direction. So, the passengers do not slow down and less congestion occurs. Beyond this, as inflow rates increase, congestion increases, especially at the left staircase. Nevertheless, as soon as the next train door is being targeted, the congestion dissolves. For the filling process *mixed*, no congestion occurs at the staircases at any time and for any inflow rate, see figure 3.22 (bottom). The filling process *re-fro* does also not show congestion.

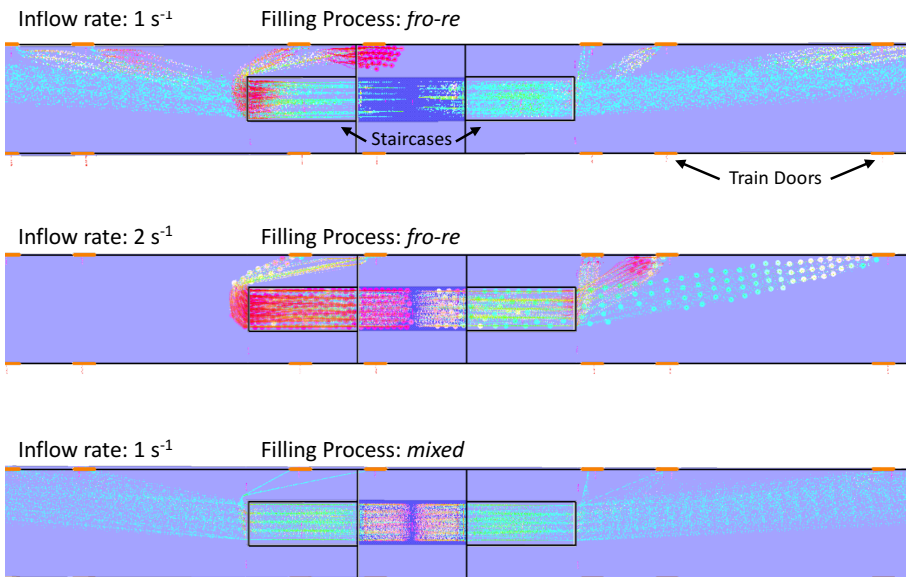


Figure 3.22.: Visualisation of the trajectories in the staircase area for the inflow rates 1 s^{-1} and 2 s^{-1} , and the filling processes *fro-re* and *mixed*.

Looking at the occurring densities around the staircases, gives a more detailed overview of the situation. For the analysis, the densities in the measurement areas with IDs 60 to 66 (cf. figure 3.20b) are considered. Figure 3.23 shows the maximum densities that

occur at the example of the ICE. As the temporal component is not taken into account here, it can be seen that there is not much difference between the filling processes *re-fro* and *fro-re*. However, it plays a major role whether crowding with high densities occurs at the beginning or at the end of the filling process. To take this into account, the individual evaluations of the density measurements over time need to be included.

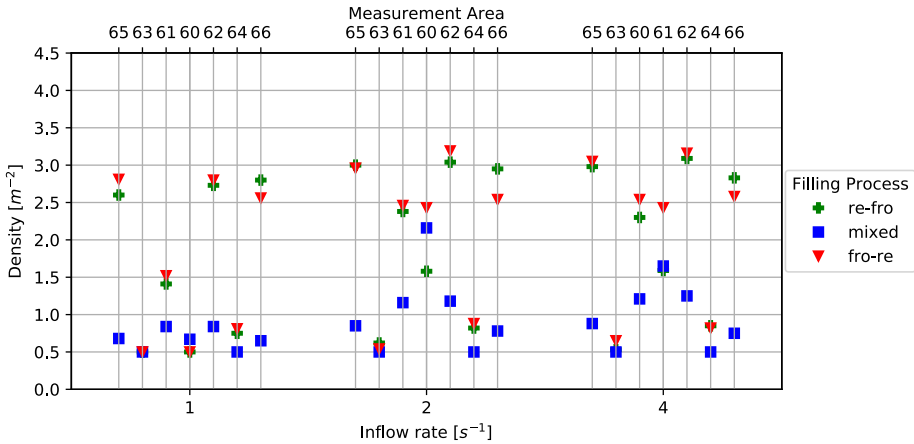


Figure 3.23.: Maximum densities for the ICE with different inflow rates.

Figure 3.24 shows the densities over time, which occur on the platforms in the staircase area in the measurement area with ID 66, at the example of the ICE with the door status *open* and figure 3.25 for the door status *close*. Both cases show similarities, but also huge differences for the occurring densities. Figure 3.24 shows that for the *fro-re* process, high densities occur especially at the beginning of the filling, while for the

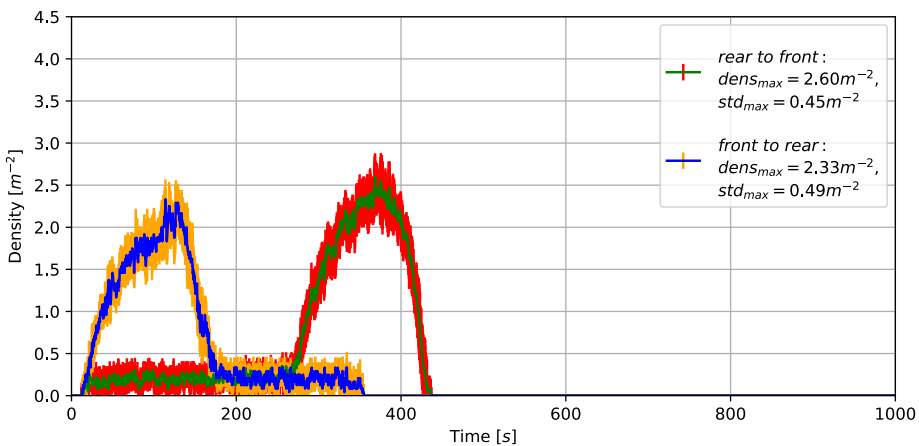


Figure 3.24.: Time-dependent densities with mean values and standard deviation for the ICE, the door status *open* and an inflow rate of 2 s^{-1} .

re-fro process the densities increase relatively late. In the first case, this is a safety-relevant problem. High densities at the staircases at the beginning of filling mean that many passengers are moving up. This can lead to dangerous crowding with fatal outcomes in case of pushing or similar. In the opposite case, if high densities occur at the end of the filling process, this mainly depicts the entry situation with a small cluster of passengers in front of the train doors. Since no, or only a few passengers, are moving up, the situation is not considered critical.

For the door status *close*, which is presented in figure 3.25, the effect for the *re-fro* process is the same. The densities rise at the end of the filling process. A difference, which attracts attention, is the duration of the high-level densities. As the peak with open doors falls off again during the entry process, the densities with closed doors last until these are opened after 600s. As mentioned above, this is not a safety relevant factor, because there are no passengers following. For the *fro-re* process, it is the opposite. Here, the door status has a huge influence on the densities in the staircase area. As the doors are closed, the cluster of waiting passengers in front of the doors near the access, will not disperse, and the congestion persist, which inevitably affects the following passengers and the whole evacuation process. Higher densities in this area occur than for the *open* door status, because other passengers have to go through to reach the rear train doors, but are blocked from the waiting passengers at the same time. After all following passengers have passed, a constant density, which represents the cluster of waiting passengers, lasts until the doors open.

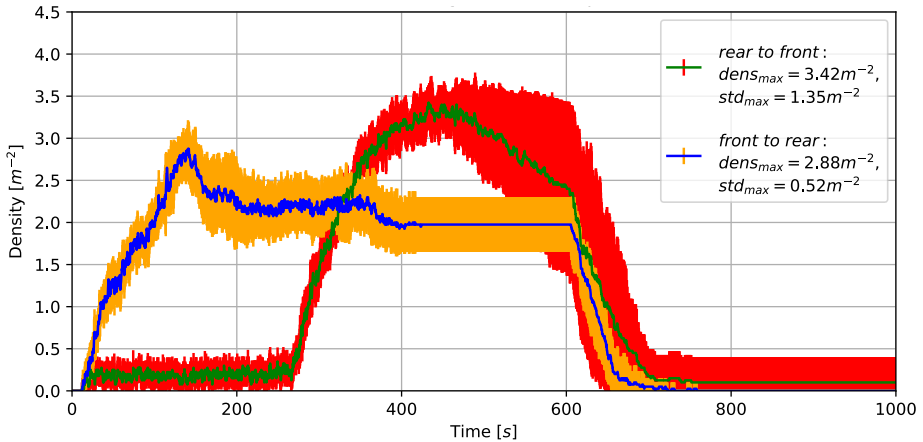


Figure 3.25.: Time-dependent densities with mean values and standard deviation for the ICE, the door status *close* and an inflow rate of 2 s^{-1} .

Taking these results into account, it nevertheless could make sense to keep the doors closed to ensure a sensible distribution of the passengers. But, according to the assessments so far, the process *fro-re* should be dispensed with. However, the filling processes will be examined in more detail in the next section. Additionally, as mentioned above, a constant inflow rate to the platforms of 2 s^{-1} per staircase and about 5 s^{-1} for the whole platform should not be exceeded. However, since in this study the platforms are considered separately from the station, the inflow rate should be adopted flexible in

case of occurring congestion inside the tunnel or at other places inside the station.

3.2.3.2. Filling Process

In this section, the influence of the filling processes on the evacuation time is presented. For this purpose, the distribution of the passengers over the platform is investigated. As in subsection 3.2.3.1 an inflow rate of 2 s^{-1} per staircase is recommended, only this case will be examined. Besides this, the previous results showed, that the door status has an influence on the filling process. For this purpose, all door statuses are taken into account.

Figure 3.26 shows the distribution of the passengers over the RE platform. The x-axis shows the measurement line ID numbers (cf. figure 3.20) and the y-axis shows the passing time, which corresponds to the time at which the last passenger passed the measurement line. The course of the graph provides information about the distribution. A flat curvature is equivalent to a homogeneous distribution over the platform and will ensure an optimal boarding process. A homogeneous distribution therefore means, the last passengers at each door will enter the train at the same time. So, there will be no stragglers, who delay the departure. Furthermore, the maximum times must not be neglected. Since it is an evacuation case, which is considered, a flat curve with high maximum times is worse than a steeper curve with lower times.

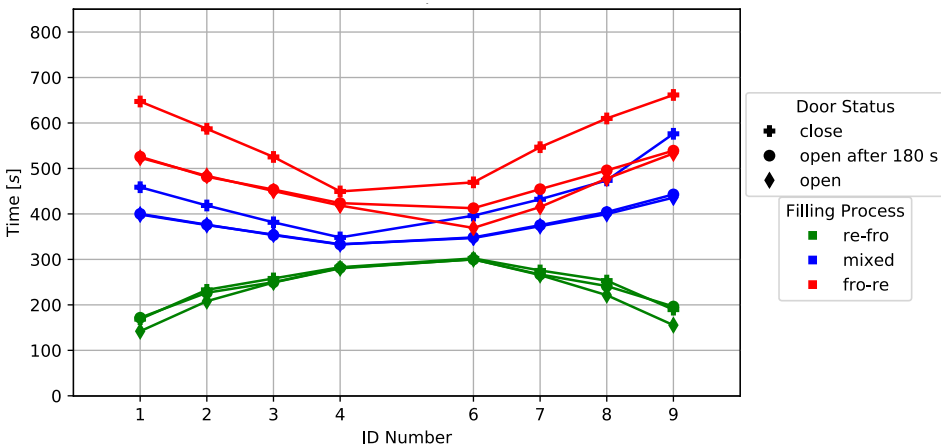


Figure 3.26.: Distribution of passengers over the platform at the example of the RE and an inflow rate of 2 s^{-1} .

In the presented example, the filling process *re-fro* shows the best results. The graphs show the flattest curvature and the maximum times are the lowest. The process *mixed* shows similar flat curves. Nevertheless, the maximum times are higher than for the *re-fro* process. The *fro-re* process has again the worst results. The maximum times are the highest, even though they are partly lower than in the *mixed* process. Additionally, the graphs have a steep descent and ascent.

Figure 3.27 shows two visualisations of the trajectories from the simulation data after a time of 150 s, with the *re-fro* process on the top and the *fro-re* process on the bottom.

As mentioned in section 2.3.2.3, the filling process *re-fro* corresponds to the case with total regulation. The passengers should use the doors, which are most far away from the staircases, first. This avoids congestion and crowding at any point on the platform and more passengers can enter the platform, see figure 3.27a. The filling process *fro-re* corresponds to the most realistic case without any regulation. The passengers take the first available and free door, to know themselves being in the save area. As figure 3.27b shows, this leads to congestion at the staircases, because waiting passengers cause a tailback. In comparison to the *re-fro* process, fewer passengers have reached the platform, which at the end results in increasing boarding times.

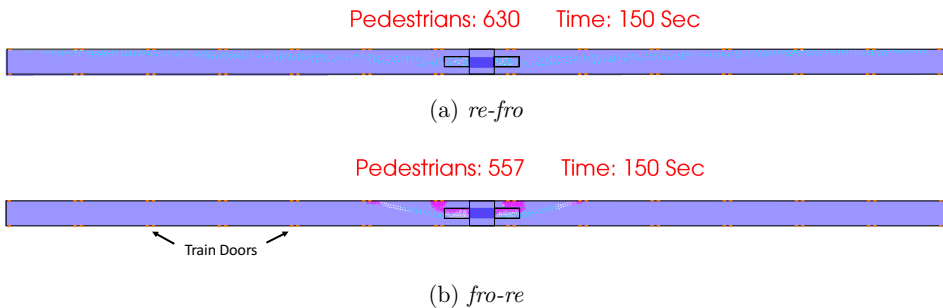


Figure 3.27.: Visualisation of trajectories for the filling processes *re-fro* and *fro-re*.

As a conclusion, a regulated and ordered filling process from the rear doors to the front doors is recommended, which is supported by security personal or the federal police. This leads to a homogeneous distribution of the passengers over the platform, avoids congestion and will ensure an overall faster boarding process.

3.2.3.3. Door Status

In this section, the different door statuses are analysed in more detail. As in the last subsection (3.2.3.2) the filling process *re-fro* was detected to be the best option, this is the only filling process, which is considered here. In figure 3.28 the boarding times for the three door statuses, *open*, *open after 180 s* and *close* are presented. The boarding times are defined as the time difference between the first and the last passenger, who entered a train. For the statuses *open* and *open after 180 s* the boarding process is influenced by the filling process. It can be found, that opening the train doors after 180s results in faster boarding times than for opened doors from the beginning. For the door status *open after 180 s* the passengers have to wait 180s before they can enter the train. So, small groups of passengers can accumulate in front of the train doors. Hence, when entering the train, the distance between two passengers is smaller, than for those who enter the train without waiting in front of the doors first, which leads to smaller boarding times. Nevertheless, the time difference between the boarding times is smaller than the waiting time of 180s. This shows, that keeping the doors closed for some time might be a good solution to minimise the evacuation times.

Keeping the doors closed until all passengers have distributed over the platform, leads to the smallest boarding times, which is obvious, because the filling process does not

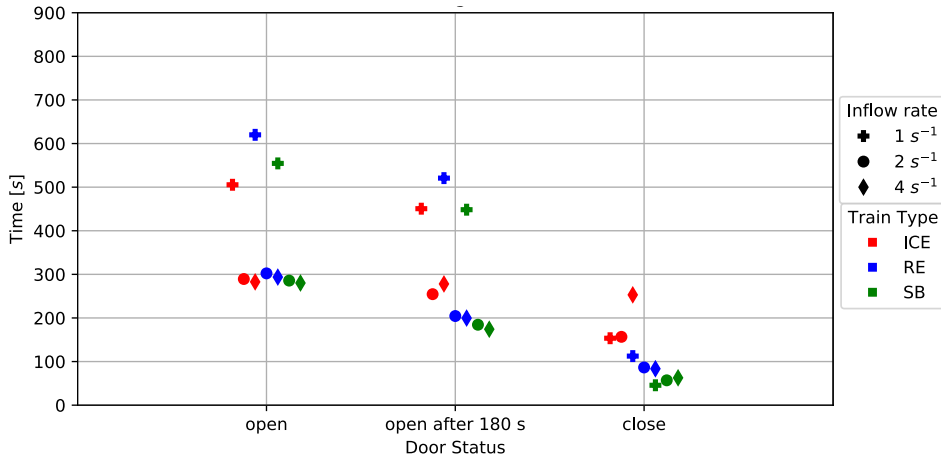


Figure 3.28.: Boarding times in dependency of the door statuses.

affect the boarding process. As mentioned in section 2.3.2.3, the doors are opened after 600 s, when all passengers have been distributed in front of their destination door. However, even here the differences to the boarding times of the other two door statuses is much smaller than 600 s. This could lead to the conclusion, that keeping the doors closed is the best option. Nevertheless, the evacuation time must not be neglected to make a statement about the best door status. The boarding and evacuation times for the example of the RE and an inflow rate of 2 s^{-1} are shown in table 3.4. Although the boarding time of the door status *open after 180 s* is almost 100 s smaller than for *open*, the difference in the evacuation times is less than 10 s. For the door status *close* the difference is about 300 s. As the evacuation time for the first two statuses only almost 400 s, closing the doors for 600 s might have been too long and the results would have been better, if the doors had been opened earlier.

Door status	open	open after 180 s	closed
Boarding time [s]	302	204	86
Evacuation time [s]	393	384	686

Table 3.4.: Boarding and evacuation times for different door statuses of the RE.

As a conclusion, it is recommended to keep the train doors closed at the beginning of the filling process anyway. It reduces the boarding times a lot and despite this, closed doors are helpful for the orientation and the distribution, because it prevents the passengers to become stressed, because they know, that there is enough time to catch the train. Moreover, it is recommended to decide individually when to open the doors, but to keep it close until most of the passengers have at least entered the platform.

3.2.3.4. Train Types

In this section, the differences between the three train types are outlined. As the best variations of the inflow rate, filling process and door status have already been found in subsections 3.2.3.1 to 3.2.3.3, only these variations will be used for the analysis here. Nevertheless, without analysing any simulation data there are a few obvious differences, which also have to be considered. The trains have a different number of doors and different door widths (cf. table 2.2). Additionally, the capacity of the train wagons varies (cf. table 3.5 line 1). To be able to compare the results of the different train types, relative and absolute values will be used.

In the first step the number of evacuees, who have entered a train within the first five minutes are analysed, see table 3.5 lines 2 and 3. The most passengers entered the RE in five minutes, followed by the SB and the ICE. For the RE this is equivalent to 67% of the train capacity (line 1), whereas the ICE and the SB reach only about 53% of their capacity after five minutes.

Nr.	Train type	ICE	RE	SB
1	Train capacity	1170	1350	1440
2	Number of evacuees in five minutes	625	900	766
3	Percentage of train capacity [%]	53.42	66.67	53.19
4	Maximum evacuation time [s]	460	393	360
5	Raw boarding time [s]	100	79	36
6	Evacuation flow [s ⁻¹]	2.54	3.44	4.00

Table 3.5.: Comparison of the different train types with the results of an *open* door status, the filling process *re-fro* and an inflow rate of 2 s⁻¹.

In a second step, the maximum evacuation times are analysed in line 4 of table 3.5. The minimum evacuation time can be found for the SB with 360s, which is surprising at the first moment, because after 300s only 53% of the passengers had been evacuated. This small differences between the evacuation times and the five-minute values can be explained with the influence of the filling and the boarding processes. As the process *re-fro* is considered, the first passengers had to overcome a long distance to their destination doors. This has a corresponding negative effect on the five-minute values. Looking back at the distribution of passengers in figure 3.26, it was found that most of the passengers have already entered and distributed on the platform after five minutes. They just did not enter their destination train door. If looking additionally at the raw boarding times in line 5 of table 3.5, which are calculated by equation 3.1, the influence of the boarding process gets clearer.

$$time_{boarding} = \frac{passengers/door}{flow_{door}} [s] \quad (3.1)$$

The raw boarding time indicates how long it takes until a defined number of passengers, which correspond to the door capacity, had entered the train through a single door. The total opening width of the trains also plays a role here. Table 2.2 showed that this is about 25% for the SB and 6% for the ICE. This ratio can be seen on a similar scale for the raw boarding times. In the case of SB this takes 36s, while in case of the ICE

100s are required. So, if all passengers have already distributed on the platform, and only had to enter the train through one of the doors, the raw boarding time indicates how long this process will last. This also explains why the SB has a smaller evacuation times than the other train types.

The last aspect which is taken into account is the evacuation flow J_{evac} in line 6 of table 3.5, which indicates how many passengers can be evacuated per second. Therefore, the train capacity is divided by the evacuation time, as shown in equation 3.2. As the SB showed the best results for the evacuation times and has the highest capacity, the evacuation flow is also the highest here, followed by the RE and the ICE.

$$J_{evac} = \frac{capacity_{train}}{time_{evac}} [s^{-1}] \quad (3.2)$$

The comparison of the train types has shown that using the RE the highest number of passengers can be evacuated in five minutes. Whereas, the best overall results were shown by the SB, with the highest evacuation flow rate. However, it should be borne in mind that this train, and therefore its capacity, was made up of three individual trains. This assumption was made because it is technically possible, and in this way valuable personnel is saved. If this adaption is not convertible, the RE is the better choice. The ICE showed the overall worst results.

3.2.3.5. Overall Assessment

In the sections above, the supposedly worse variants were neglected during the evaluation. Hence, figure 3.29 shows an overall view of the evacuation times, with all crowd management combinations. To ensure comparability of the values, especially between the individual train types, the times are shown relative to the train capacity. Wherein the capacity of the ICE describes the 100% values. The most effective variations were defined to be the SB and the RE with the filling status *re-fro*, the door status *closed*

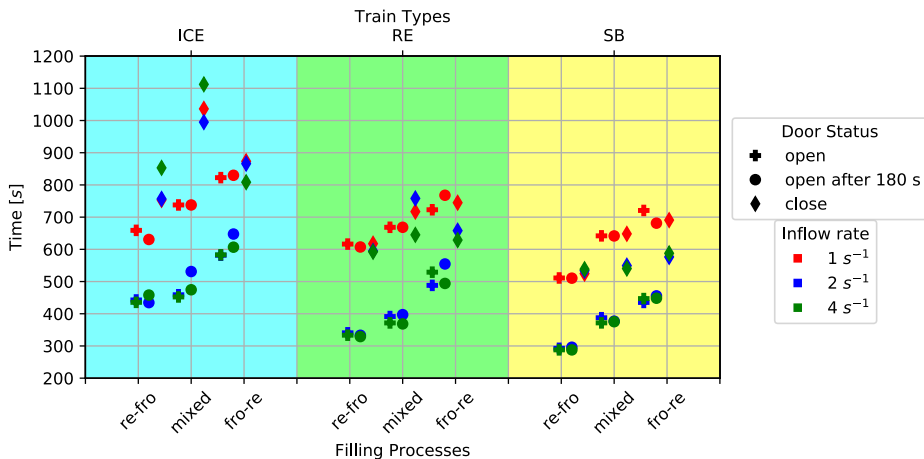


Figure 3.29.: Overview of the evacuation times, considering all crowd management measures.

after x minutes and an inflow rate between 2 s^{-1} and 4 s^{-1} . When looking at the results in figure 3.29, the *re-fro* process is mostly the best choice, which confirms the results of the analysis above. The differences between the door statuses *open* and *open after 180 s* are negligible, whereas the values of the *close* door status are higher. The reason for this was outlined before, as well as the benefits to keep the doors closed anyway.

As the evacuation times are relative to the train capacity, the train types can also be compared. The RE and the SB were chosen to be the best option, for the *re-fro* process, which is confirmed. For the other inflow processes, the SB also shows the best result, which is explained by the train design. As the SB has three doors per train section, the total opening width is the highest (cf. table 2.2) and the passengers per door are accordingly less. This in turn leads to smaller clusters of waiting passengers in front of the train doors, which causes less congestion. Additionally, the entrance is plain, which leads to a faster boarding. Hence, RE and SB are recommended to be a good choice for the evacuation. The ICE is not suitable. It has longer evacuation times, and its train design with small door width and staircases might hinder the evacuation flow. Nevertheless, for a real large-scale evacuation all available train types need to be used. The results just give an overview, which trains should be preferred if possible.

3.2.3.6. Double-sided Filling

All investigations have also been conducted with two trains, one at each track of the platform. This on the one hand ensures the safety of the passengers, as both platform edges are secured by a train. On the other hand, this also means double number of passengers, which might cause other problems. Figure 3.30 shows the overall assessment of the maximum evacuation times. To make the values comparable between the different train types, these are plotted relative to the ICE values. While for the one-sided filling process the values of interest lie between 300 s and 600 s, the values are now between 500 s and 1,000 s, which is almost the double. With an equal inflow of 2 s^{-1}

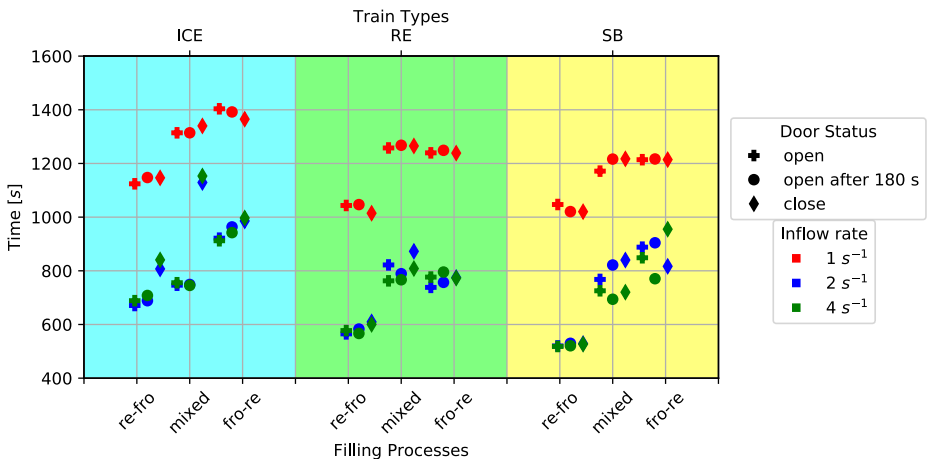


Figure 3.30.: Overview of the evacuation times, considering all crowd management measures for the double-sided case.

but a doubled passenger number, equation 2.2 shows that the doubled time would be needed to fill the platforms. So, this result is plausible, which can also be seen in the boarding times of the trains in figure 3.31. Here, the boarding for the RE and the ICE with open doors takes almost 600 s, whereas in the one-sided case less than 300 s were needed, see figure 3.28.

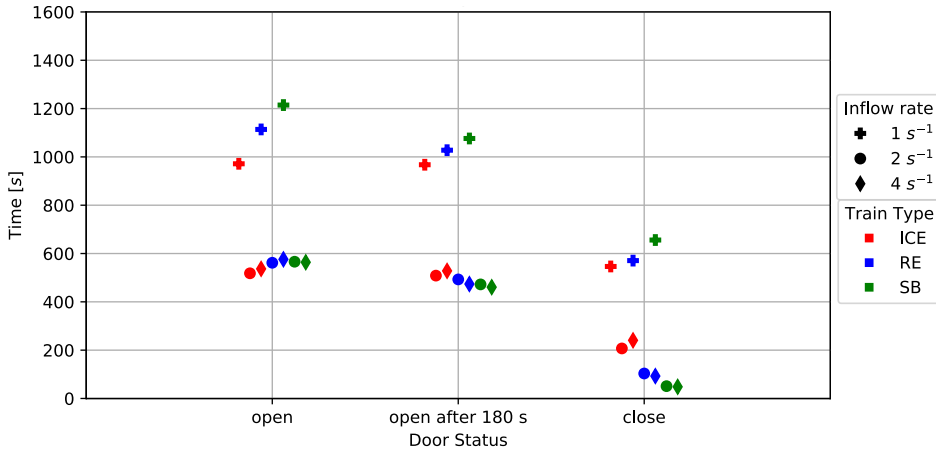


Figure 3.31.: Boarding Times for the filling process *re-fro* in the double-sided case.

Besides this, the point of most interest are the occurring densities. Figure 3.32 shows the maximum density values. Comparing it to the one-sided case in figure 3.23, only a few values increased. In the *fro-re* process, the one-sided case showed occurring congestion and therefore high densities at the beginning of the filling process, caused by passengers entering the first train doors or waiting in front of it. Upcoming passengers

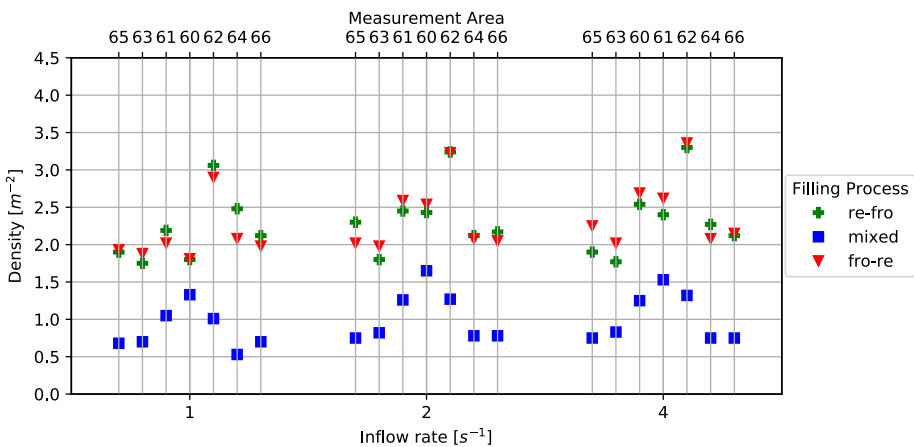
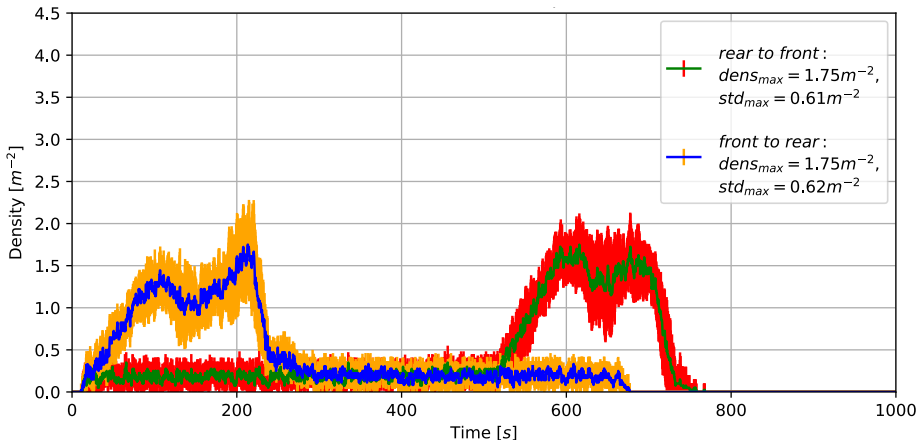


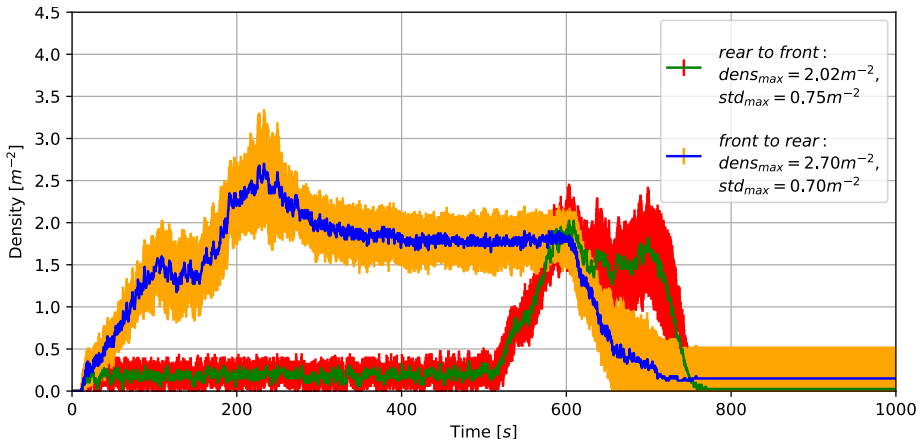
Figure 3.32.: Maximum densities for the ICE with different inflow rates for the double-sided case.

had to go through, and the densities raised in the staircase area. For the double-sided case it is the same, but here more space is considered, so there is less space to let upcoming passengers pass. Thereby, the door capacity and the door flow of the trains play a major role for the arising density values. This becomes clearer by looking at the time-dependent densities.

Figures 3.33 and 3.34 show the results of the time-dependent densities as a function of the filling processes *fro-re* and *re-fro* in dependency of the door statuses *open* and *close* for the examples of the ICE and the RE. As the overall filling process for the double-sided case lasts longer, a general observation for both, the *close* and *open* door status,

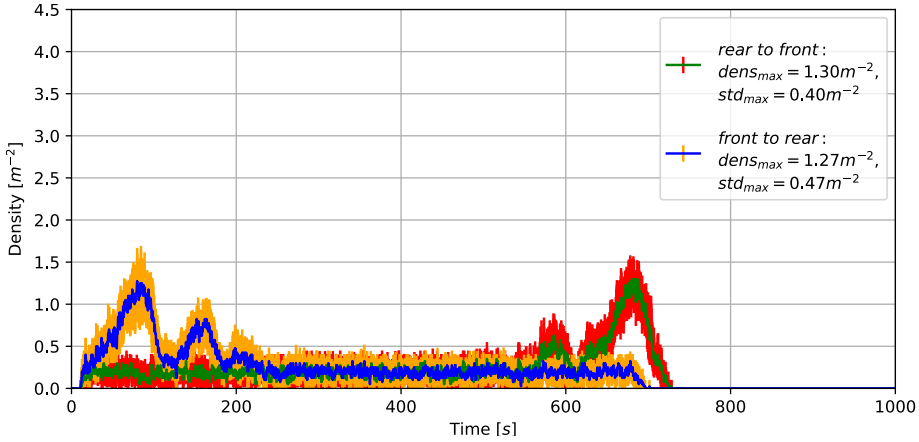


(a) Time-dependent densities for open doors.

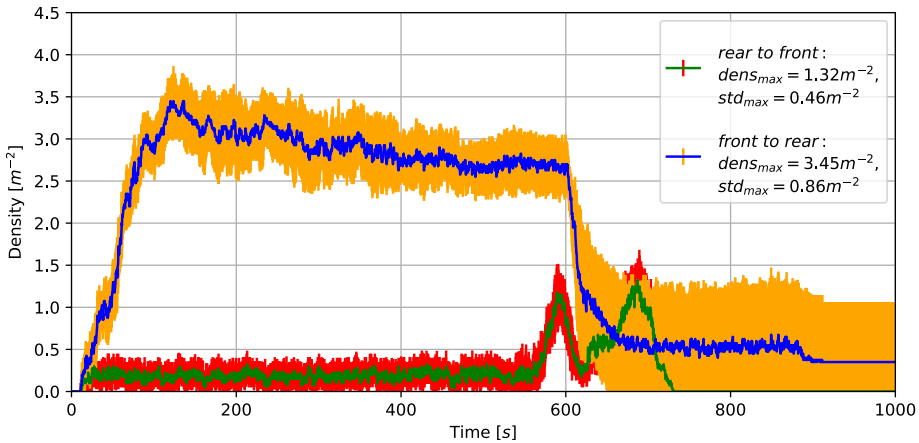


(b) Time-dependent densities for close doors.

Figure 3.33.: Time-dependent densities with mean values and standard deviation for the door statuses *open* and *close* as function of the filling process for a double-sided ICE filling.



(a) Time-dependent densities for open doors.



(b) Time-dependent densities for close doors.

Figure 3.34.: Time-dependent densities with mean values and standard deviation for the door statuses *open* and *close* as function of the filling process for a double-sided RE filling.

is that for the process *re-fro*, the occurrence of higher density values shifts backwards, while the values have similar levels. Besides this, for the *open* door status, the door flow is decisive for the density values. The door flow for the RE is 0.95 s^{-1} and for the ICE 0.45 s^{-1} , see table 2.2. Hence, although the RE has the higher door capacity with 75 passengers, in comparison to 45 passengers for the the ICE, see table 2.4, the density values for the ICE are higher for both filling processes, compare figures 3.33a and 3.34a. Compared to the one-sided case, the values do not reach higher levels. But as the time, which is needed to fill the platform is doubled, also the duration of the boarding process increases. Here, especially for the *fro-re* process at the ICE, two peaks can be observed. The first can be traced back to boarding passengers, which accumulate in front of the

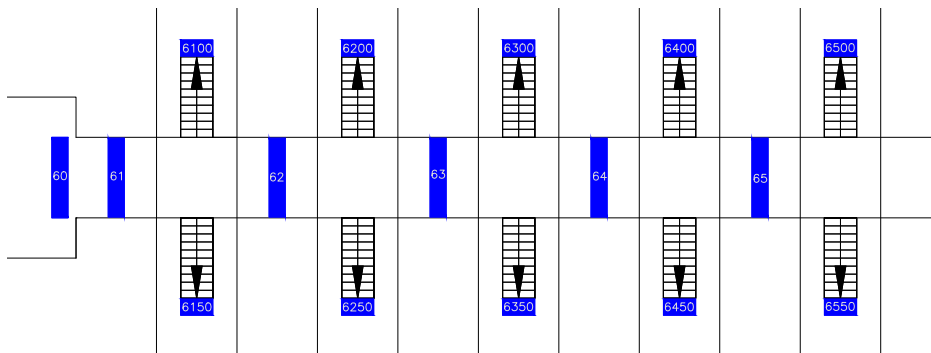
front train doors. The second is caused by upcoming passengers who have less space to move out of the way, as passengers gather in front of the doors on both sides of the platform.

For closed doors, the door capacities tip the scales for the density values. Hence, for the *fro-re* process, the RE stick on a higher level (figure 3.34b) than the ICE (figure 3.33b), because more passengers wait in front of the close train doors and following passengers further increase the densities by using the little available space to pass by. Nevertheless, in comparison to the one-sided case, the values show only slight differences for the *fro-re* process. Since the filling process for the double-sided case takes a little less than 600 s and the closed doors opened after 600 s, the one-sided or double-sided filling only has an effect on the total evacuation time if the doors were opened earlier. For the *re-fro* process, the differences are decisive. For the one-sided case, the densities reach a high level, as passengers wait in front of all doors before they open after 600 s. For the double-sided case, not all passengers have reached the platform, when the doors open. So, lower densities occur in front of the first train doors.

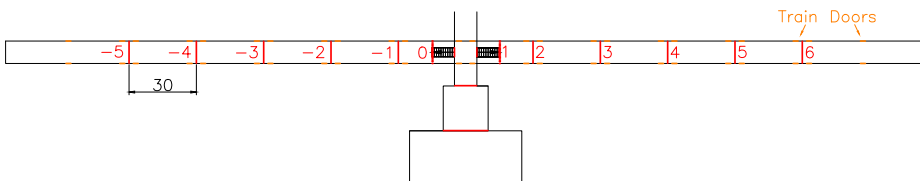
3.2.4. Multivariate Crowd Management Measures

This section presents the evaluation of detailed multivariate crowd management measures. These are an extension to the previous studies in section 3.2.3. The measures presented there, have been expanded and carried out on the entire station geometry. Whereas previously, for example, only three inflow rates and three variation of the filling process were considered, five inflow rates and eleven filling processes are now presented. The aim of this significantly more detailed study, especially of the filling process, is to show how the evacuation time improves or worsens depending on how well the corresponding measures are implemented.

For the evaluation of the data, again different measurement areas and measurement lines are defined, see figures 3.35 and 3.36. The measurement areas for density evaluation are located in the entrance hall in front of the entrance to the tunnel, in the tunnel in the middle between two platforms as well as immediately behind each staircase, see figure 3.35a. The measurement lines are positioned at the entrance, at the tunnel entrance, on the platforms at the staircases and along the platform at each train wagon to measure the distribution of the passengers. The exact positions and designations for the measurement areas (MAs) along the platform can be taken from figure 3.35b. Additionally, for the evaluation of the passing times of the different station sections the other measurement lines are used, which designations can be found in figure 3.36.



(a) Measurement areas (rotated view)



(b) Measurement lines along the platform

Figure 3.35.: Measurement areas for the evaluation of the densities and measurement lines along the platform for the evaluation of passengers distribution in setup 4.

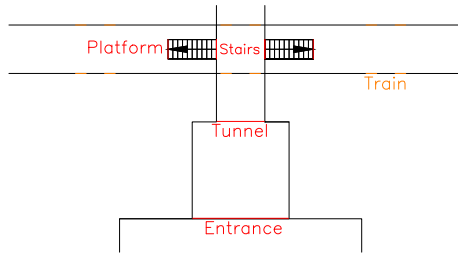


Figure 3.36.: Measurement lines at transitions for the analysis of the different station sections in setup 4.

3.2.4.1. Densities

Passenger safety is a priority at all times, so the first step is to look at the densities occurring in the tunnel and in the staircase areas. Two methods are used to evaluate the densities. First, the maximum densities occurring for each individual case are determined and compared. In a second step, the temporally occurring densities for individual cases are considered in order to draw conclusions about the temporal occurrence of high densities. This is an essential aspect for assessing safety. As mentioned in the previous sections, high densities that occur at the beginning of the filling process pose a significant safety risk due to passengers moving up.

Figure 3.37 gives an overview about the maximum densities which occur for different inflow rates by filling platform 5. Only inflow rates up to 6 s^{-1} are taken into account, as no further increase can be detected beyond that. As can be seen, the densities increase with increasing inflow rate. At first, the values in the individual measuring ranges differ only slightly from each other. The differences between the individual

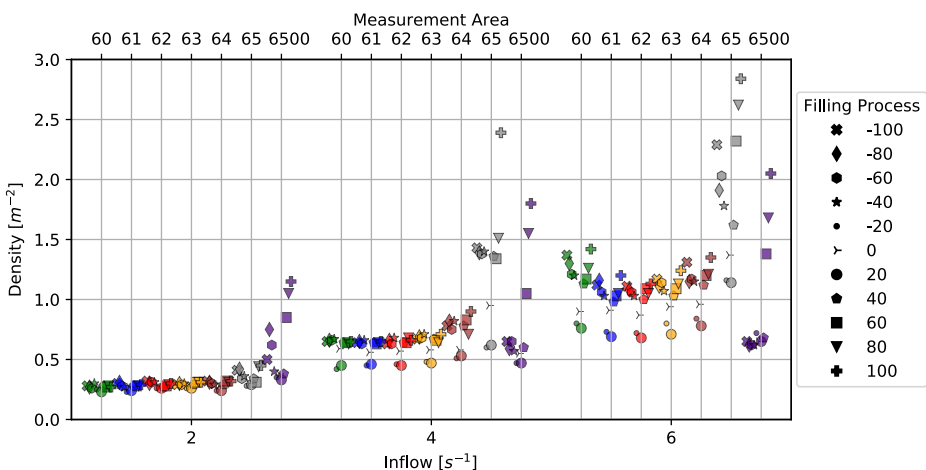


Figure 3.37.: Maximum densities for different inflow rates at the example of platform 5.

filling processes are also hardly visible at lower inflow rates. These are initially only visible on the platform. With increasing inflow rates, however, it can be observed that, in addition to the densities on the platform, those in the tunnel, in front of the respective platforms, in particular increase sharply, which also makes the differences in the filling types visible there. For an inflow rate of 6 s^{-1} also the densities in the entry hall increase slightly. This is caused by the cross-section narrowing between the entrance hall and the tunnel entrance.

When looking additionally at the time-dependent densities in the following, several things catch the eye. If looking at the individual cases independently of each other, it is noticeable that the filling process, especially for the *fro-re* process, has a great influence on the occurrence of congestion on the platform in the staircase area, but also inside the tunnel. Figure 3.38 shows this with the example of platform 2 and an inflow rate of 4 s^{-1} . Here, for the cases with a high proportion of passengers using the front doors first, the densities on the platforms are significantly higher than in the reverse case, where no relevant peaks are visible. This also affects the densities inside the tunnel. In general, passengers reduce their speed on staircases, so that slight congestion occurs when there is an inflow of 4 s^{-1} . This can be seen in an increase in densities near the stairs compared to those in the front measurement areas. If congestion also occurs at the platforms in the staircase area, this causes backlogs and the densities in the tunnel rise.

If looking at all door opening times for one case, it is noticed that these also have an influence on the development of congestion and high densities. This is most noticeable when filling the platform from the front to the back, see figure 3.39. If the doors are opened at the beginning of the filling process, the densities are relatively low. Passengers wait here only briefly before boarding the train. As a result, the following passengers have more space overall to spread out. However, if passengers have to wait a long time in front of the doors, they take up a lot of space. For the following passengers it becomes difficult to give way, so they have to go through which increases the densities especially in the staircase area. Nevertheless, as mentioned in the evaluation of the previous studies, it may make sense to keep the doors closed for longer. In general, filling the platform from the back to the front is considered more sensible, so that there are no backlogs on the stairs due to waiting or boarding passengers. Figure 3.40 shows the result for this case. Here the densities on the platforms have almost the same level independent of the door opening time. Keeping the doors closed can therefore be a good tool to encourage passengers to pass through.

Besides the densities in the staircase area, the tunnel must not be neglected. If critical densities occur here, dangerous situations for example in case of pushing can quickly arise because there are no possibilities for the passengers to get out of the way and reduce the pressure in the system. In order to avoid these, special consideration must be given to the time-delayed backlogs that occur in the various tunnel sections. Figure 3.41 shows in the marked area that congestion in the rear section of the tunnel (ID 65) leads to backlogs and rising densities in the front sections in a very short time. Depending on the distance between the individual sections, this takes less than 30 seconds and less than two minutes until the tailback has reached the entrance area. This temporal component is important for controlling the inflow rate. Immediate action is required. If too high densities are reacted too late, this can have fatal consequences. The densities

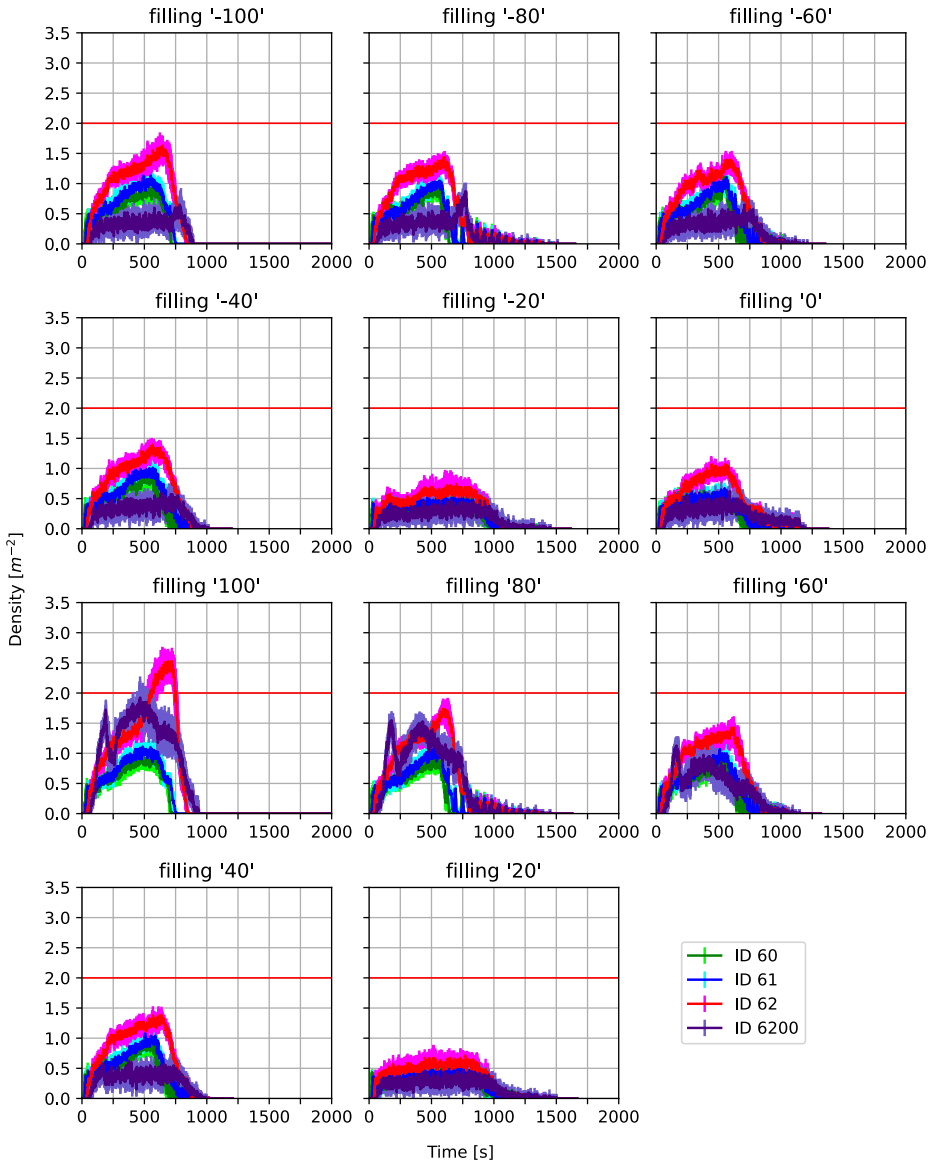


Figure 3.38.: Time-dependent densities as a function of the filling process for the example of platform 2 with an inflow rate of 4 s^{-1} .

in the tunnel are also strongly dependent on the distance from the platform to the entrance. Thereby the following applies for the same inflow, the greater the distance between the platform and the entrance, the lower the densities, compare figures 3.38 with B.1 in the appendix B. The reason for this is that the crowd spreads out over

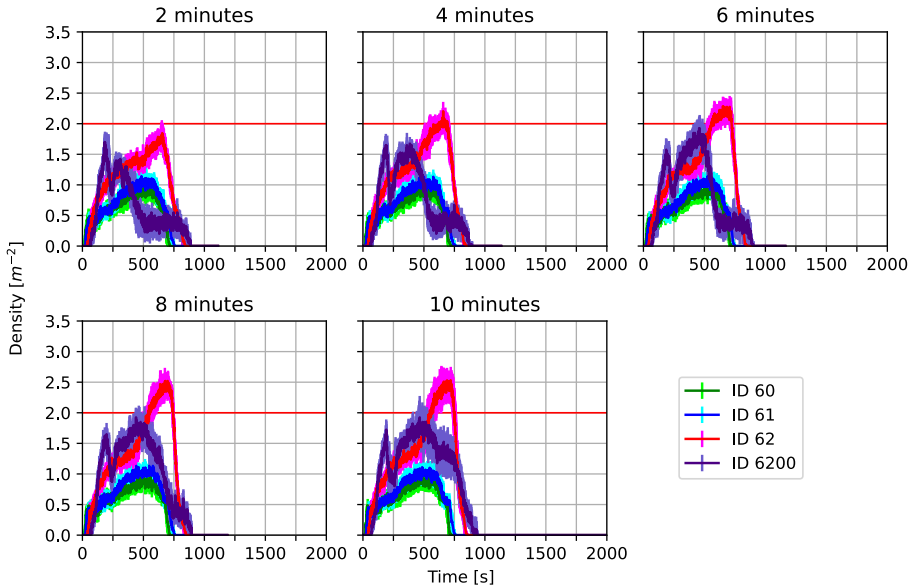


Figure 3.39.: Densities in dependence of the door opening times at the example of the filling process “100” (*fro-re*) on platform 2 with an inflow of 4 s^{-1} .

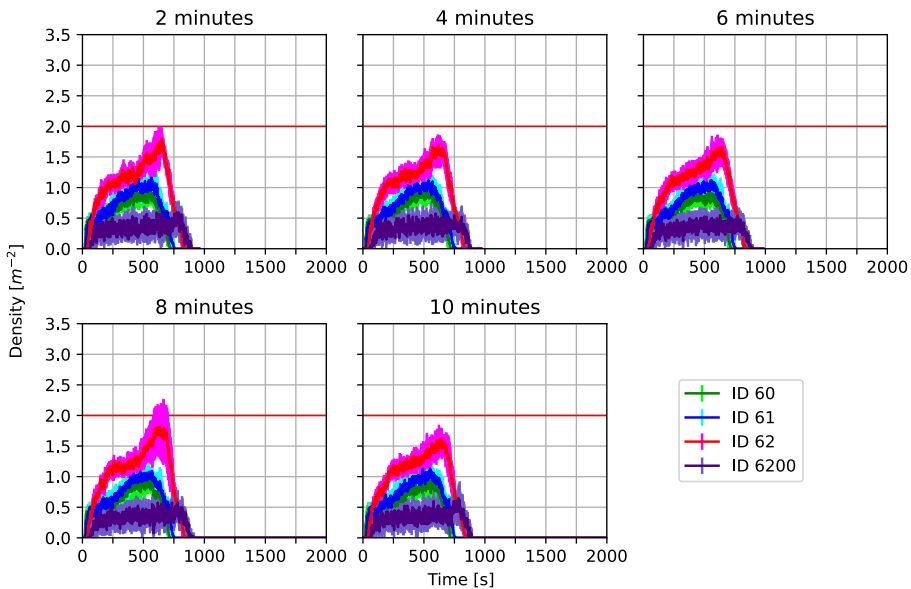


Figure 3.40.: Densities in dependence of the door opening times at the example of the filling process “-100” (*re-fro*) on platform 2 with an inflow of 4 s^{-1} .

distance. Thus, more passengers reach their free walking speed, and it takes longer until congestion occurs if the walking speed is reduced at the staircases and the walking movement is additionally obstructed by waiting passengers on the platform. This phenomenon is therefore independent of the filling process, even though this can have an additional negative effect.

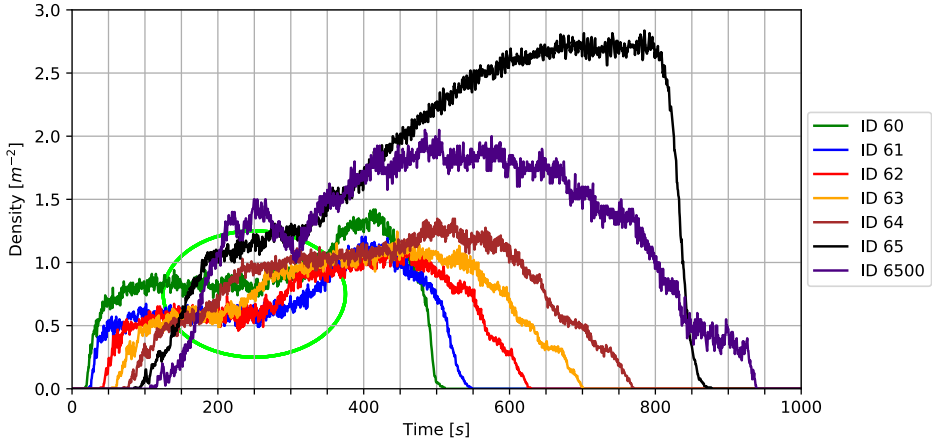


Figure 3.41.: Time-dependent delay in rising densities at the example of the filling process “100” on platform 5 with an inflow of 6 s^{-1} .

What is also noticeable in the comparison of the densities depending on the inflow rates is that there is hardly any difference between 6 s^{-1} and 12 s^{-1} , see figures B.2, B.3 and B.4 in appendix B. This suggests that the capacity of the geometry is already fully utilised at an inflow of 6 s^{-1} . Nevertheless, densities above 2 s^{-1} arise for almost every filling process. With an inflow of 4 s^{-1} , the densities are below this value and reach only 1.5 s^{-1} except in short peaks for some filling processes, see figure B.1 in appendix B. For this reason, an inflow of 4 s^{-1} can be assumed as safe. However, it must always be assessed individually in the respective situation whether throttling of the inflow rate is to be carried out for safety reasons. In the next section, the total evacuation times are considered in more detail, which also provide information about the optimal inflow rate.

3.2.4.2. Total Evacuation Times

In this section, the evaluation of the total evacuation times is carried out. In the following, total evacuation times are therefore defined as the maximum times which are required by the passengers to pass a measurement line. This refers to the evacuation times of the respective sections. These can also be referred to as *passing times*. As already mentioned in chapter 3.2.2, these values can also be used to create optimised arrival and departure plans for the trains. Figure 3.42 shows the times after 75% of passengers have passed the transitions, which were shown in figure 3.36, and 3.43 show the maximum values. For the different inflow rates, the times at which the filling at

the entrance is theoretically completed are marked. For an inflow rate of 2 s^{-1} this is 1,080 s, for 4 s^{-1} 540 s and for 6 s^{-1} 360 s.

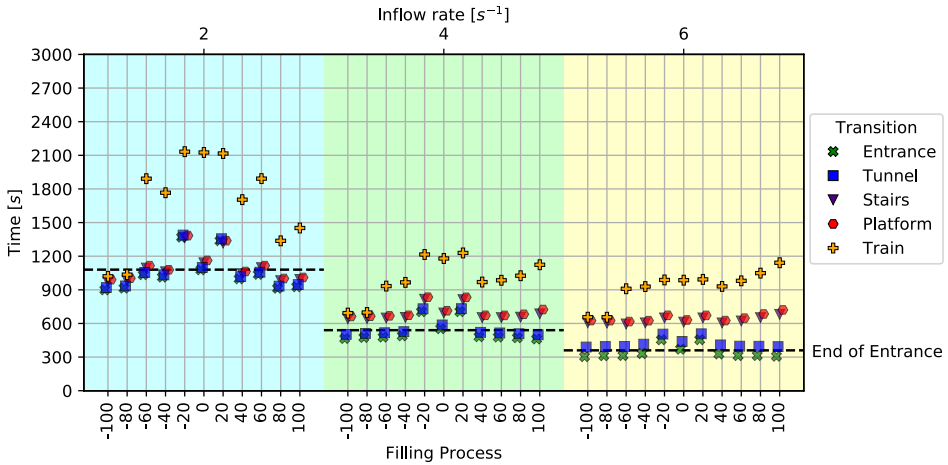


Figure 3.42.: Passing times of 75% of the passengers at the transitions between the station sections with different inflow rates.

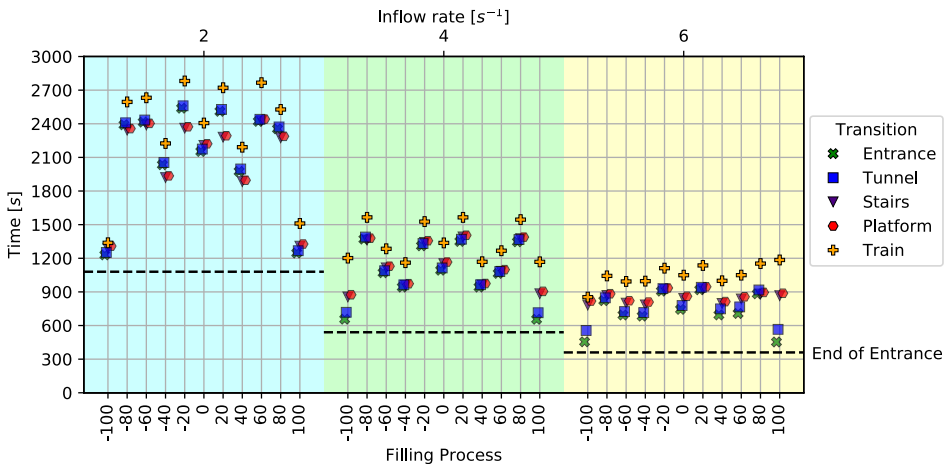


Figure 3.43.: Maximum passing times at the transitions between the station sections with different inflow rates.

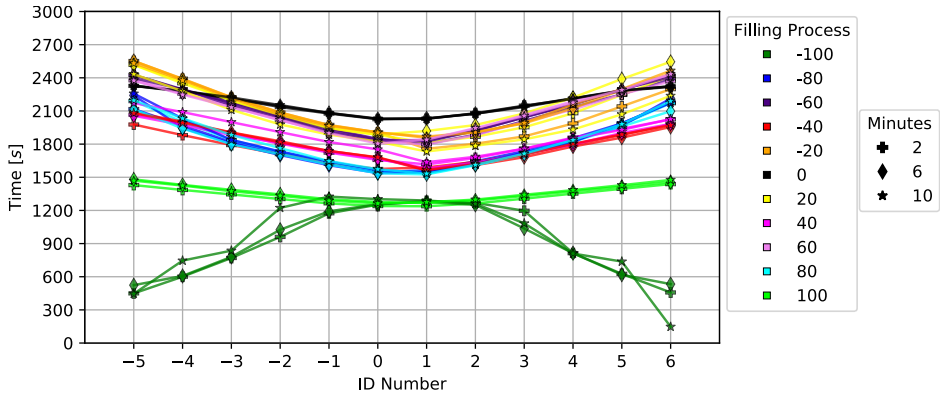
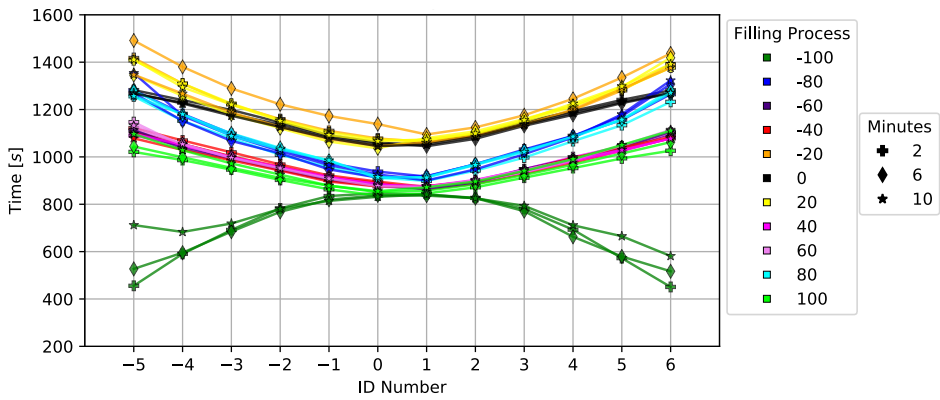
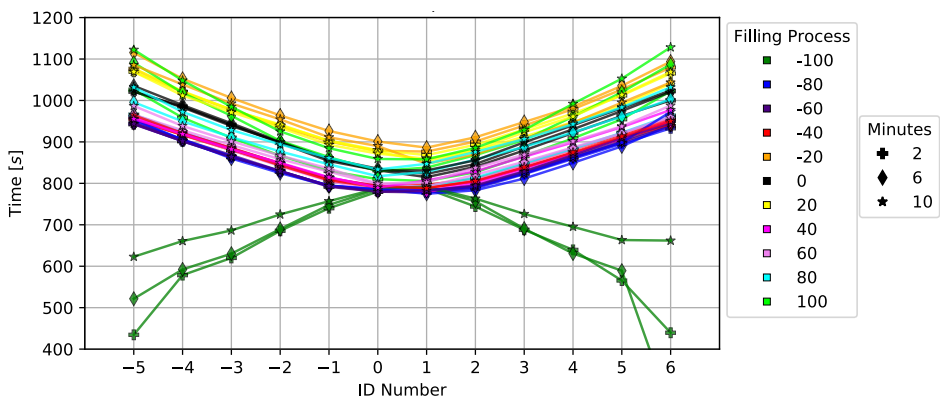
At the entrance, the filling processes should not yet have any influence on the passing times. In the 75% case this is also largely true. Here, the passing times of the first sections, i.e. at least up to the tunnel entrance, are at a similar level. For the rear sections and especially the times on the platform, clear differences become apparent between the filling processes depending on the individual inflow rates. While for 2 s^{-1} no clear structure can be observed, the values between 4 s^{-1} and 6 s^{-1} follow an increasing

course from the *re-fro* process “-100” with the lowest values to the *fro-re* process “100” with the highest values. The reason this progression only becomes visible at high inflow rates is due to the relationship between the times needed to cover the distances to the measurement lines, the inflow rate itself and the capacity of the most critical bottleneck, which here are the staircases. From the hand calculation, it can be seen that approximately 385 s would be needed until all passengers had passed the stairs. The total number of passengers is halved according to the number of staircases. Only with an inflow rate of 6 s^{-1} this value would be attainable. Below this, the passing times are determined by the inflow rate, as fewer passengers arrive at the staircase than it could actually hold. This means that, especially with a proportion of equally distributed passengers, longer passing times occur, because one passenger per door is generated at each source-dependent time step, so that both the first and the last train door are head to in each time step. Accordingly, the times increase compared to the *re-fro* process at least by the time needed to walk the distance between the first and the last door. This effect becomes even clearer with the maximum values in figure 3.43 and is explained further in the following section with the help of the length measurement lines.

3.2.4.3. Filling Processes – Distribution of Passengers over the Platform

The observation of the length evaluation lines provides information about the filling process of the platform. For this purpose, the times are evaluated which were reached after a defined number of passengers, here 95 % of the total number, have passed the measuring lines. The closer these times are to each other, the better the filling process can be rated, as this means uniform filling, which reduces the dwell time of the trains, so more passengers can be evacuated per time unit. However, the times themselves must not be neglected. High times that are close to each other have a lower rating than times that are far apart, but having an overall lower total evacuation time. It should also be taken into account at which point the higher times occur, at measurement lines with a long distance to the staircases or at measurement lines close to it. The latter is more favourable, as any stragglers have a shorter way to enter the train and thus delay the departure time less than stragglers who can only find space in one of the rear train wagons.

Figures 3.44 to 3.46 show the passing times at the length measurement lines of platform 3 with an inflow rate of 2 s^{-1} , 4 s^{-1} and 6 s^{-1} . At the first view, the results of the three cases only differ in the maximum times that occur, while the curves seem to be similar. However, if looking more closely at the graphs of the individual inflows, a shift in the extremes (processes “100” and “0”) can be observed. The first thing that immediately attracts attention in all cases is the big difference between the results for the filling process “-100”, which corresponds to the 100 % implementation rate of the filling process *re-fro*, and the other processes, including the gradations of the process *re-fro*. Although the corresponding curves are steep with time differences between the outer and middle measurement lines of several minutes, the overall evacuation times are below those of the other filling processes and the curve slopes towards the ends. This means, as mentioned above, that stragglers have less influence on the departure time. Based on the results of the previous studies in chapter 3.2.3.2, it could be expected that the filling process “100”, which is the 100 % implemented filling process *fro-re*,

Figure 3.44.: Passenger distribution with an inflow of 2 s^{-1} .Figure 3.45.: Passenger distribution with an inflow of 4 s^{-1} .Figure 3.46.: Passenger distribution with an inflow of 6 s^{-1} .

would show the worst results. The gradations of the processes *fro-re* and *re-fro*, which have different proportions of the equal distribution, would represent an improvement or deterioration of these results accordingly. However, these expectations are only partially fulfilled. Looking more closely at the results for the inflow 6 s^{-1} in figure 3.46, the results are most in line with the described expectations. The filling process “100” shows significantly higher evacuation times than the process “-100” and the values for the process “0”, which corresponds to an optimal equal distribution, lie between these two. The corresponding gradations of the distribution from the back to the front behave in such a way that they show correspondingly worse times with decreasing *re-fro* proportion. Since especially in the gradations between “0” and “100” the processes influence each other, due to waiting passengers at the staircases, the results improve only up to a certain degree.

With the inflow rates of 2 s^{-1} and 4 s^{-1} the process “100” with a furthermore quite flat curve shows the second-best times. Here, the equal distribution of passengers performs significantly worse. The gradations of the processes *fro-re* and *re-fro* are correspondingly worse in both cases. The reason for this is the inflow rate and the resulting passing times at the entrance. Since in the previous studies in chapter 3.2.3 only the platforms were considered, but not the way from the entrance to there, the influence becomes visible here for the first time. If calculating the time, which 2,160 passengers need to reach the platform by the two 4 m wide staircases, by hand, equation 2.2 results in a raw filling time of approximately 770 s. With an inflow rate of 2 s^{-1} , however, 1,080 s would be needed until all passengers had passed the entrance area, which is considerably longer than the raw filling time. The possible capacity is therefore not exhausted. In addition, according to equation 2.1, the walking times from the entrance to the destination door have to be added, to consider the last passengers entering the station. To reach the first door about 115 s are needed and for the last door about 250 s. Since the low utilisation also does not result in high densities or any kind of congestion (cf. section 3.2.4.1), the filling process is mainly dependent on the walking times. Here, also the implementation of the equal distributed passengers has a huge influence. As mentioned in section 3.2.4.2 one passenger per door is generated at each source-dependent time step. So, one of the last passengers, who enter the station, has to walk to the furthest train door. This is why the results of the “-100” and “100” processes are so close to each other, whereas their gradations with a portion of equal distribution show worse results. For the inflow rate 4 s^{-1} only 540 s are needed until all passengers have passed the entrance. Adding up the walking times, the total time is only slightly less than the raw filling time, so the capacity is almost exhausted. Thus, the walking time has less influence on the overall filling process and slight increases in the densities can be seen, cf. section 3.2.4.1. However, these do not reach critical values and thus have little influence on the overall filling process, so that the values of the length measurement lines are still close together. For an inflow rate of 6 s^{-1} only 360 s are needed until all passengers have passed the entrance. This is less than half of the raw filling time at the staircases. Here the filling processes have a correspondingly greater influence. There is a sharp increase in densities, which leads to backlogs and significantly influences the distribution of passengers. As mentioned above, the results are therefore most in line with expectations.

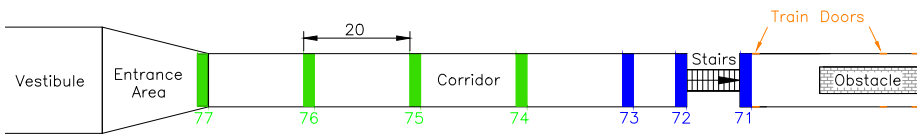
3.2.4.4. Interim Conclusion

The multivariate analysis of the different crowd management measures presented has shown the mutual dependencies of the individual measures on each other. Some measures have a greater, others a lesser impact on the overall process. First and foremost are the filling process and the inflow rate. The results of the filling processes clearly show that it is of great necessity that the concept is implemented sensibly, otherwise it can lead to negative developments. Ideally, sufficient, well-instructed, and trained personnel should be used for this purpose. However, since in the event of an evacuation it can be assumed that there will be fewer staff, it is necessary to consider how an optimal filling of the platforms can nevertheless be ensured. If the control of the trains allows it, it would be conceivable for the doors to be opened one after the other, in order to encourage passengers in this way to use the furthest train doors first.

The evaluation of the different inflow rates has shown that they have a decisive influence on the development of congestion and critical densities. If too high inflow rates are selected, life-threatening situations can quickly arise, e.g. in case of pushing, as there are no possibilities within the station to reduce the resulting pressure or to remove passengers in an emergency. The systems should be checked in advance for a maximum permissible inflow rate. Furthermore, it must be ensured that individual reduction of the inflow is possible at any time in order to be able to react to critical situations as quickly as possible. Furthermore, it has been shown that possible inflow rates depend very much on local conditions. Irrespective of new constructions or conversions, this can already be of importance for existing larger facilities. The distance from the entrance to the destination plays a major role here and can be considered in a platform-dependent time schedule.

3.3. Applicability to Variable Geometries

In these final studies, the various crowd management measures are transferred to another geometry. On the one hand, this represents an idealised train station which avoids corners where passengers have to change their walking direction by 90 degrees or more. On the other hand, it shows that the presented crowd management measures can also be applied to other geometries. Since the geometry is not a specific station geometry, the terminology, which was presented in figure 2.8, is used in the following. Additionally, it is no longer spoken of passengers, but of people in general. Figure 3.47 furthermore shows the location and designations of the measurement areas and measurement lines. It should be noted that the number of measurement areas varies with increasing corridor length. These areas are spaced at 20 m intervals and are marked in green, see figure 3.47a.



(a) Fixed- (blue) and variable (green) measurement areas in dependency of the corridor length.



(b) Measurement lines along the *Event Access Area*.

Figure 3.47.: Measurement areas and lines for setup 5.

For the investigations, not only the different crowd management measures are varied, but also the dimensions of the geometry. These vary on the one hand in the width of the staircase, which represents a critical bottleneck and decisively determines the inflow rate. On the other hand, the length of the corridor is varied. In this way, the influence of the distance from the *Entrance Area* to the *Event Access Area* is considered. These result in a total of 26,400 combinations for the simulation.

In addition, the influence of obstacles is investigated for this geometry. Their influence has not been considered so far, but is of great importance, especially for the filling process. In the case of a train station, obstacles for example represent the existing interior, such as benches, showcases, vending machines, rubbish bins or small information and lounge houses. Figure 3.48 shows setup 5 including obstacles. Since this is a symbolised representation of obstacles, no individual objects are shown, but everything

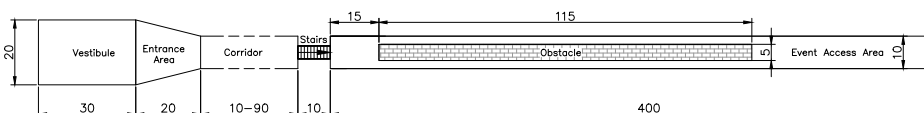


Figure 3.48.: Setup 5, including obstacles.

is represented in an idealised obstacle of $5\text{ m} \times 115\text{ m}$, which is located 15 m behind the staircase. As described in chapter 2.3.2.4, only selected cases of all crowd management measures are considered to analyse the influence of the obstacle.

3.3.1. Hand Calculation

From the evaluation of the previous studies, it is known that the capacity of the geometry is determined by the bottlenecks. If the selected inflow rate is lower than the capacity, congestion is only caused by the selected filling process, for example. If the inflow rate exceeds the capacity, further congestion is to be expected, which can then be positively or negatively influenced by the filling process. To determine the capacity of the system, the equations described in chapter 2.2 are used. Table 3.6 shows the results for the individual staircase widths and table 3.7 for the inflow rates. It should be noted that especially the times for the inflow rates do not consider any congestion. For example, with an inflow rate of 2 s^{-1} it will therefore take at least $1,080\text{ s}$ until all people have passed the entrance. Filling the platform by a 4 m wide staircase takes only about 770 s , according to manual calculation. The capacity is therefore not reached at this point. For occurring congestion, this means that it is purely caused by the chosen filling process and not by the inflow rate. This will be taken into account accordingly in the following when evaluating the densities and distribution of the people.

Staircase width [m]	4	6	8	10
Filling time one-sided [s]	771	514	385	308
Filling time double-sided [s]	1542	1028	770	616

Table 3.6.: Hand calculation: Filling times for different staircase widths.

Inflow rate [s^{-1}]:	2	4	6	8	10	12
Passing times one-sided [s]	1080	540	360	270	216	180
Passing times double-sided [s]	2160	1080	720	540	432	360

Table 3.7.: Hand calculation: Passing times at the entrance for different inflow rates.

3.3.2. Densities

Passenger safety is always a priority, so the first step of the evaluation of the simulation data, is to look at the densities occurring in the entrance area, the corridor and in the staircase area. For this purpose, the densities in the different measurement areas are evaluated and compared. The evaluation of the time-dependent densities in the measurement areas with ID 71 (platform access), ID 72 (staircase access) as well as in the variable measurement areas with IDs 73-77 shows in particular the influence of the filling process, the door opening times and the geometry changes. The influence of the different inflow rates is considered individually for each case.

In the first step, the influence of the door opening times is taken into account. Therefore, a case with an inflow rate of 2 s^{-1} and a stair width of 4 m is chosen. As tables 3.6

and 3.7 showed that the capacity of the geometry is not utilised in this case, all differences in the curvatures are directly attributable to the different door opening times. Figure 3.49 and figures C.1 and C.2 in appendix C show the densities for different filling processes and door opening times of 2 min, 6 min and 10 min. Overall, it can be observed that the densities for all gradations of the process *re-fro* show only slight

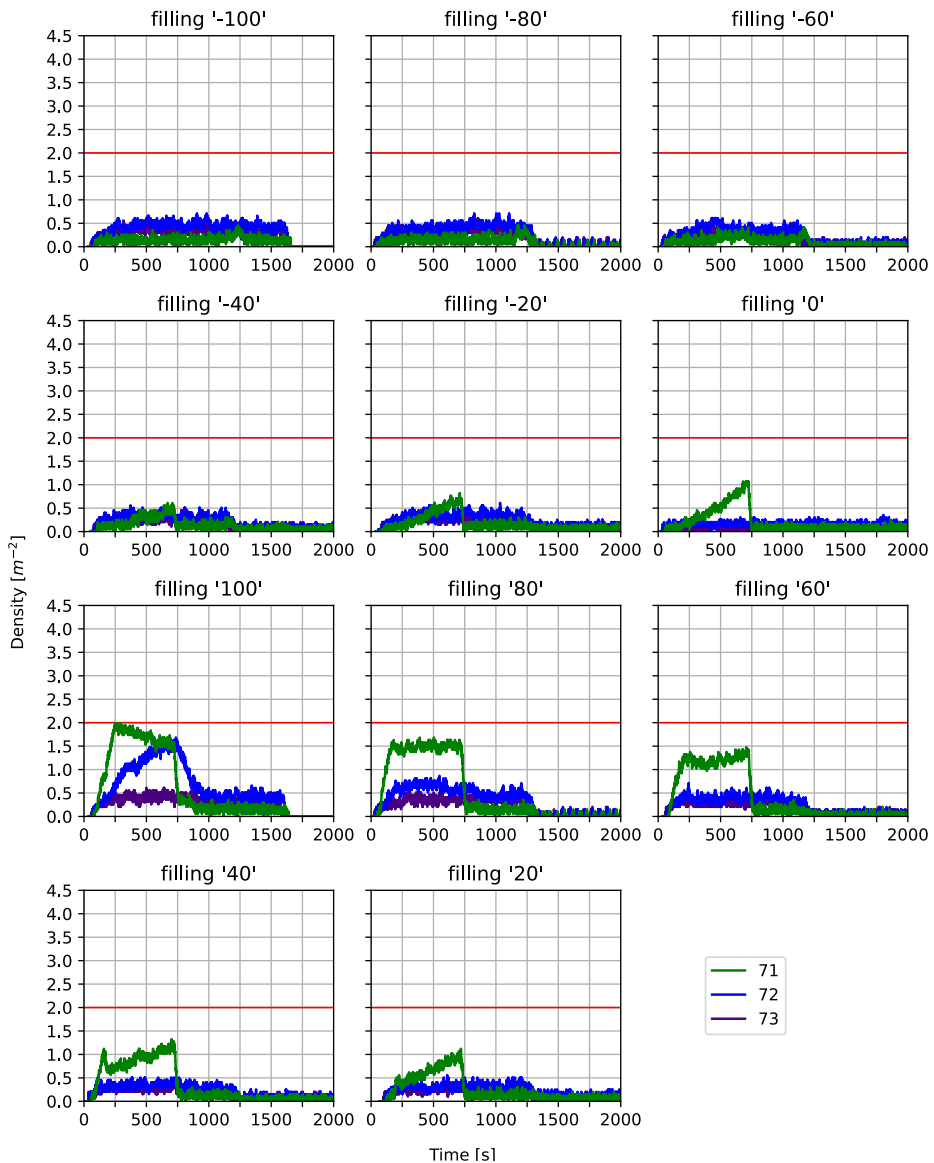


Figure 3.49.: Time-dependent densities for a corridor of 10 m, a staircase of 4 m, an inflow rate of 2 s^{-1} , and a door opening time of 10 min.

differences, see figure 3.49. For the other processes, the densities particularly in front of the staircase (ID 72) increase with increasing door opening times and the dwell time of the high densities in the staircase area of the *Event Access Area* (ID 71) lasts longer. The reason for this is that not all people have reached the final exits, when these are opened after a short time. So, there are fewer people waiting and after the opening point they enter the exits quickly. For the *fro-re* process, following people are not hindered by waiting people after this point. If in turn the doors open late, more people wait in front of the closed exits and block the way for following people, especially in the area of the staircase. This makes it difficult for them to go through, which further increases the density in this area. For tactical reasons, it may nevertheless be advisable to keep the train doors closed for a longer time, to ensure an optimal filling of the *Event Access Area* first. Hence, for the further investigation, only the results with a door opening time of 10 min are taken into account.

As already briefly shown, the filling process has a major influence on the formation of congestion and high densities not only in the classic station geometry but also here. For the example in figure 3.49, which shows the densities of the case with a short corridor length of 10 m, a staircase width of 4 m and an inflow rate of 2 s^{-1} , it is clearly visible that for the *re-fro* filling process and its gradations, no high-level densities occur. In the opposite case, borderline high densities are recorded in the staircase area of the *Event Access Area*, which, due to the number of following people, causes backlogs in the corridor (ID 72). Thereby, the densities decrease with an increasing proportion of equally distributed people, see figure 3.49 case “100” to “20”.

However, the inflow rate at the entrance is decisive for the occurrence of high densities and backlogs. The implementable inflow rate in turn is strongly dependent on the geometry. Figure 3.49 and figure C.3 in appendix C show that the length of the corridor can have a positive influence on the development of congestion and associated high densities. The longer the distance from the entrance area to the most critical bottleneck, in this case the staircase with the directly adjacent final exits, the lower the occurring densities in the staircase area. As already shown in chapter 3.2.2, the reason for this is the walking speed of the people. If a bottleneck follows immediately behind the entrance, the people do not reach their free walking speed before they have to slow down again. However, since all people strive to reach their destination quickly, which means at least at their free walking speed, this inevitably leads to congestion, since this effort is hindered by people slowing down. The threshold for congestion is therefore much lower. In a long corridor, the free walking speed can be reached and maintained for some time. This causes the crowd to disperse. When reaching the bottleneck, which requires a reduction in speed, it therefore takes longer until a visible backlog occurs, see figure C.3.

The width of the staircase, has a greater influence than the length of the corridor. The staircase represents a bottleneck by its very nature, as the walking speed is greatly reduced at this point compared to the flat corridor. If the inflow rate for a staircase width of 4 m is increased to 4 s^{-1} , also for the *re-fro* process congestion occur with densities that are far above the limit value of 2 m^{-2} , see figure 3.50. With a stair width of 4 m, a maximum inflow rate of 2 s^{-1} is therefore recommended. Figures C.4 to C.6 in appendix C show that increasing the staircase width makes it possible to increase the inflow rate. If considering the filling processes of *re-fro*, the inflow rate

can be increased by approximately two persons per second for every two additional metres of staircase width without causing significantly higher densities. The indicator for these values is a maximum density value of 2 m^{-2} in the measurement area inside the corridor, especially in front of the staircase (ID 72), which only lasts for a short time. Densities in the *Event Access Area* are allowed to exceed this value for the *re-fro* processes, as this only represents waiting people and no people are following.

Of course, in most cases the geometry is already predefined, but this must be taken into account, especially in the case of new buildings or conversions. Likewise, accesses at events can be influenced accordingly by appropriate barriers. With regard to the width of a staircase, it is important to ensure that there are sufficient railings. Young people also walk freely in the middle, but especially older passengers or those with heavy luggage prefer to walk along the railing.

All these results apply to the one-sided case, which means that only the exits of one side of the *Event Access Area* are used. This would be conceivable for event entrances, for example. The other side would then consist of a boundary, e.g. by special event barriers, an adjacent building or similar. For safety reasons on a platform, however, a double-sided filling may be preferred. This is therefore also briefly considered in the following. Figure C.7 in appendix C shows the densities of the double-sided case with a small corridor length, a staircase width of 4 m and an inflow rate of 2 s^{-1} . As the double number of people use the geometry, the overall process last longer, on the one hand. For the densities of the processes *re-fro* (“-100” to “-20”) in figure C.7, there are no differences to the one-sided case in figure 3.49 except these longer time values. On the other hand, since both sides are used, a larger total area is occupied by waiting and boarding passengers. Following passengers therefore have less space to avoid the crowd and have to go through. Figure C.7 shows, this has a negative effect, especially for the filling process *fro-re* and its gradations, which leads to increasing densities, compared to the one-sided case in figure 3.49.

If the inflow rate is now increased for the cases with wider staircases and longer corridors, the increase is not equivalent to the one-sided case. Figure C.8 shows the case of a 6 m staircase and an inflow rate of 4 s^{-1} . Taking the *re-fro* processes into account, this shows still good values. Looking on the other hand at the densities of the cases with 8 m and 10 m wide staircases and an inflow rate of 6 s^{-1} in figures C.9 and C.10 in appendix C, the densities inside the corridor increase over the limit values. Hence, for the double-sided case, an inflow rate between 4 s^{-1} and 6 s^{-1} is the very limit. Besides this, the filling process from the front to the back should be dispensed with in any case.

The same recommendation applies to the use of obstacles. As mentioned above, the idealized obstacle of $5 \text{ m} \times 115 \text{ m}$ represents various facilities such as display boards, rubbish bins, benches, ticket machines or food stands. Looking at the evaluation of the densities especially at the beginning of the *Event Access Area* for the case with a short corridor and a low inflow rate of 2 s^{-1} , figure 3.51 shows that there is a clear increase in densities, compared to the case without obstacles in figure 3.49. The reason for this is that people aiming for final exits at the back of the *Event Access Area* have a significantly reduced free area to get to their destination. This is especially critical if people are already waiting in front of the nearest exits. The space they occupy makes it difficult to get through, and since there are several final exits in the area of the

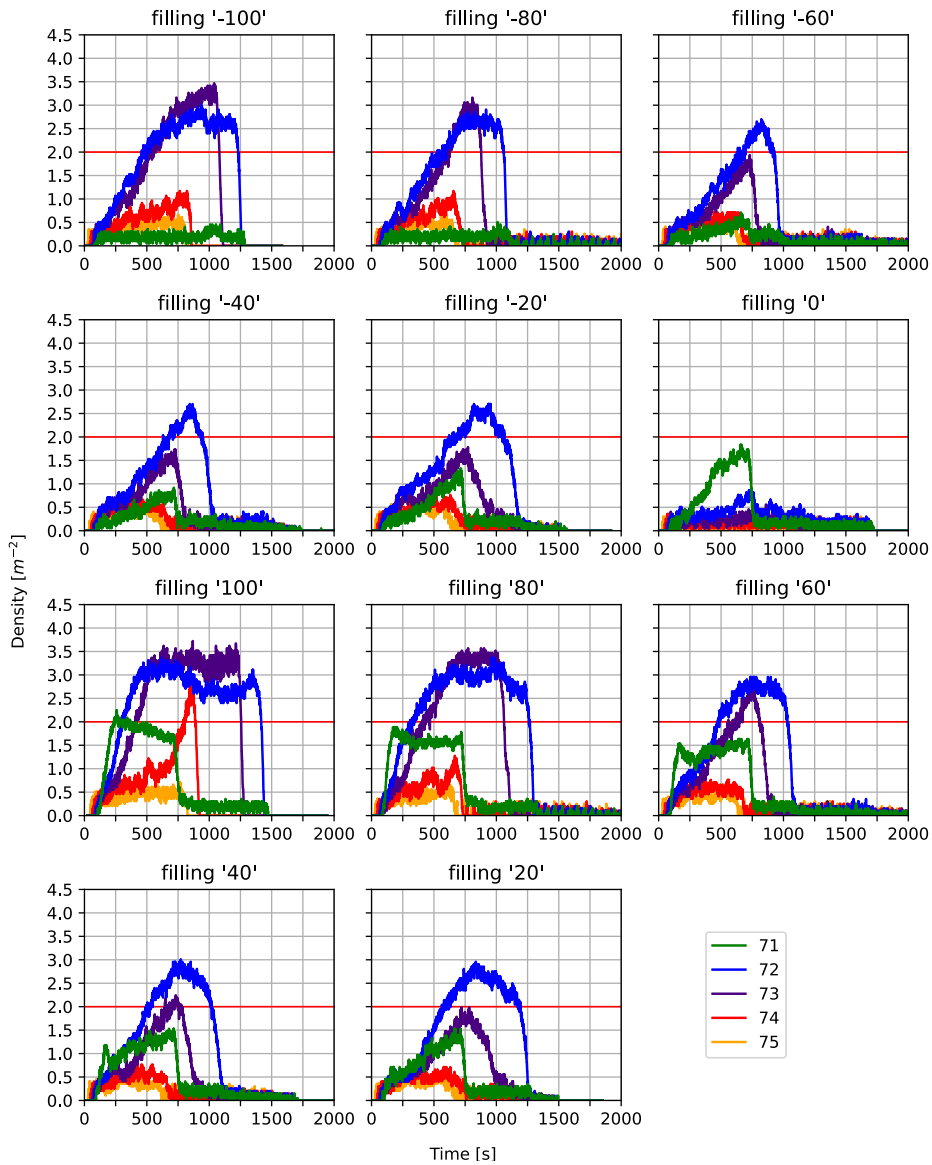


Figure 3.50.: Time-dependent densities for a corridor of 50 m, a staircase of 4 m, and an inflow rate of $4 s^{-1}$.

obstacle, it is not possible to pass by on the other side for people having one of these exits as final goal.

This situation would be exacerbated in the case of double-sided use. There, the second side may also be blocked by waiting people. So, there would be nothing left but to move through the waiting people on one side or the other. However, this leads to very

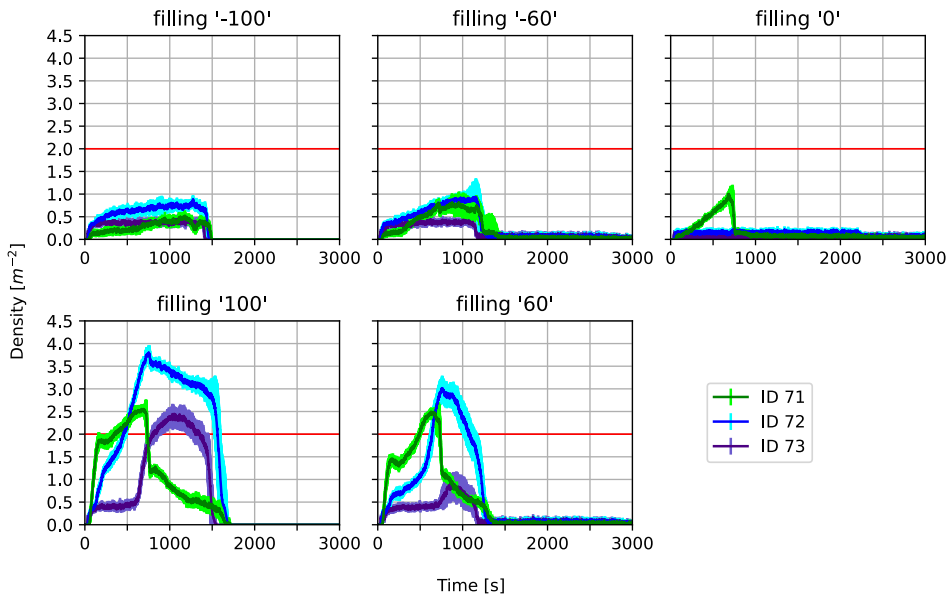


Figure 3.51.: Time-dependent densities for a one-sided filling with obstacle, a corridor of 10 m, a staircase of 4 m, and an inflow rate of 2 s^{-1} .

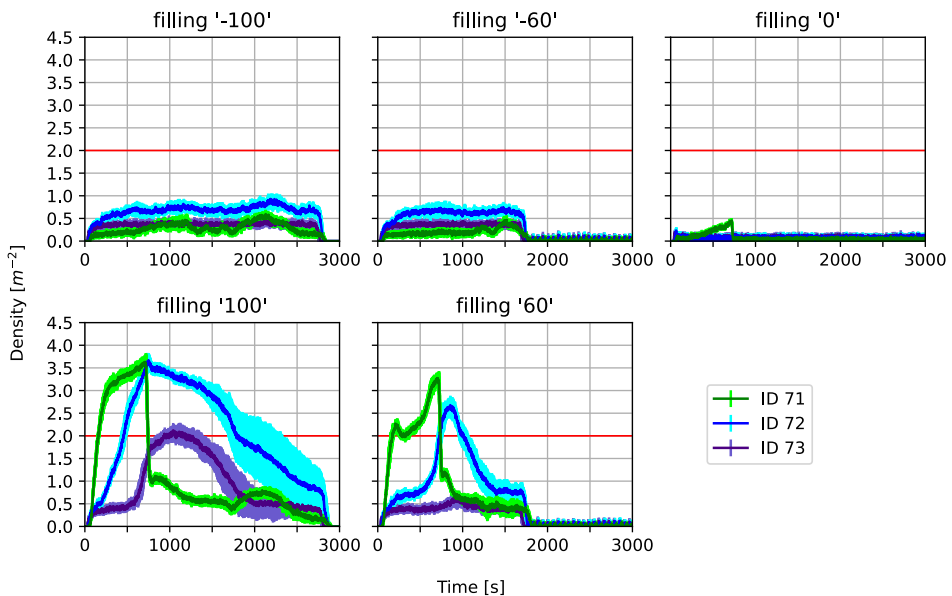


Figure 3.52.: Time-dependent densities for a double-sided filling with obstacle, a corridor of 10 m, a staircase of 4 m, and an inflow rate of 2 s^{-1} .

high densities with almost 4 m^{-2} on the *Event Access Area* and in the corridor in front of the staircase, see figure 3.52. As the area is limited by the obstacle and the exits to the side and there are thus no possibilities for evasion, this can lead to life-threatening situations under certain circumstances. For these reasons, a filling process from the back to the front should be implemented in any case.

Considering a geometry with a longer corridor and a wider staircase, better density values are recorded for an inflow rate of 2 s^{-1} and the one-sided case, see figure C.11 in appendix C in comparison to figure 3.51. Nevertheless, to increase the inflow rate with increasing stair width is only conditionally possible for a strict implementation of filling process *re-fro*, see figures C.12 and C.13 in appendix C. For the other filling processes, an increase in the inflow rate despite a wide staircase of 8 m leads to backlogs up to the middle of the corridor, with densities approaching 4 m^{-2} . For the double-sided case, an increase of the inflow rate is not possible for any filling process or geometry variation. Figure 3.53 shows the densities of the 100% implemented *re-fro* process (“-100”) with an inflow rate of 4 s^{-1} and the most favourable geometry variation with a staircase width of 8 m and the longest corridor with a length of 90 m. Nevertheless, the values reach levels beyond all limits.

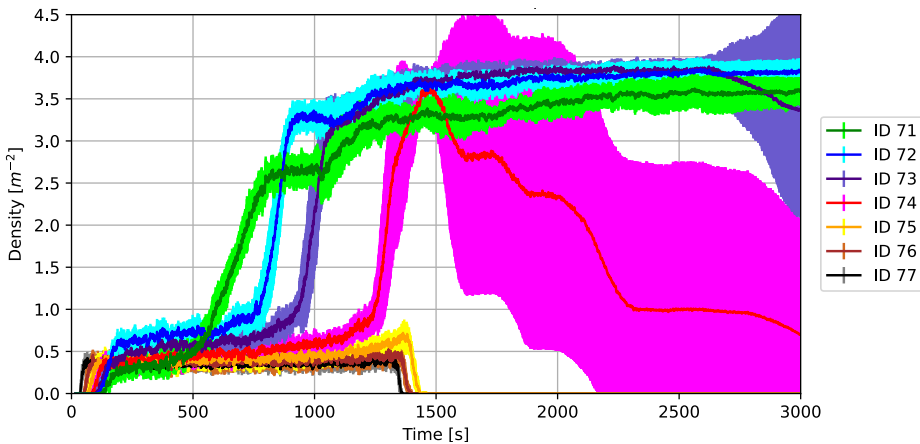


Figure 3.53.: Time-dependent densities of the filling process “-100” (*re-fro*) for the double-sided filling with obstacle, a corridor of 90 m, a staircase of 8 m, and an inflow rate of 4 s^{-1} .

3.3.3. Maximum Evacuation Times and Peoples Distribution along the Event Access Area

In the following, the filling process is considered on the basis of the length measurement lines and the maximum evacuation times. The evaluation of the length measurement lines is, as previously also described in the sections 3.2.3 and 3.2.4, a very good way to assess the distribution of people on the *Event Access Area*. This in turn provides information about the effectiveness of the chosen filling process. The location and

designation of the measurement lines were shown in figure 3.47b. The maximum evacuation times at the final exits allow further conclusions to be drawn about the filling process, as they also consider the door opening times. In the length measurement lines, these only have an influence if waiting people block the way for following people. Since the chosen setup has significantly longer walking distances on the *Event Access Area* than the classic station geometry with two entrances placed in the centre of the platform, the influence of the walking distances during the filling process must also be taken into account.

Figure 3.54 shows the maximum evacuation times depending on the filling process for different inflow rates. The maximum evacuation times result from the time the last person needs to enter a final exit. It can be clearly seen that the evacuation times for an inflow rate of 2 s^{-1} are significantly higher than for 4 s^{-1} . As already mentioned in the evaluation of the densities, the reason here is also the utilisation of the natural capacity of the geometry, which is described by the bottleneck of the staircase. As shown in section 3.3.1, the filling at the entrance takes longer at an inflow rate of 2 s^{-1} than the filling of the *Event Access Area* via the staircase. At 4 s^{-1} this circumstance has already been reversed. Taking into account the walking times, the inflow and the filling are approximately in balance, which means that the evacuation times are lower overall. The difference between the evacuation times with inflow rates of 4 s^{-1} and 6 s^{-1} is smaller. People pass the entrance in a much shorter time, but this also creates congestion, which slows down the process of filling. A further increase of the inflow rate has therefore no further positive effect on the evacuation time. Hence, between 6 s^{-1} and 12 s^{-1} , no major differences are visible.

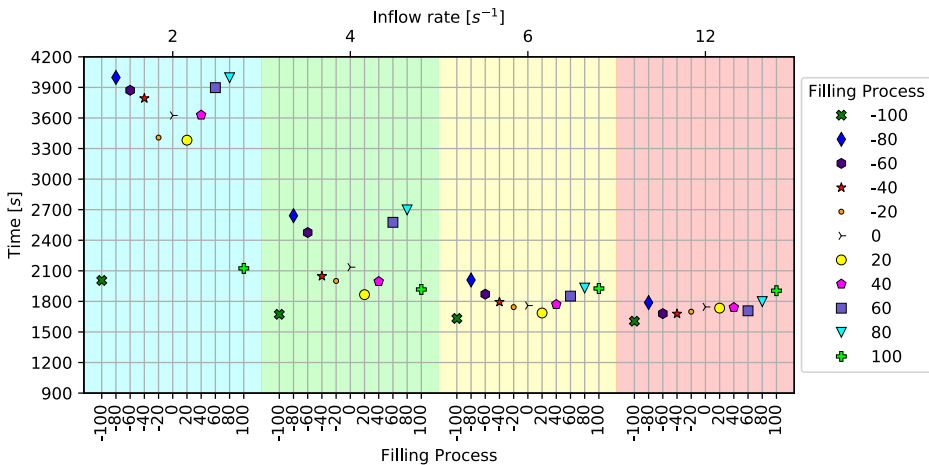


Figure 3.54.: Maximum evacuation times for different inflow rates, a corridor of 90 m and a staircase of 4 m.

What is striking in addition to the general time level between the inflow rates are the differences in the filling processes. While at inflow rates of 2 s^{-1} and 4 s^{-1} all processes with a share of equally distributed people show significantly higher values than the extremes *re-fro* and *fro-re*, an increase from *re-fro* to *fro-re* can be seen especially in

the maximum inflow rates. As described in section 2.3.2.4, an equal distribution of people means that with each source-dependent time step one person is introduced into the system for each train door. This means that the maximum occurring times are correspondingly higher, since here the walking times have a strong impact.

The equal distribution of people as a deviation from the desired process was chosen here for model-related reasons. Since each person that is introduced into the system must be assigned a corresponding goal, the modelling of deviating people is not possible in any other way. The fact that this strongly influences the processes when considering maximum values can therefore be seen as a limitation of the method.

In order to clarify this limitation and still be able to make a statement about the filling processes, figure 3.55 shows the results of the length measurement lines with the values of the passing times for the last person entering the measurement lines. Figure 3.56 shows the same case, but with the times that are needed until 50 % of the people have entered the measurement lines. Here the difference becomes clear very quickly. The curves of the 50 % values reflect the filling processes very well. For the filling processes from the back to the front, a very even distribution can be observed, whereas with the *fro-re* processes the times increase continuously from measurement lines 1 to 12. Up to an implementation rate of 60 % of the selected process, the times are correspondingly better. After this point, the proportion of equally distributed people predominates and the times increase. Accordingly, the case of 100 % equal distribution has the worst values. For the maximum values, the curves look quite different. Here, the course of the curves with a proportion of equally distributed people mainly reflects the difference in the walking distances, which is approximately 300 s between the first and the last measurement line. For this reason, these curves are parallel to each other. A qualitative statement about the filling processes is not possible.

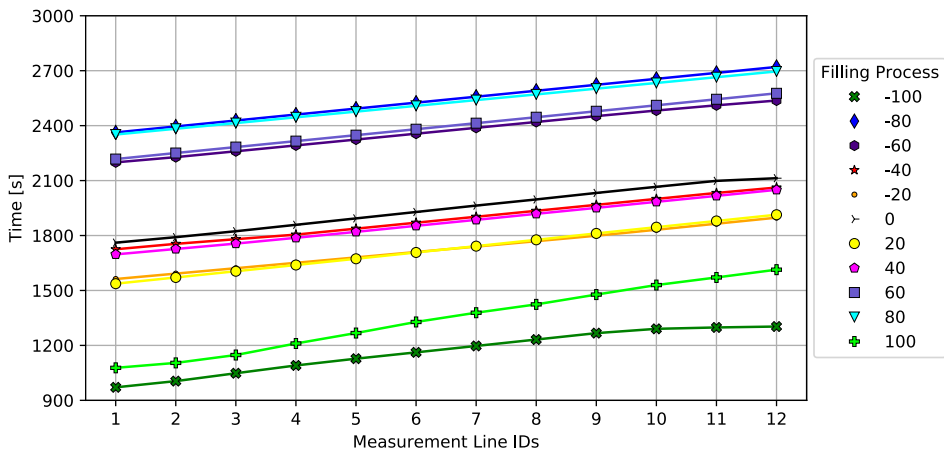


Figure 3.55.: Distribution over the *Event Access Area* in dependency of the filling process for the maximum number of people.

Taking these findings into account, the results for the case with obstacle are considered below. Looking at the results of the length measurement lines, both the maximum time values and the 50 % values have to be taken into account for the evaluation of people's

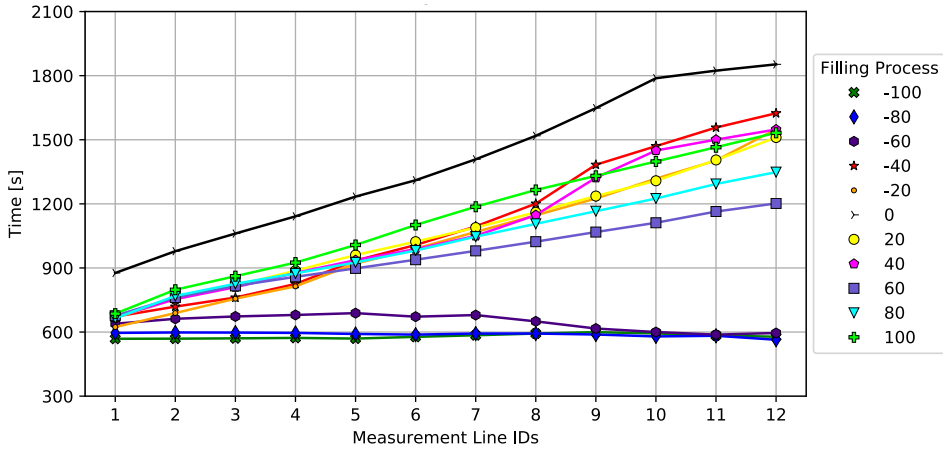


Figure 3.56.: Distribution over the *Event Access Area* in dependency of the filling process for 50% of the people.

distribution. The maximum values are shown in figure 3.57 and the 50% values in figure 3.58. By narrowing the cross-section through the obstacle, the flow in this area is throttled, which has a great influence on the filling process. Looking at the 50% values, it can be found that the difference between *re-fro* and *fro-re* becomes larger than for the case without obstacles. Moreover, the course of the curves is influenced by the obstacle. For all filling processes, the time values rise steeply between the first and the second measurement line. For the process *re-fro*, the time values at the measurement lines behind the obstacle additionally drop off, which can be particularly observed in figure 3.57 for case “-100” and in figure 3.58 for case “-60”. This effect occurs because

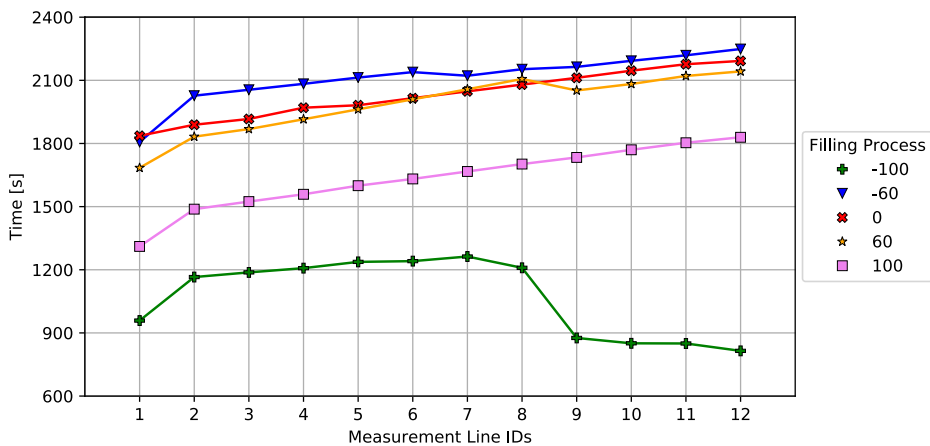


Figure 3.57.: Distribution over the *Event Access Area* with obstacle in dependency of the filling process for the maximum number of people.

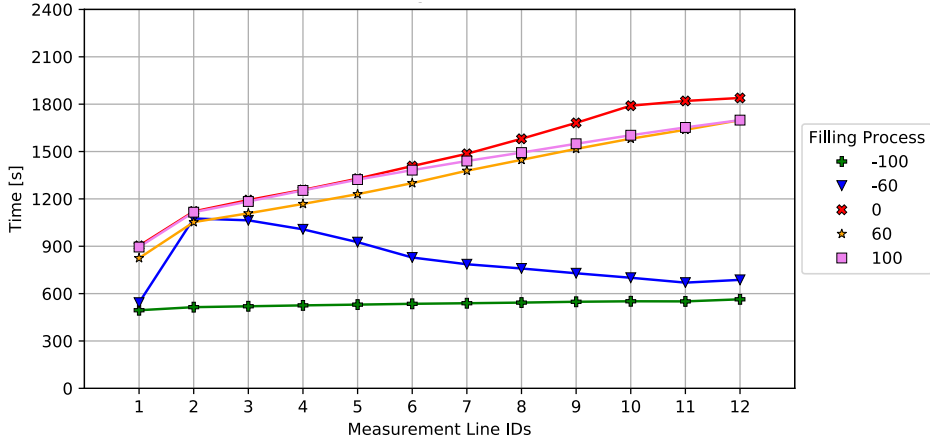


Figure 3.58.: Distribution over the *Event Access Area* with obstacle in dependency of the filling process for 50% of the people.

both sides next to the obstacle are initially available to the people when considering the *re-fro* process. At the doors in the area of the obstacle, the space is limited, which increases the overall times.

Comparing the maximum and the 50% values, in figures 3.57 and 3.58, with each other, the influence of the equal distribution can be observed again. While the filling processes with a proportion of equally distributed people in the 50% case still show similar time values to the two extremes *fro-re* and *re-fro*, their maximum values have risen sharply again, see figure 3.57. Nevertheless, the curvatures show the influence of the obstacles, too.

In these studies, it has been found, that the influence of the equal distributed people does not only depend on the walking paths of the last people, but also on the general implementation of the people by the sources. The people are implemented in such a way that for the mixed processes at each time step there are people for both processes, *fro-re* or *re-fro* and the equal distribution. It was taken into account that the people have enough time to leave the area of the sources before new people are created in the next time step. At this point, however, there are temporary delays in producing people for the equal distribution, which makes the process take longer overall and further increases the influence on the maximum evacuation times. This is a model limitation and can be considered respectively.

3.3.4. Interim Conclusion

The evaluation of the transferred multivariate crowd management measures on a variable geometry has shown that an applicability of the examined measures is also possible on other geometries. Furthermore, it became apparent that the effectiveness of the individual measures strongly depends on the structure of the geometry. The width of the most critical bottleneck, for example, has a decisive influence on the greatest possible inflow rate. The inclusion of obstacles also showed that this is a factor that should not

be neglected. Particularly on narrow platforms, this can lead to great difficulties when another filling process than from the back to the front is implemented. These findings can help to optimise the design of platforms, for example by installing facilities further away from the staircases or to distribute them more widely so that larger gaps are created. When transferring this to event technology, where obstacles are represented e.g. by sales stands, their placement should also be critically questioned.

Besides this, the usage of sources to create new people during the simulation has been detected to be another modelling limitation. Especially the implementation of equal distributed passengers, to model people who do not follow the ordered filling process, causes problems. As the people do not leave the sources as fast as it was expected, a time delay of producing new people occurs, which creates an imbalance between the processes *re-fro* or *fro-re* and the equal distribution. Nevertheless, this problem can be solved by implementing the sources more sensitive. Therefore, a detailed analysis of the sources should be conducted in future works.

4. Conclusion

The aim of this thesis was to investigate the pedestrian dynamics within a train station in order to evaluate and increase the capacity of the station in the event of an extraordinary event with a resulting excessively high passenger volume. In particular, methods were presented which, by means of simulation studies, make it possible to identify critical bottlenecks within a station or other geometries, in order to develop various crowd management measures on this basis and to examine their effectiveness in increasing capacity. Since an extraordinary event is assumed, where personnel and material resources may be limited, various assumptions were made for the study. For example, the station is available solely for this purpose. Thus, there are no disruptions caused by passengers alighting and moving through the station. For safety reasons, it is assumed that the trains have already arrived at the platforms before the passengers enter the platform. Furthermore, all the measures considered are designed to operate without additional material and with as little personnel as possible. An example of this is the inflow regulation via the entrance doors.

The approach of the methodology in the first step is to look at the system without any form of measures. Specifically, this means that all available entrances are used, and all platforms are filled simultaneously. Here, the bidirectional flow, which occurs when several opposite entrances are used, poses a particular problem. The crossing passenger flows obstruct each other and thus cause major congestion in the access routes. This in turn can lead to dangerous crowding with serious consequences, e.g. in case of pushing. Based on this result, initial measures are developed in a second step to improve the overall process. The results are reviewed again and further measures are then developed on this basis. In this way, various measures are successively checked for their effectiveness. In addition to the increase in capacity, the safety of all people plays an overriding role. In the case of the exclusive use of a single entrance or several adjacent entrances, the simultaneous filling of the platforms was generally classified as critical, since the passenger flows also block each other here. The resulting measure was a separate filling of the platforms. At this point, a method for creating detailed arrival and departure schedules was also proposed. This is developed from the times that the passenger groups need to pass through the individual sections of the station. In addition, the cross-section narrowing between the entrance area and the tunnel, as well as the staircases, were identified as further critical bottlenecks. Congestion occurs there, which can lead to dangerous crowding. As a measure, a reduction of the inflow would have eliminated these congestion to a large extent. However, it was found that additionally a software limitation comes into play here. The stairs require routing around 90-degree corners. Since all passengers choose the shortest route in the simulation, regardless of whether a further route would be faster, this favours congestion in front of the stairs. In the further investigations, various approaches were therefore presented to how the influence of the software limitation can be minimised and at the

same time qualitative statements on the measures are possible.

Based on the findings about the identified bottlenecks, various crowd management measures to increase the capacity of the system were thus presented in the final steps. Their interaction was examined in a multivariate analysis. This particularly includes the inflow to the system, which is a crucial setting to avoid congestion and dangerous crowding. Therefore, when assessing a station for the use during an exceptional event with greatly increased passenger volumes, a maximum inflow should be set in advance. Nevertheless, it must be possible to reduce the inflow rate at any time in order to be able to react to extraordinary events as quickly as possible. The filling process of the platforms, i.e. whether they are filled from the back to the front or from the front to the back, also plays a decisive role in avoiding congestion, especially in the staircase area. This is particularly important with regard to the use of escalators. The evaluation has shown that filling from the back to the front generally has a positive influence on the overall filling. Congestion is avoided and by distributing the passengers to the train doors, an even filling is guaranteed and the dwell time of the trains is reduced accordingly. Since the implementation of this filling method requires a lot of personnel, the effect of different degrees of implementation on the entire process was illustrated. Opposite filling from front to back, which corresponds to the most probable filling without the use of personnel, generally has a negative effect. Here, congestion is favoured, especially in the area of the staircases. As a result, lower inflow rates have to be set to ensure the safety of people. In addition, the use of escalators, for example, is not possible due to the high risk of backlogs. Filling from the front to the back also results in longer dwell times of the trains, as the people on the platforms are unevenly distributed in time, which means that stragglers, for example, have to cover a very long distance before boarding the train.

In summary, the simulation studies can be used to uncover general critical bottlenecks in a system and thus successively develop and test measures for improvement. However, it must not be assumed that there is an absolute, universally valid solution. As the last studies of variable geometry have shown, many measures are strongly dependent on the existing infrastructure and must be flexibly adaptable depending on the situation. Likewise, all results must be considered critically at all times, taking into account the software limitations accordingly.

5. Outlook

The methodology presented in this thesis for increasing the capacity of train stations in the case of extraordinary events with greatly increased passenger volumes is only one component in the overall context of evacuation planning or the transport planning of major events. Taking this overall context into account, the studies can be expanded accordingly. A detailed analysis of the people arriving at the station, for example, would give conclusions about required restraint areas. In addition, further measures can be investigated, which can also be used in the planning of events where both large personnel and material efforts can be made. This could include, for example, way finding systems in more complex geometries with intermediate waiting areas. Similarly, the impact of arriving passengers could be investigated with and without separation of passenger flows. Considering the new function in JPScore, the *trains*, it would also be possible to run longer scenarios, which take into account the situation-dependant use of different measures as well as detailed train schedules.

In addition, existing concepts, which were developed, for example, for the transport of spectators at critical football matches, can also be examined. In this way, entire concepts or only individual parts of it can be critically assessed and optimised, considering the experience gained. In addition, the components of existing concepts can be used in other scenarios within the same building and tested in advance for their effectiveness. The possibilities for this are manifold. In addition, the required effort to investigate changes in the planning concept considering the same building, after initial application, is relatively low in relation to the benefits.

Bibliography

- [1] Nirajan Shiwakoti, Zhiyuan Liu, Trent Edward William Hopkins, and William Young. An overview on multimodal emergency evacuation in an urban network. In Brendan O’Keeffe, editor, *Australasian Transport Research Forum 2013 Proceedings*, pages 1 – 10. Australian National Audit Office, October 2013.
- [2] Todd Litman. Lessons from Katrina and Rita: What major disasters can teach transportation planners. *Journal of Transportation Engineering*, 132(1):11–18, 2006.
- [3] Daniel Baldwin Hess and Julie C. Gotham. Multi-modal mass evacuation in Upstate New York: A review of disaster plans. *Journal of Homeland Security and Emergency Management*, 4(3), 2007.
- [4] John L. Renne, Thomas W. Sanchez, and Todd Litman. Carless and special needs evacuation planning: A literature review. *Journal of Planning Literature*, 2011.
- [5] Pamela Murray-Tuite, Brian Wolshon, and Deborah Matherly. Evacuation and emergency transportation - techniques and strategies for systems resilience. *TR News - Transportation Systems Resilience - Preparation, Recovery, and Adaptation*, 311(September - October):20–26, 2017.
- [6] Evangelos I. Kaisar, Linda Hess, and Alicia Benazir Portal Paloma. An emergency evacuation planning model for special needs populations using public transit systems. *Journal of Public Transportation*, 15(2), 2012.
- [7] Hossam Abdelgawad and Baher Abdulhai. Large-scale evacuation using subway and bus transit: Approach and application in city of Toronto. *Journal of Transportation Engineering*, 138(10):1215–1232, 2012.
- [8] Tanka Nath Dhamala and Iswar Mani Adhikari. On evacuation planning optimization problems from transit-based perspective. *International Journal of Operations Research*, 15(1):29–47, 2018.
- [9] Fatemeh Sayyady and Sandra D. Eksioğlu. Optimizing the use of public transit system during no-notice evacuation of urban areas. *Computers & Industrial Engineering*, 59(4):488–495, 2010.
- [10] Ressort Verkehr Verkehrspolitik Allgemeiner Deutscher Automobile-Club (ADAC). *Staubilanz 2018*, January 2019.
- [11] AG Fukushima UAG Evakuierungsplanung. Rahmenempfehlung für die Planung und Durchführung von Evakuierungsmaßnahmen einschließlich der Evakuierung für eine erweiterte Region (RE Evakuierungsplanung), August 2014.

- [12] Presidenza del Consiglio dei Ministri Dipartimento della Protezione Civile. Proposta di aggiornamento - Aggiunte e varianti alle parti A3, B, C1 e C2 della pianificazione nazionale d'emergenza dell'area vesuviana, March 2001.
- [13] Presidenza del Consiglio dei Ministri Dipartimento della Protezione Civile. Aggiornamento dei Piani di Emergenza Per il Rischio Vulcanico Nell'area Vesuviana e Nell'area Flegrea - Piano di allontanamento definitivo - Rapporto finale. Technical report, Universita' Degli Studi di Roma "La Sapienza" - Dipartimento Idraulica Trasporti e Strade, November 2006.
- [14] Luke David VanLandegen and Xuwei Chen. Microsimulation of large-scale evacuations utilizing metrorail transit. *Applied Geography*, 32(2):787–797, 2012.
- [15] Anzahl der Besucher und Reisenden ausgewählter Bahnhöfe in Deutschland pro Tag im Jahr 2017. URL: <https://www.handelsdaten.de/deutschsprachiger-einzelhandel/travel-retail-taegliche-anzahl-besucher-reisenden-bahnhoefe>, 2017.
- [16] Ye Pu, Hong Xu, and Xin Nie. Study on the bottleneck of urban rail transit station based on the operation safety. In *IOP Conference Series: Materials Science and Engineering*, volume 392, August 2018.
- [17] Zhibin Jiang, Wei Fan, Wei Liu, Zhu Bingqin, and Jinjing Gu. Reinforcement learning approach for coordinated passenger inflow control of urban rail transit in peak hours. *Transportation Research Part C: Emerging Technologies*, 88:1–16, 2018.
- [18] Serge P. Hoogendoorn, Miklos Hauser, and Nuno Rodrigues. Application of microscopic pedestrian flow simulation to station design evaluation in Lisbon train stations. In TRB, editor, *Transportation Research Board Annual pre-print CD-Rom*, pages 1–18. Transportation Research Board (TRB), January 2004.
- [19] Bernd Belka. *Maßnahmenkatalog zur Verringerung von hohen Personendichten beim abströmenden Personenstrom am S Bahnhof Merkur Spiel Arena*. Special Security Services Deutschland SSSD GmbH, September 2019.
- [20] You Wu, Jie Xu, Limin Jia, and Yong Qin. Estimation of emergency evacuation capacity for subway stations. *Journal of Transportation Safety & Security*, 10(6):586–601, 2018.
- [21] Maria Davidich, Florian Geiss, Hermann Georg Mayer, Alexander Pfaffinger, and Christian Royer. Waiting zones for realistic modelling of pedestrian dynamics: A case study using two major German railway stations as examples. *Transportation Research Part C*, 37 (2013):201–222, 2013.
- [22] Mira Küpper and Armin Seyfried. Analysis of space usage on train station platforms based on trajectory data. *Sustainability*, 12(20), 2020.
- [23] Pierre Patterson. Passenger waiting strategies on railway platforms - Effects of information and platform facilities - Case study: Schweden and Japan. Master's

- thesis, KTH, School of Architecture and the Built Environment (ABE), Transport Science, March 2011.
- [24] Mira Küpper and Armin Seyfried. Waiting passengers and social groups on platforms – automatic identification based on trajectories. Proceedings of the 10th International Conference on Pedestrian and Evacuation Dynamics (PED2021), Melbourne (Australia), November 29-30, 2021, 2021.
- [25] Usman Tasiu Abdurrahman, Anson Jack, and Felix Schmidt. Effects of platform screen doors on the overall railway system. In *8th International Conference on Railway Engineering (ICRE 2018)*, volume 2018, page 6 pp., 2018.
- [26] Yoongho Ahn, Tomoya Kowada, Hiroshi Tsukaguchi, and Upali Vandebona. Estimation of passenger flow for planning and management of railway stations. In *Transportation Research Procedia*, volume 25 (2017), pages 315–330, 2017.
- [27] Ulrich Weidmann. *Der Fahrgastwechsel im öffentlichen Personenverkehr*. PhD thesis, ETH Zürich, 1994.
- [28] Lu Zhilin. Großräumige Evakuierung über das Verkehrsmittel Schiene – Einstiegszeiten in Züge und Engstellen im Bahnhof mittels Feldstudien und Simulationen. Master’s thesis, Bergische Universität Wuppertal - Fakultät für Maschinenbau und Sicherheitstechnik, August 2019.
- [29] John. J. Fruin. *Pedestrian Planning and Design*. Elevator World, New York, 1987 (Original work published 1971).
- [30] Ulrich Weidmann. Transporttechnik der Fußgänger. Technical Report Schriftenreihe des IVT Nr. 90, Zweite ergänzte Auflage, Institut für Verkehrsplanung, Transporttechnik, Strassen- und Eisenbahnbau, ETH Zürich, ETH Zürich, March 1993.
- [31] Stefan Holl, Maik Boltes, and Armin Seyfried. Level-of-Safety-Konzept für den Fußverkehr bei Großveranstaltungen. In Christoph Groneberg, editor, *Veranstaltungskommunikation*, pages 253–277, Wiesbaden, 2019. Springer Fachmedien Wiesbaden.
- [32] Tobias Schrödter, Mohcine Chraibi, and Armin Seyfried. Modeling of position finding in waiting processes on platforms. In Iker Zuriguel, Angel Garcimartin, and Raul Cruz, editors, *Traffic and Granular Flow 2019*, pages 233 – 240, Cham, 2020. Springer International Publishing.
- [33] Jupedsim official webpage. URL: <https://www.jupedsim.org>. Accessed: October 2021.
- [34] Antoine Tordeux, Mohcine Chraibi, and Armin Seyfried. Collision-free speed model for pedestrian dynamics. In Victor L. Knoop and Winnie Daamen, editors, *Traffic and Granular Flow '15*, pages 225–232. Springer International Publishing, 2016.

-
- [35] Arne Graf. Automated routing in pedestrian dynamics. Master's thesis, Fachhochschule Aachen - Campus Jülich - Studiengang: Technomathematik, October 2015.
- [36] Qiancheng Xu, Mohcine Chraibi, and Armin Seyfried. Anticipation in a velocity-based model for pedestrian dynamics. *Transportation Research Part C: Emerging Technologies*, 133:103464, 2021.
- [37] Jupedsim source code. URL: <https://github.com/JuPedSim/jpscore>.
- [38] Christian Dittmer. Technical data of the train series dbpza 551. URL: <https://www.deutsche-reisezugwagen.de>. Accessed: September 2021.
- [39] DB Fernverkehr AG. Fahrzeuglexikon für den Fernverkehr. Technical report, Deutsche Bahn AG, June 2021.
- [40] Technical specifications of the train series 423. URL: <https://web.archive.org/web/20060821212052/http://www.et423.de/techndaten.html>, 2006. Accessed: November 2021.
- [41] Stefan Holl and Armin Seyfried. Validität von Evakuierungssimulationen. *vfd-Zeitschrift*, 1:35–41, 2010.
- [42] Anna Braun, Mohcine Chraibi, and Lukas Arnold. Investigation of the capacity of train stations in case of a large-scale emergency evacuation. In Melanie Weber, Laura Bieker-Walz, Robert Hilbrich, and Michael Behrisch, editors, *SUMO User Conference 2019*, volume 62 of *EPiC Series in Computing*, pages 68–77, 2019.
- [43] Klattenhoff Paula DB AG. Der ICE 4, das Flaggschiff des Fernverkehrs. Technical report, Deutsche Bahn AG, October 2020.

A. Initial conditions of JPScore

Example of a configuration file for JPScore

```

<?xml version="1.0" encoding="UTF-8" ?>
<JuPedSim project="Subway-Project" version="0.7"
  xmlns:xsi="http://www.w3.org/2001/XMLSchema-instance"
  xsi:noNamespaceSchemaLocation="../../xsd/jps_ini_core.xsd">

  <header>
    <seed>1234</seed>
    <max_sim_time>6000</max_sim_time>
    <num_threads>4</num_threads>
    <geometry>02-geometry-final.xml</geometry>
    <trajectories format="plain" fps="4">
    <file location="11-trajectories.txt" />
    </trajectories>
    <logfile>11-log</logfile>
    <output path="11-results-01" />
    <show_statistics>false</show_statistics>
  </header>

  <!--events_file>/04-events.xml</events_file-->
  <!--schedule_file>/05-schedule.xml</schedule_file-->

  <!--traffic_constraints>
    <file>06-traffic.xml</file>
  </traffic_constraints-->

  <!--train_constraints>
    <train_types>07-train_types.xml</train_types>
    <train_time_table>08-ttt.xml</train_time_table>
  </train_constraints-->

  <routing>
    <goals>
      <goal id="101" final="true" caption="goal_101">
        <polygon>
          <vertex px="8" py="115" />
          <vertex px="8" py="117" />
          <vertex px="7" py="117" />
          <vertex px="7" py="115" />
          <vertex px="8" py="115" />
        </polygon>
      </goal>
      <goal id="102" final="true" caption="goal_102">
        <polygon>
          <vertex px="22" py="115" />
          <vertex px="22" py="117" />
          <vertex px="23" py="117" />
          <vertex px="23" py="115" />
          <vertex px="22" py="115" />
        </polygon>
      </goal>
      <goal ...
      ...
    </goals>
  </routing>

```

```

<agents operational_model_id="3">
  <agents_distribution>
    <group group_id="101" agent_parameter_id="1" room_id="1000"
      subroom_id="1" number="45" goal_id="101" router_id="1" />
    <group group_id="102" agent_parameter_id="1" room_id="1000"
      subroom_id="1" number="45" goal_id="102" router_id="1" />
    ...
  </agents_distribution>
  <agents_sources>
    <source group_id="101" id="101" time_min="0.0" time_max="6000"
      frequency="300" percent="0.0625" rate="4" N_create="160"
      agents_max="1600" greedy="true" />
    <source group_id="102" id="102" time_min="0.0" time_max="6000"
      frequency="300" percent="0.0625" rate="4" N_create="160"
      agents_max="1600" greedy="true" />
    ...
  </agents_sources>
</agents>

<operational_models>
  <model operational_model_id="3" description="Tordeux2015">
    <model_parameters>
      <solver>euler</solver>
      <stepsize>0.05</stepsize>
      <exit_crossing_strategy>8</exit_crossing_strategy>
      <floorfield delta_h="0.0625" wall_avoid_distance="0.8"
        use_wall_avoidance="true" />
      <linkedcells enabled="true" cell_size="2.2" />
    </model_parameters>
    <agent_parameters agent_parameter_id="1">
      <v0 mu="1.1" sigma="0.1" />
      <v0_upstairs mu="0.7" sigma="0.167" />
      <v0_downstairs mu="0.7" sigma="0.188" />
      <bmax mu="0.25" sigma="0.00000" />
      <bmin mu="0.25" sigma="0.00000" />
      <amin mu="0.25" sigma="0.00000" />
      <tau mu="0.5" sigma="0.001" />
      <atau mu="0.0" sigma="0.00000" />
      <T mu="1" sigma="0.001" />
    </agent_parameters>
  </model>

  <route_choice_models>
    <router router_id="1" description="ff_global_shortest">
      <!--write_VTK_files>true</write_VTK_files-->
    </router>
  </route_choice_models>

</JuPedSim>

```


B. Evaluation Final

In the following, additional results which have been referred in chapter 3.2.4 are shown. These are:

- Figure B.1.: Time-dependent densities as a function of the filling process for the example of platform 5 with an inflow rate of 4 s^{-1}
- Figure B.2.: Time-dependent densities as a function of the filling process for the example of platform 3 with an inflow rate of 6 s^{-1}
- Figure B.3.: Time-dependent densities as a function of the filling process for the example of platform 3 with an inflow rate of 8 s^{-1}
- Figure B.4.: Time-dependent densities as a function of the filling process for the example of platform 3 with an inflow rate of 12 s^{-1}

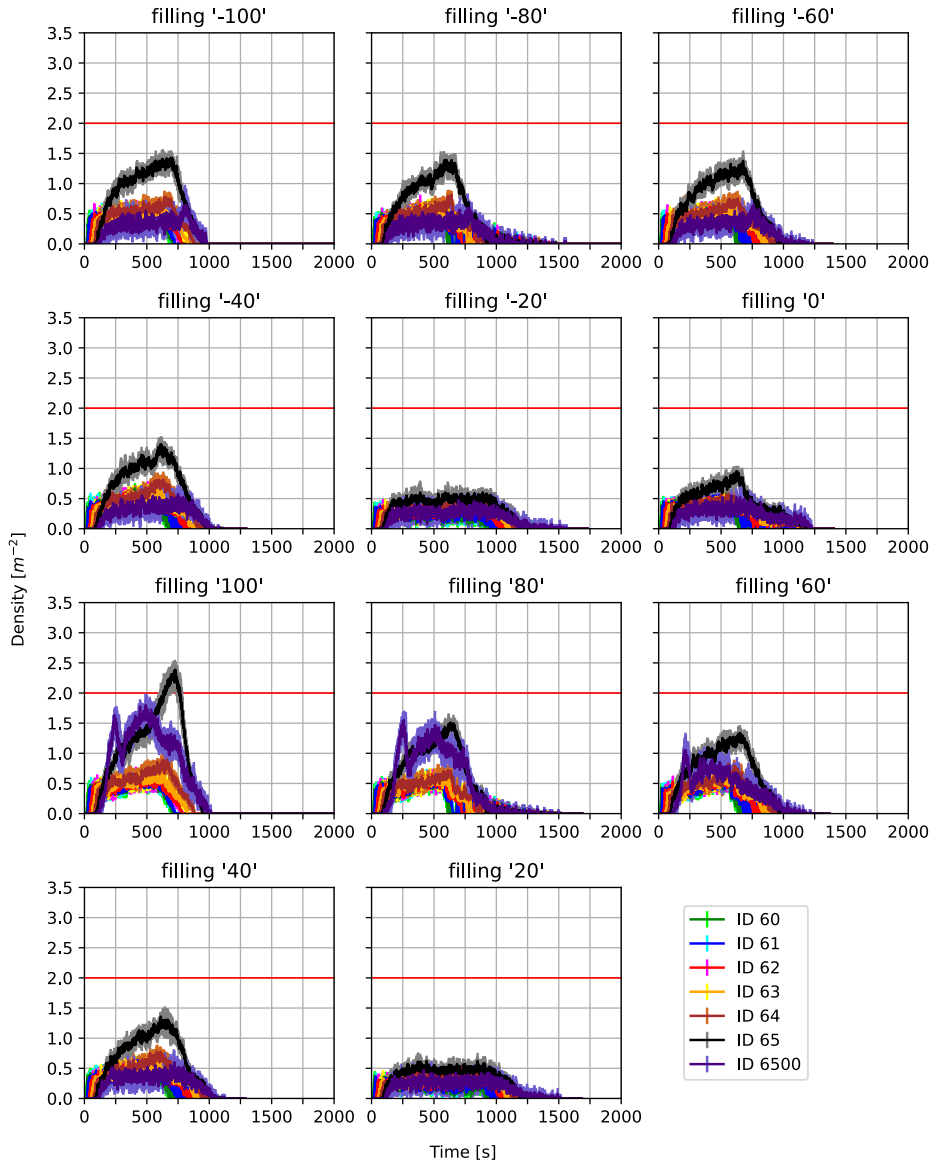


Figure B.1.: Time-dependent densities as a function of the filling process for the example of platform 5 with an inflow rate of 4s^{-1} .

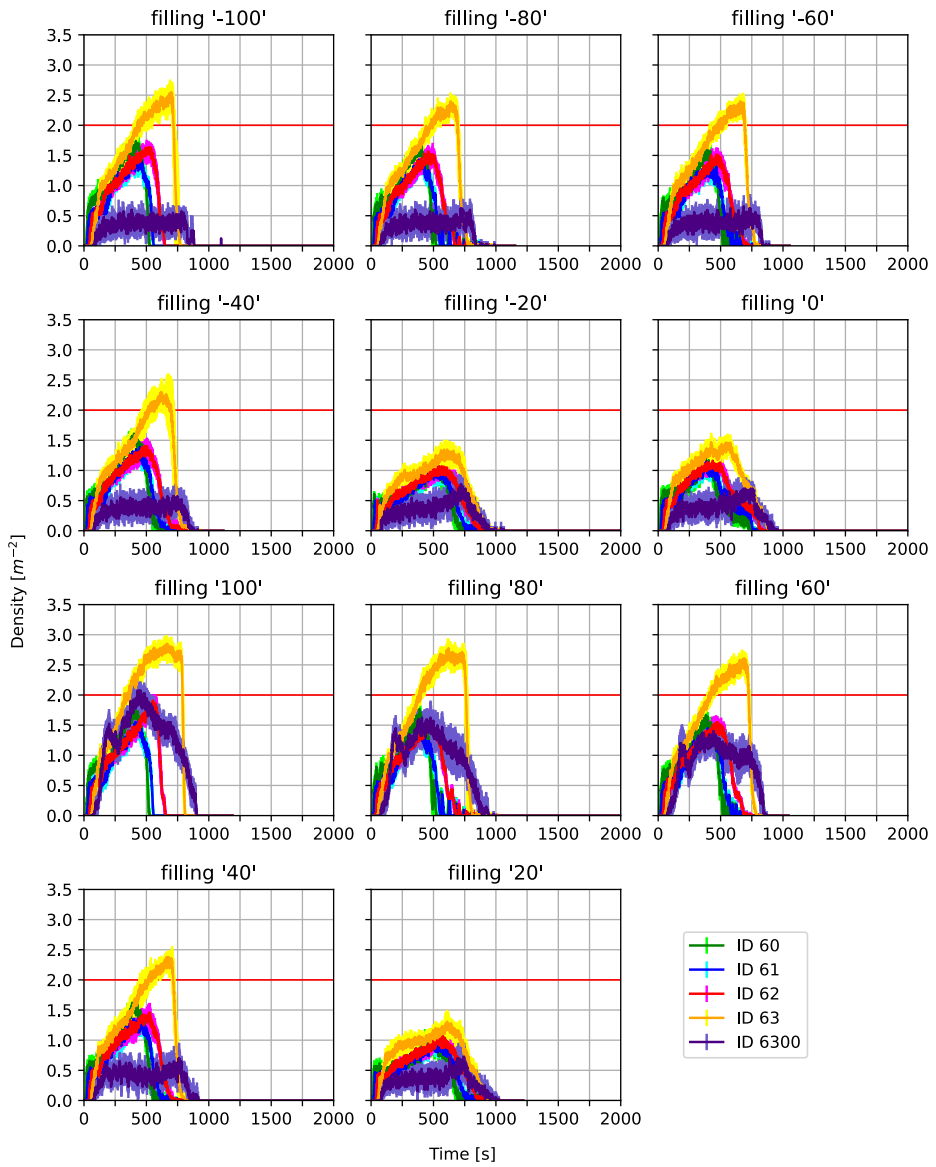


Figure B.2.: Time-dependent densities as a function of the filling process for the example of platform 3 with an inflow rate of $6 s^{-1}$.

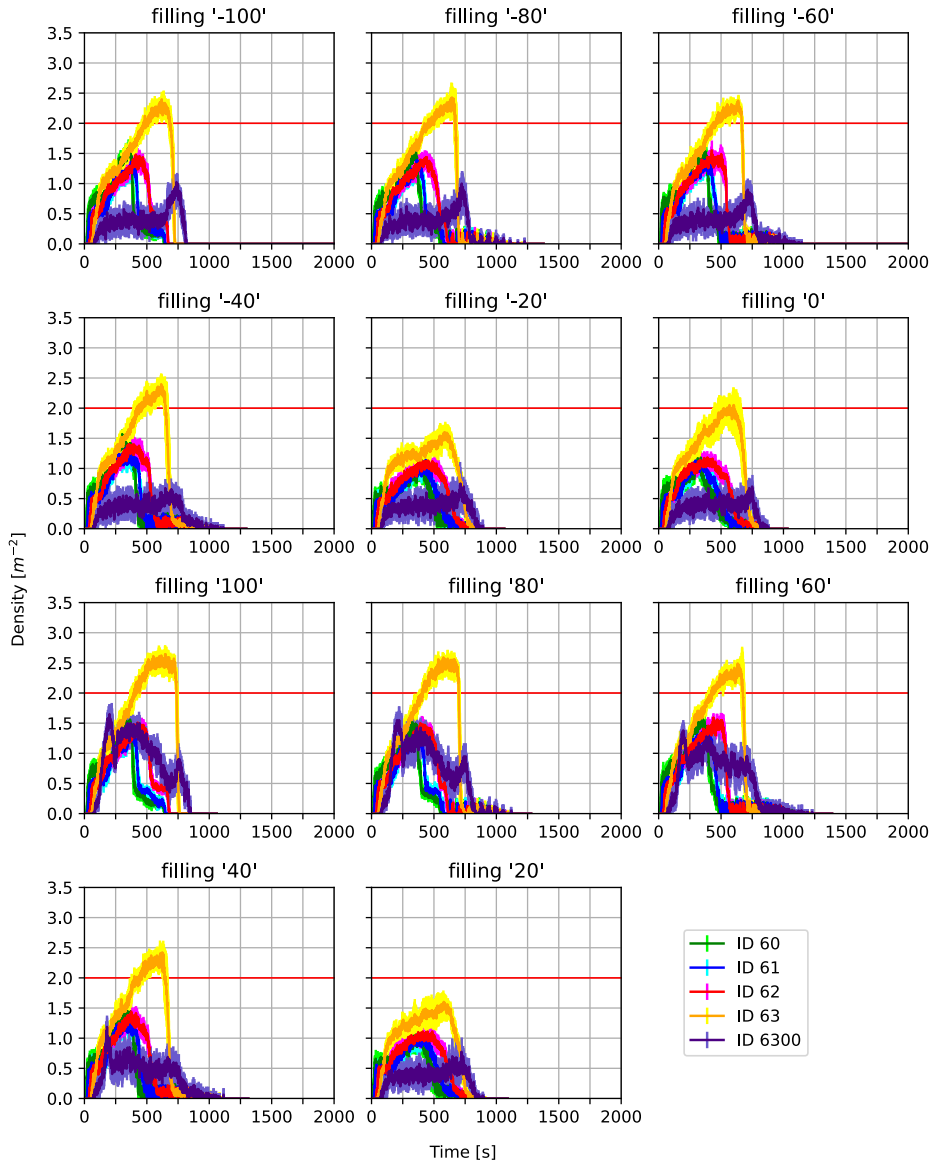


Figure B.3.: Time-dependent densities as a function of the filling process for the example of platform 3 with an inflow rate of 8 s^{-1} .

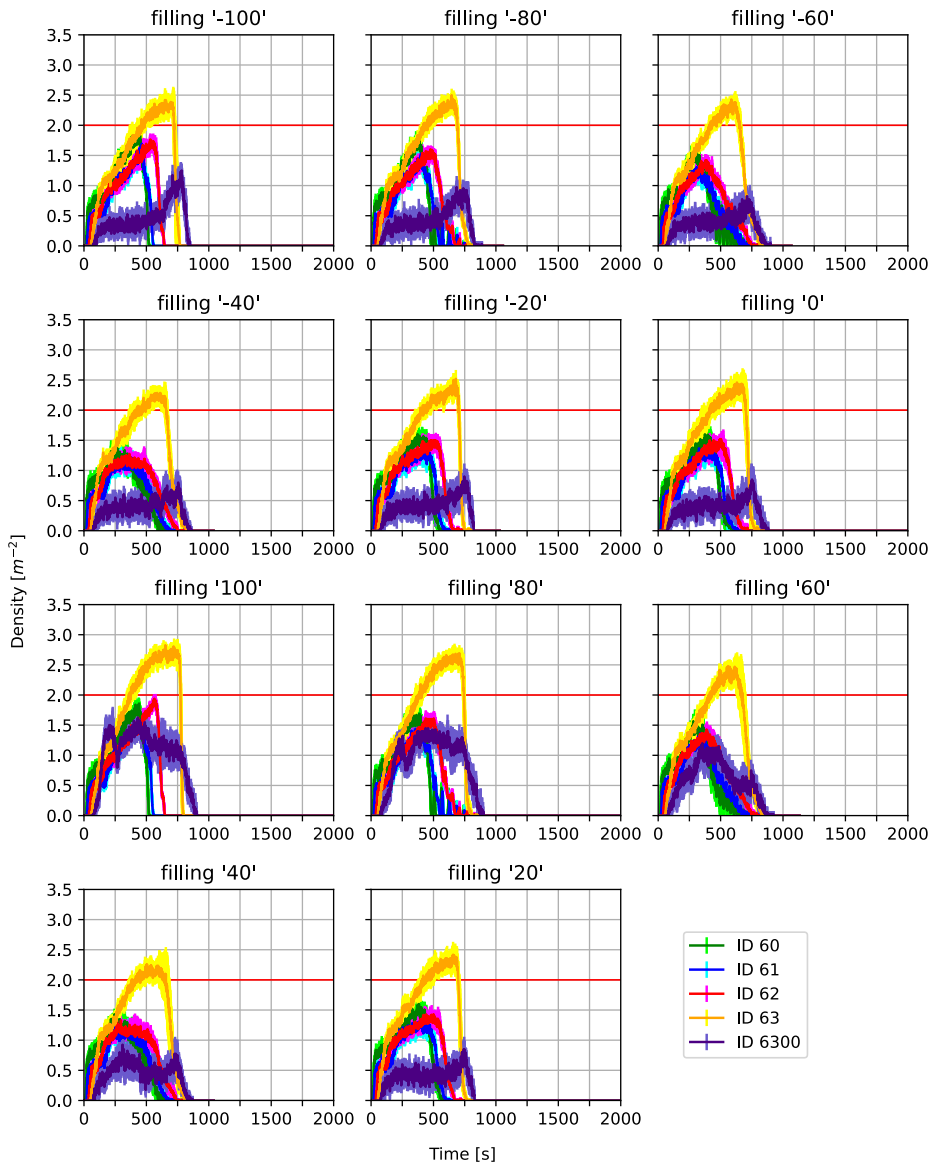


Figure B.4.: Time-dependent densities as a function of the filling process for the example of platform 3 with an inflow rate of 12 s^{-1} .

C. Evaluation Easy

In the following, additional results which have been referred in chapter 3.3 are shown. These are:

- Figure C.1.: Time-dependent densities for the filling processes “100” to “20” (*fro-re*) a corridor of 10 m, a staircase of 4 m, an inflow rate of 2 s^{-1} , and a door opening time of 2 min
- Figure C.2.: Time-dependent densities for the filling processes “100” to “20” (*fro-re*) a corridor of 10 m, a staircase of 4 m, an inflow rate of 2 s^{-1} , and a door opening time of 6 min
- Figure C.3.: Time-dependent densities for the filling processes “100” to “20” (*fro-re*) a corridor of 90 m, a staircase of 4 m and an inflow rate of 2 s^{-1}
- Figure C.4.: Time-dependent densities for the filling processes “-100” to “-20” (*re-fro*) a corridor of 50 m, a staircase of 6 m and an inflow rate of 4 s^{-1}
- Figure C.5.: Time-dependent densities for the filling processes “-100” to “-20” (*re-fro*) a corridor of 50 m, a staircase of 8 m and an inflow rate of 6 s^{-1}
- Figure C.6.: Time-dependent densities for the filling processes “-100” to “-20” (*re-fro*) a corridor of 50 m, a staircase of 10 m and an inflow rate of 8 s^{-1}
- Figure C.7.: Time-dependent densities for the double-sided filling, a corridor of 10 m, a staircase of 4 m, and an inflow rate of 2 s^{-1}
- Figure C.8.: Time-dependent densities for the double-sided filling, a corridor of 50 m, a staircase of 6 m, and an inflow rate of 4 s^{-1}
- Figure C.9.: Time-dependent densities for the double-sided filling, a corridor of 50 m, a staircase of 8 m, and an inflow rate of 6 s^{-1}
- Figure C.10.: Time-dependent densities for the double-sided filling, a corridor of 50 m, a staircase of 10 m, and an inflow rate of 6 s^{-1}
- Figure C.11.: Time-dependent densities with obstacle for a corridor of 90 m, a staircase of 8 m, and an inflow rate of 2 s^{-1}
- Figure C.12.: Time-dependent densities with obstacle for a corridor of 90 m, a staircase of 8 m, and an inflow rate of 4 s^{-1}
- Figure C.13.: Time-dependent densities with obstacle for a corridor of 90 m, a staircase of 8 m, and an inflow rate of 8 s^{-1}

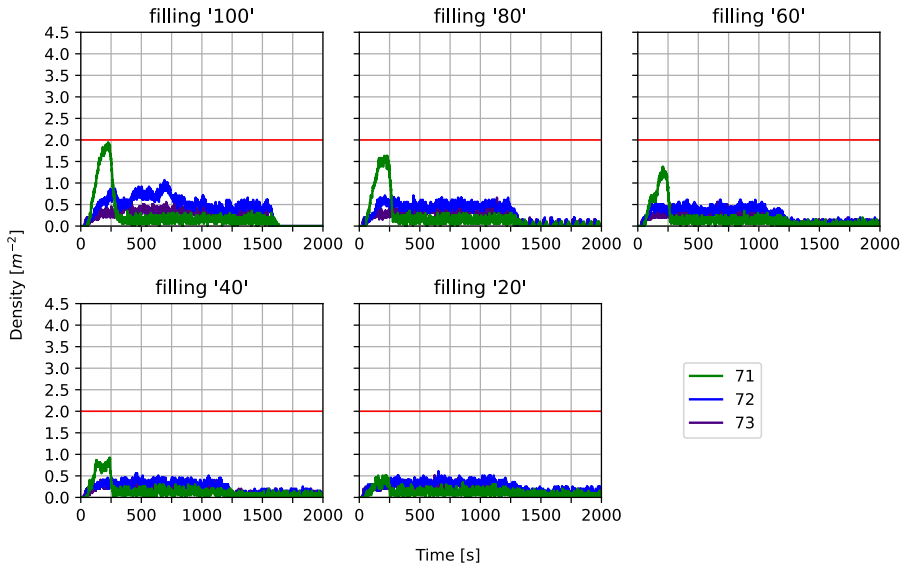


Figure C.1.: Time-dependent densities for the filling processes “100” to “20” (*fro-re*) a corridor of 10 m, a staircase of 4 m, an inflow rate of $2 s^{-1}$, and a door opening time of 2 min.

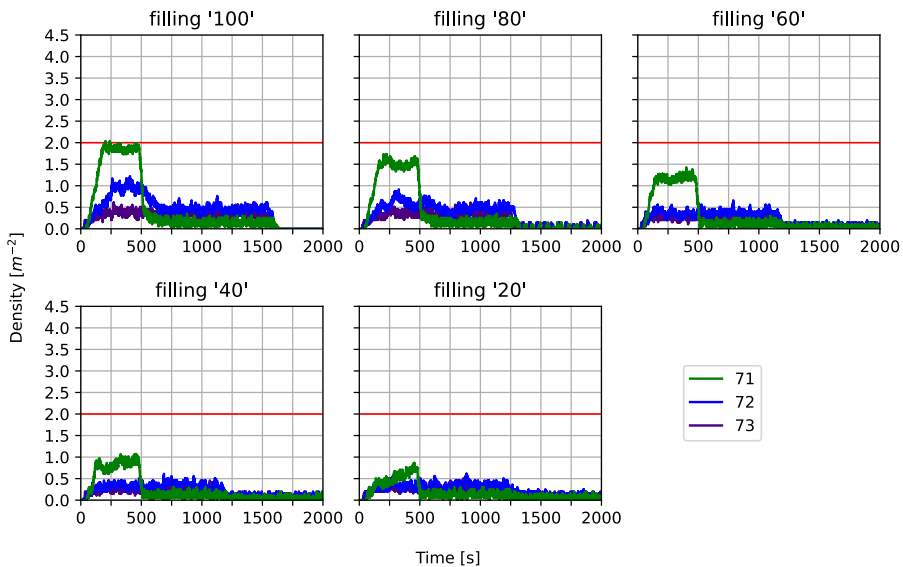


Figure C.2.: Time-dependent densities for the filling processes “100” to “20” (*fro-re*) a corridor of 10 m, a staircase of 4 m, an inflow rate of $2 s^{-1}$, and a door opening time of 6 min.

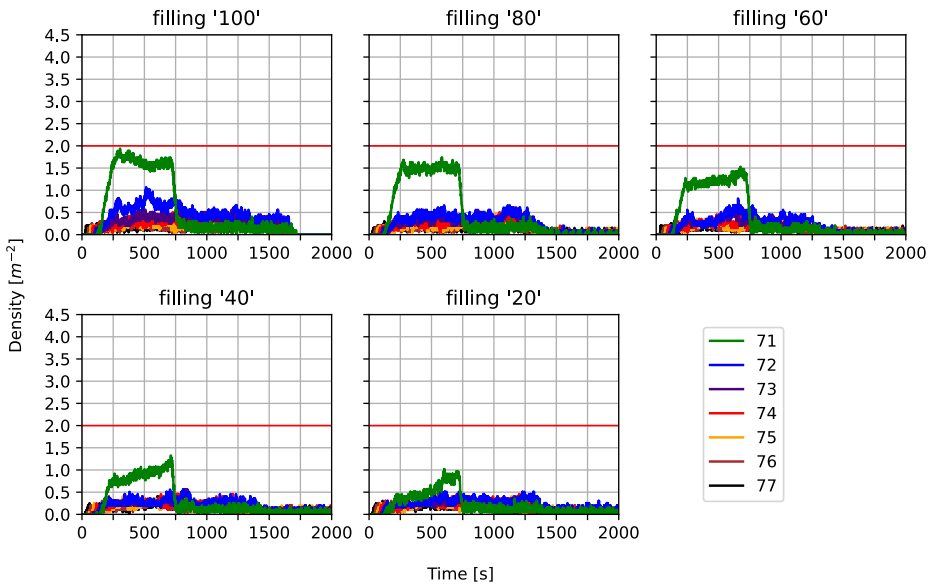


Figure C.3.: Time-dependent densities for the filling processes “100” to “20” (*fro-re*) a corridor of 90 m, a staircase of 4 m and an inflow rate of $2 s^{-1}$.

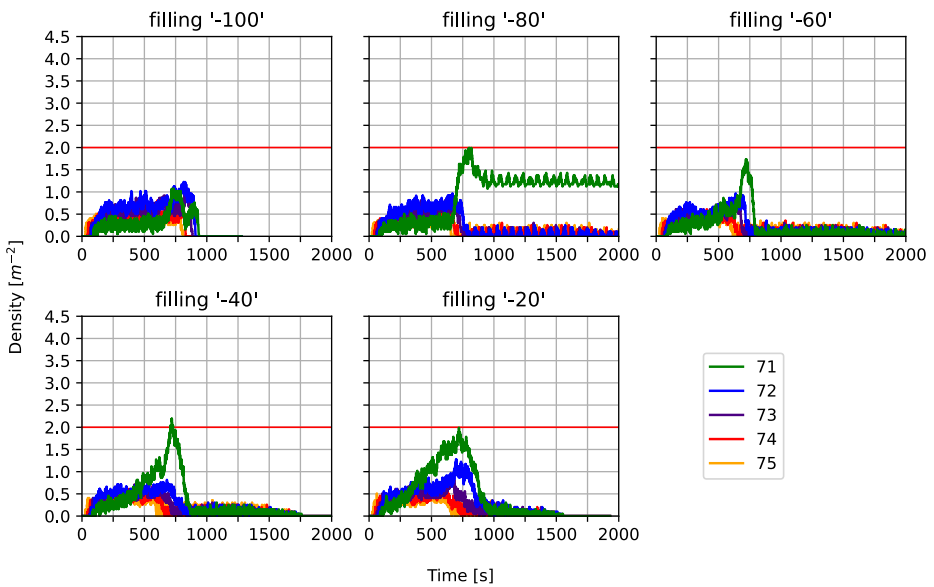


Figure C.4.: Time-dependent densities for the filling processes “-100” to “-20” (*re-fro*) a corridor of 50 m, a staircase of 6 m and an inflow rate of $4 s^{-1}$.

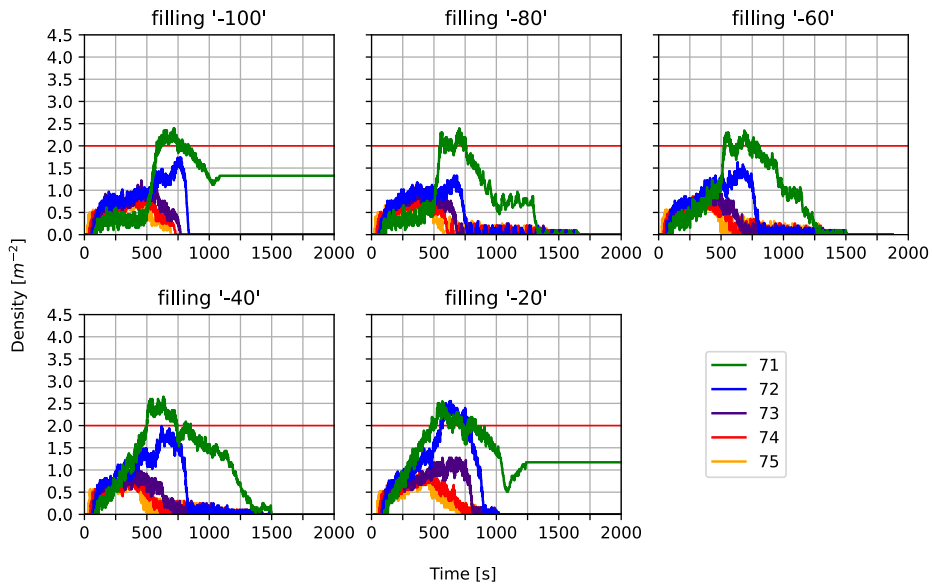


Figure C.5.: Time-dependent densities for the filling processes “-100” to “-20” (*re-fro*) a corridor of 50 m, a staircase of 8 m and an inflow rate of 6 s^{-1} .

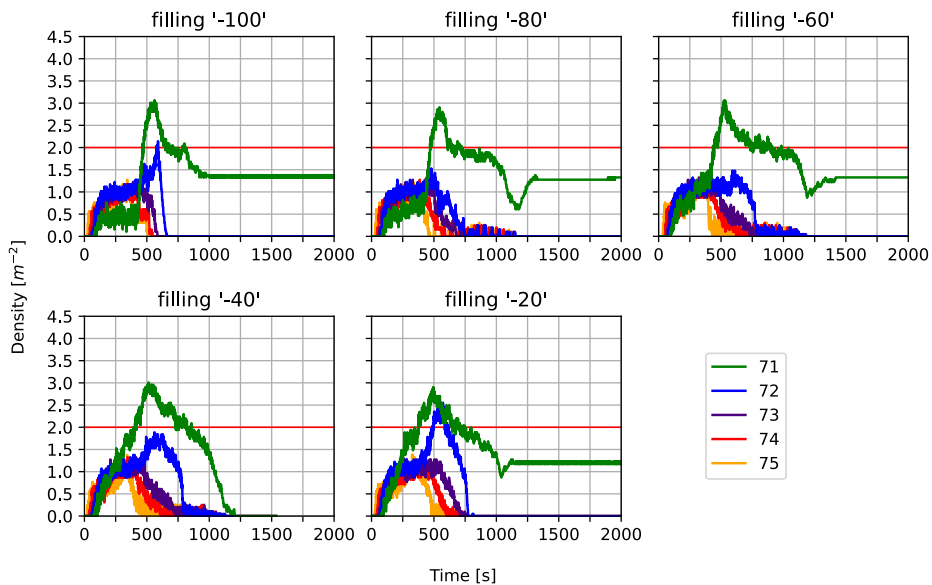


Figure C.6.: Time-dependent densities for the filling processes “-100” to “-20” (*re-fro*) a corridor of 50 m, a staircase of 10 m and an inflow rate of 8 s^{-1} .

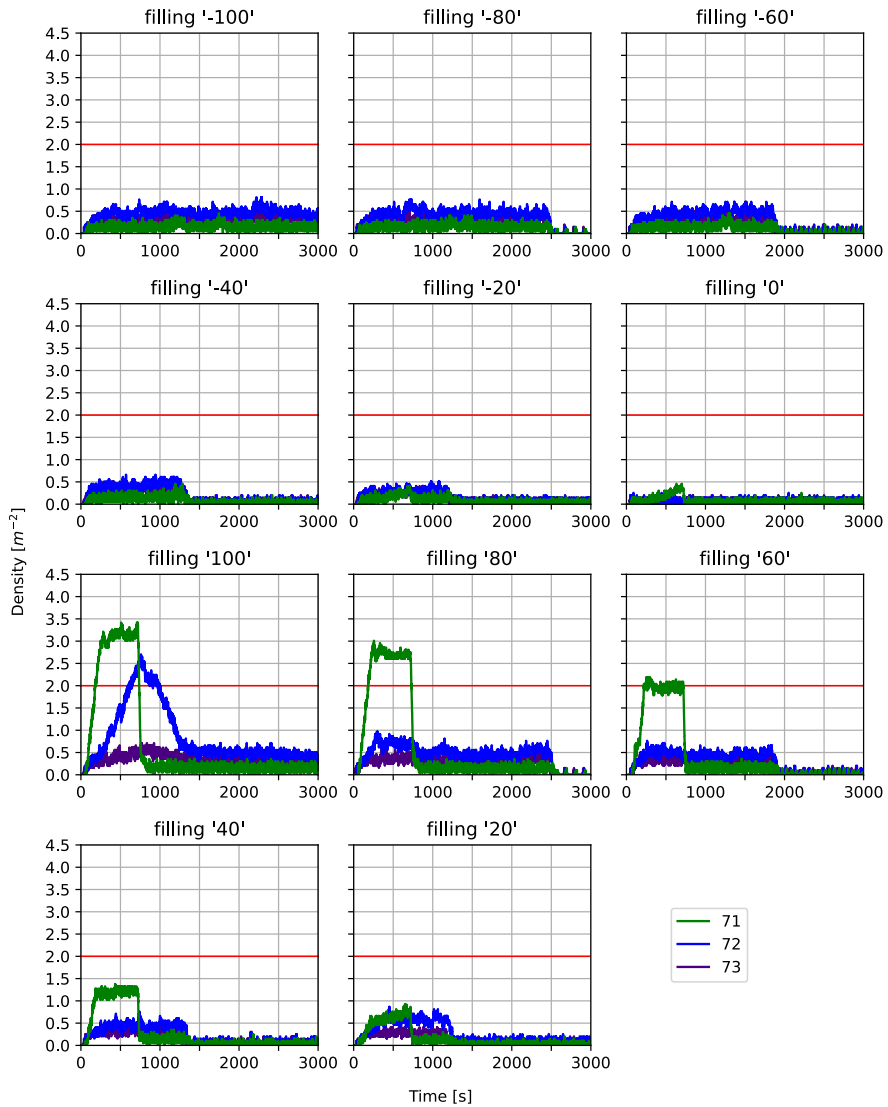


Figure C.7.: Time-dependent densities for the double-sided filling, a corridor of 10 m, a staircase of 4 m, and an inflow rate of 2 s^{-1} .

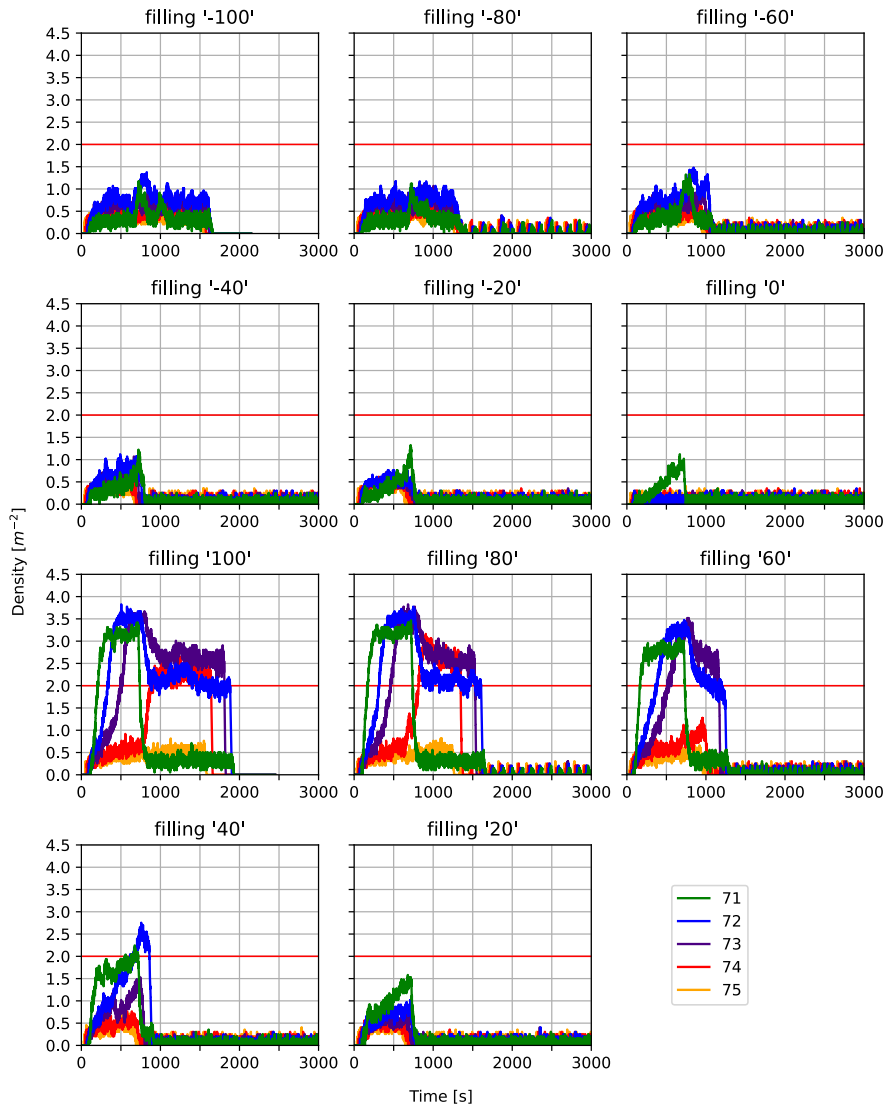


Figure C.8.: Time-dependent densities for the double-sided filling, a corridor of 50 m, a staircase of 6 m, and an inflow rate of 4 s^{-1} .

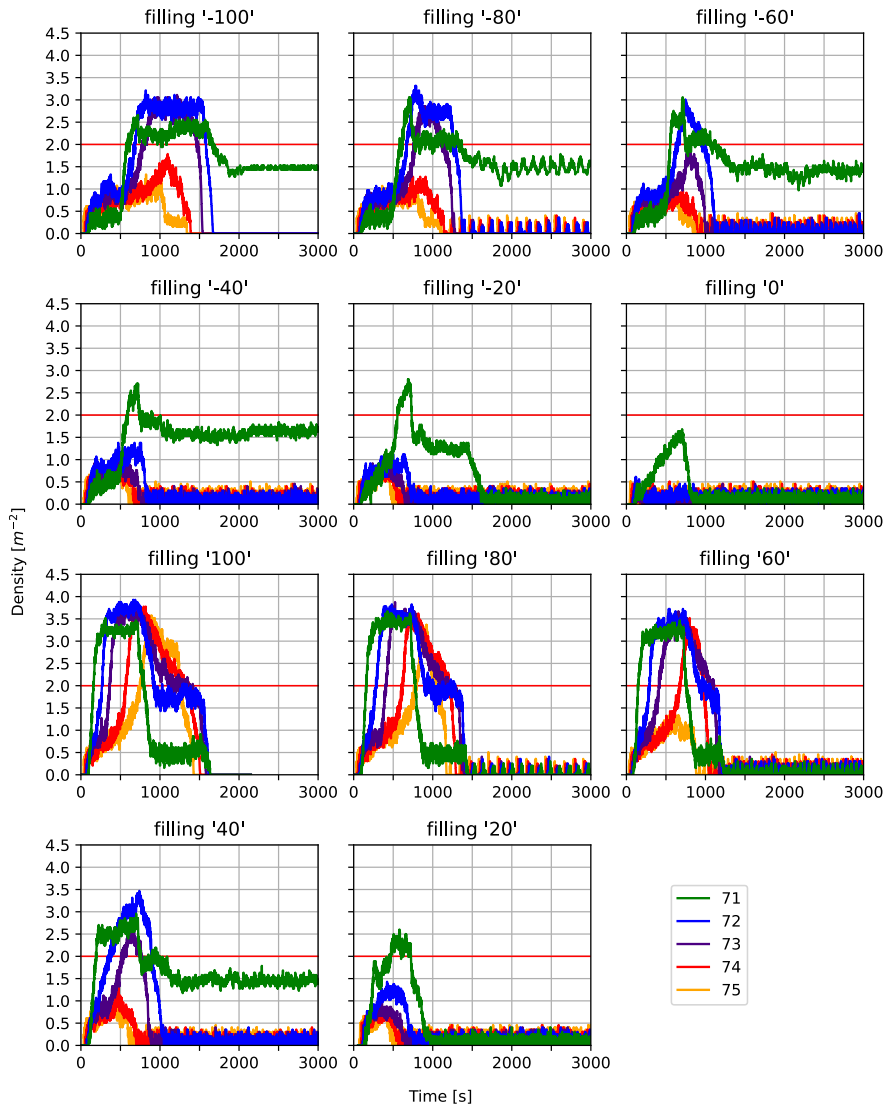


Figure C.9.: Time-dependent densities for the double-sided filling, a corridor of 50 m, a staircase of 8 m, and an inflow rate of 6 s^{-1} .

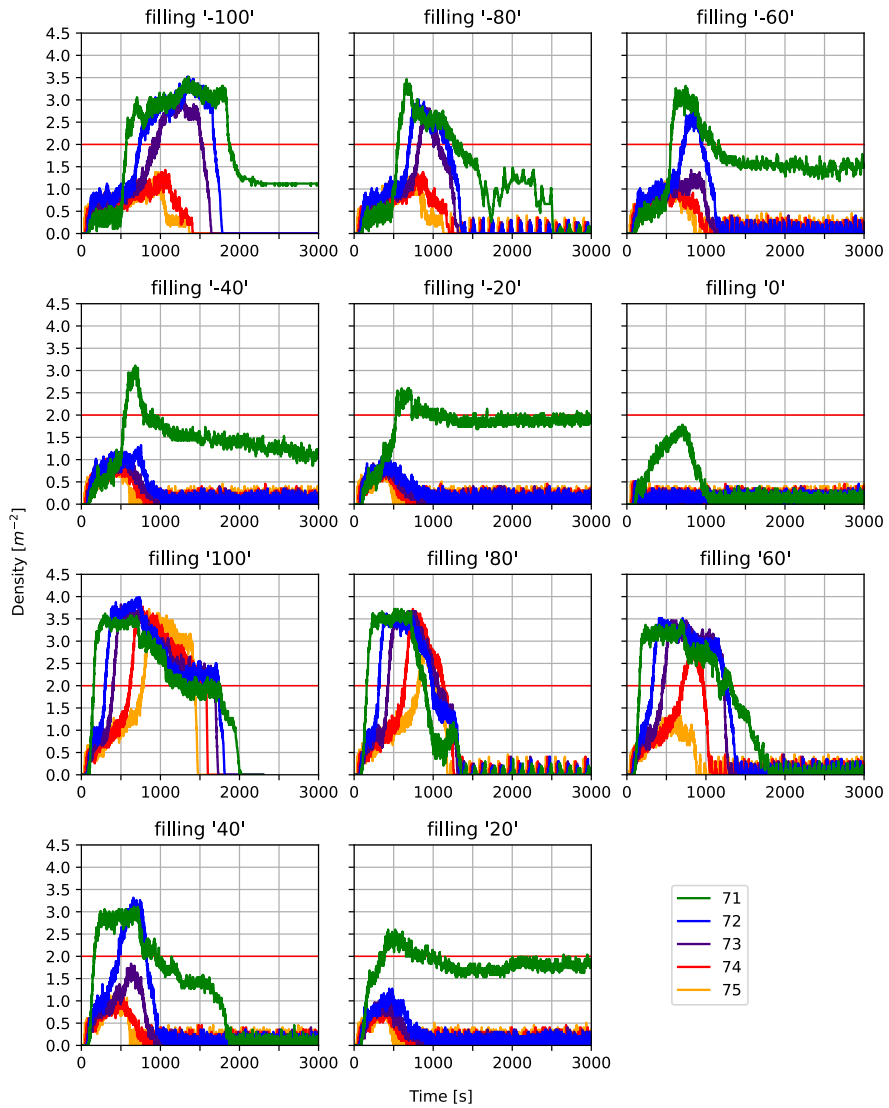


Figure C.10.: Time-dependent densities for the double-sided filling, a corridor of 50 m, a staircase of 10 m, and an inflow rate of 6 s^{-1} .

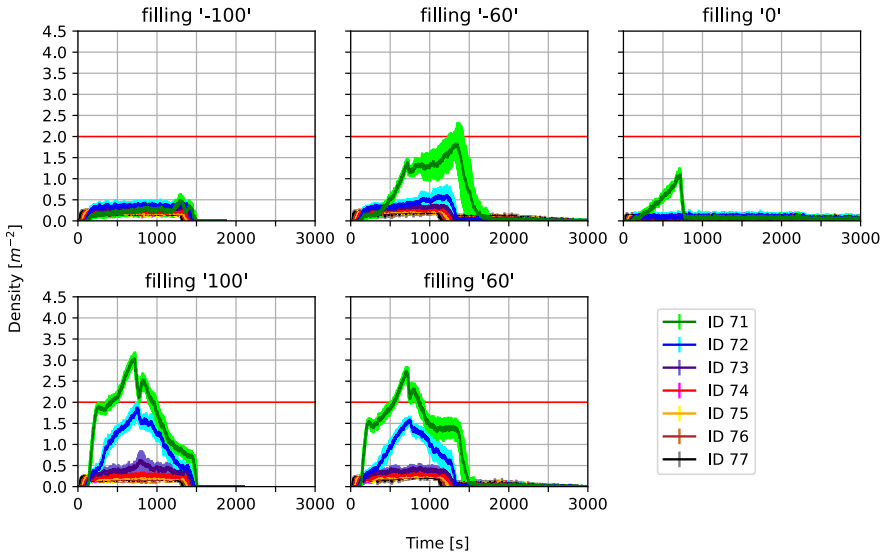


Figure C.11.: Time-dependent densities with obstacle for a corridor of 90 m, a staircase of 8 m, and an inflow rate of 2 s^{-1} .

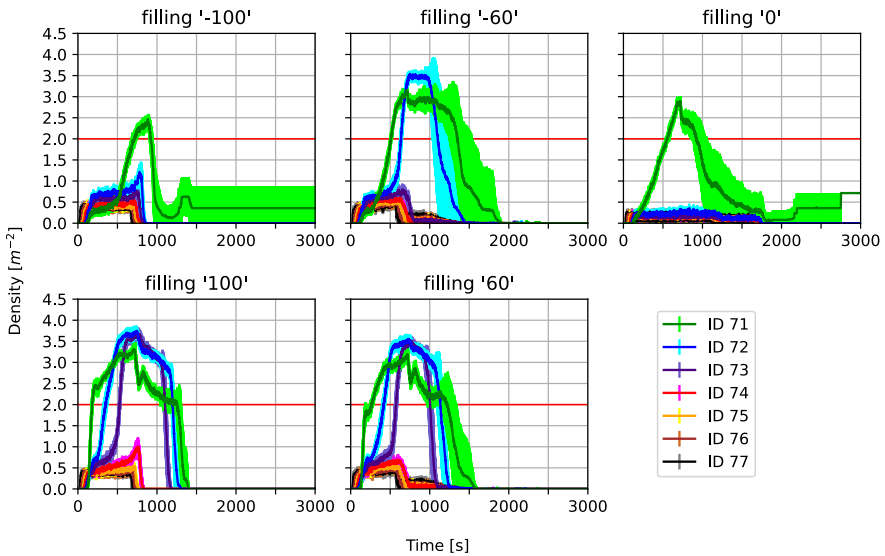


Figure C.12.: Time-dependent densities with obstacle for a corridor of 90 m, a staircase of 8 m, and an inflow rate of 4 s^{-1} .

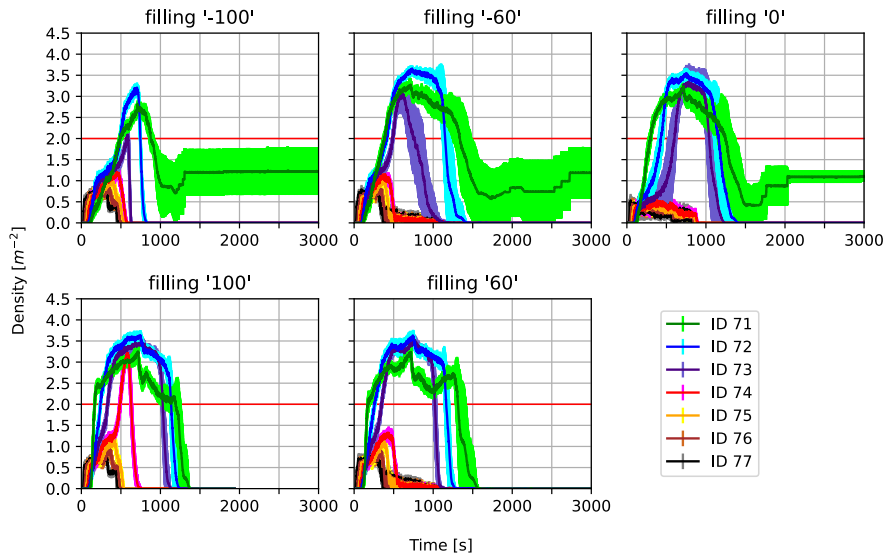


Figure C.13.: Time-dependent densities with obstacle for a corridor of 90 m, a staircase of 8 m, and an inflow rate of $8 s^{-1}$.

Band / Volume 43

Algorithms for massively parallel generic *hp*-adaptive finite element methods

M. Fehling (2020), vii, 78 pp

ISBN: 978-3-95806-486-7

URN: urn:nbn:de:0001-2020071402

Band / Volume 44

The method of fundamental solutions for computing interior transmission eigenvalues

L. Pieronek (2020), 115 pp

ISBN: 978-3-95806-504-8

Band / Volume 45

Supercomputer simulations of transmon quantum computers

D. Willsch (2020), IX, 237 pp

ISBN: 978-3-95806-505-5

Band / Volume 46

The Influence of Individual Characteristics on Crowd Dynamics

P. Georg (2021), xiv, 212 pp

ISBN: 978-3-95806-561-1

Band / Volume 47

Structural plasticity as a connectivity generation and optimization algorithm in neural networks

S. Diaz Pier (2021), 167 pp

ISBN: 978-3-95806-577-2

Band / Volume 48

Porting applications to a Modular Supercomputer

Experiences from the DEEP-EST project

A. Kreuzer, E. Suarez, N. Eicker, Th. Lippert (Eds.) (2021), 209 pp

ISBN: 978-3-95806-590-1

Band / Volume 49

Operational Navigation of Agents and Self-organization Phenomena in Velocity-based Models for Pedestrian Dynamics

Q. Xu (2022), xii, 112 pp

ISBN: 978-3-95806-620-5

Band / Volume 50

Utilizing Inertial Sensors as an Extension of a Camera Tracking System for Gathering Movement Data in Dense Crowds

J. Schumann (2022), xii, 155 pp

ISBN: 978-3-95806-624-3

Band / Volume 51

**Final report of the DeepRain project
Abschlußbericht des DeepRain Projektes**

(2022), ca. 70 pp

ISBN: 978-3-95806-675-5

Band / Volume 52

JSC Guest Student Programme Proceedings 2021

I. Kabadshow (Ed.) (2023), ii, 82 pp

ISBN: 978-3-95806-684-7

Band / Volume 53

Applications of variational methods for quantum computers

M. S. Jattana (2023), vii, 160 pp

ISBN: 978-3-95806-700-4

Band / Volume 54

**Crowd Management at Train Stations in Case of
Large-Scale Emergency Events**

A. L. Braun (2023), vii, 120 pp

ISBN: 978-3-95806-706-6

Weitere **Schriften des Verlags im Forschungszentrum Jülich** unter
<http://www.zb1.fz-juelich.de/verlagextern1/index.asp>

IAS Series
Band / Volume 54
ISBN 978-3-95806-706-6